AD-A155 020 STRESS CORROSION OF CERAMIC MATERIALS(U) NATIONAL BUREAU OF STANDARDS GAITHERSBURG MD INORGANIC MATERIALS DIV S W FREIMAN ET AL. MAY 85 N00014-84-F-0019 1/2

UNCLASSIFIED F/G 11/2 NL

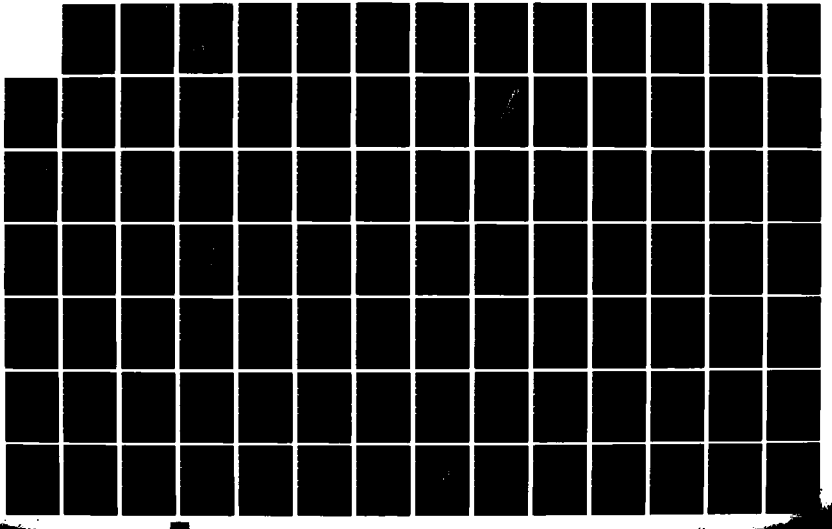

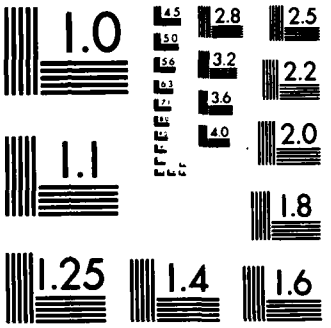

STRESS CORROSION OF CERAMIC MATERIALS

S.W. Freiman, G.S. White, A.C. Gonzalez,
E.R. Fuller, Jr. and D.C. Greenspan

Annual Report

October 1, 1983 - September 30, 1984

CNR Contract No. N00014-84-F-0019
NBS Project No. 4200454

for

Office of Naval Research
Code 431
Arlington, VA 22217

by

National Bureau of Standards
Inorganic Materials Division
Gaithersburg, MD 20899

May 1985

AD-A155020

STRESS CORROSION OF CERAMIC MATERIALS

Contents

Additional keywords: fracture; modifier ions; silicate structures; infrared spectra; stress corrosion

STRESS CORROSION OF CERAMIC MATERIALS

SUMMARY

The work during the past year can be divided into two distinct areas, namely (1) the effect of modifying ions on environmentally enhanced crack growth in glasses and (2) the relationship between crack growth and electrical failure in multilayer ceramic capacitors. Results of these investigations are summarized as follows:

(1) Environmentally Enhanced Crack Growth

During this past year work has been concentrated on understanding the role of modifier ions in silicate structures on the environmentally enhanced Si-O bond rupture mechanism described by Michalske and Freiman. To this end, crack growth studies were conducted on soda lime glass, a 33% Na_2O-67% SiO_2, and a 33% Li_2O-67% SiO_2 glass. These studies have shown that those environments and only those environments which enhance crack growth in vitreous SiO_2 do so in these glasses. However, the data suggest that the presence of Na^+ or Ca^+ may change the reactivity of the adjacent Si-O bridging bond as well as affect the elastic properties of the network so as to change the slope and position of the crack velocity-K_I curves. Ion exchange/dissolution mechanisms at the crack tip appear to come into play at low velocities, i.e. $<10^{-8}$ m/sec. Direct correlations of crack growth rates with ion exchange/dissolution were obtained for the two binary glasses. That is, those environments, e.g. water and hydrazine, that produced the largest changes in infrared spectra taken of the glass surface as a function of time also had the strongest effect on the crack growth curves.

A fracture mechanics model which incorporates effects of silica glass structures, modifying ions, and differing environments has been developed to explain the variations in slope and position of the V-K_I curve for different materials. The model assumes that the equilibrium forces acting on the Si-O bond at the crack tip can be expressed as a function of the compliance of the system and the Si-O bond force, including contributions from modifying ions and differing environments. If one inserts into the model a functional form for the Si-O bond force, and the interaction of the environment, then the model can be used to explain the trends in crack growth curves. For instance if the concerted reaction model of Michalske and Freiman is chosen as a basis for the model, the systematic shifts to higher log V-K_I slopes in less reactive environments, as observed in the binary glasses, can be interpreted as resulting from a nonlinear stress strain curve for the modified Si-O bond. Similarly, the model qualitatively explains the shift in K_I for different environments. Currently we are trying to obtain quantitative values for the parameters used in the model. With these values, we should be able to quantitatively compare the shifts predicted by the model with experimentally observed shifts in the log V vs K_I curves. In a cooperative effort with VPI, we are attempting to obtain predictions of strain enhanced reactions using molecular orbital calculations to determine the structure and reactivity of the Si-O bond. The results of this work should provide us with a clearer picture of the details of the strain enhanced reaction as well as help provide the Si-O force curve to use in our model.

Further, we have shown that while the crack growth curves for vitreous SiO_2 in liquid water and N_2 gas at 100% relative humidity overlap for crack velocities $\leq 10^{-6}$ m/s, those for soda lime glass are separated,

with that for liquid water lying at slightly lower K_I. We have ascribed the separation in the soda-lime curves to the generation of tensile stresses at the crack tip caused by ion exchange of Na^+ for H^+ in liquid H_2O, a process which would not occur in a gas or in SiO_2 which does not contain alkali ions. A quantitative estimate of these stresses gave a reasonable prediction for the observed K_I shift.

Crack growth data obtained on single crystals of α quartz indicates that the regularity of its crystal structure compared to vitreous SiO_2 has little or no effect on the environmentally enhanced crack growth.

(2) Crack Growth and Electrical Failure in Ceramic Capacitors

The primary goal of this task during this past year was to establish a link between electrical failure in multilayer ceramic capacitors and the presence of cracks in the material. A second objective was to devise a test which could distinguish between "good" and "bad" capacitors.

Crack growth data was obtained by indentation procedures on discs of Z5U capacitor ceramic which had been especially prepared by AVX Corp. and which did not contain electrode layers. Because we had previously shown that there is a strong interaction between cracks and the metal electrode layers, leading to crack propagation resistances well above that for the ceramic alone, we felt it important to obtain independent data from the ceramic.

Leakage currents were measured for multilayer capacitors (at 50 V) with and without the presence of indentation induced cracks. Both indented and unindented capacitors were submitted to a short soak in a NaCl solution, cleaned and dried. Uncracked capacitors or those with small cracks, showed no change in leakage current, while those containing cracks

which were large enough to cut through two electrode layers, showed at least an order of magnitude increase in current. A test similar to this could be used to screen capacitors for cracks.

AVX supplied other specimens of Z5U capacitor ceramic which contained two metallized electrode layers, each ~60 μm below the surface. By monitoring the leakage current from these specimens after indentation and during loading in a test machine, it could be shown that the growth of the small cracks under mechanical stress lead to sizeable increases in leakage current. The time required for this increase to occur could be predicted from the crack growth parameters determined on the unelectroded material.

ENVIRONMENTALLY ENHANCED CRACK GROWTH IN SODA LIME GLASS

S.W. Freiman, G.S. White and E.R. Fuller, Jr.
Inorganic Materials Division
National Bureau of Standards
Washington, DC 20234

ABSTRACT

Crack growth data is presented for soda lime glass in various chemical environments. It is shown that the same environments which govern crack growth rates in vitreous silica also do so in soda lime glass. The slopes and positions of the soda lime crack growth curves are shown to differ from those in vitreous silica. It is hypothesized that the differences between the behavior of soda lime glass and silica are due to the effects of the modifier ions, Na^{+} and Ca^{+2}, on the reactivity of the Si-O bond or through changes in the elastic properties of the bridging network. It is shown that sodium ion exchange and silica dissolution may also be important to crack growth, particularly at low crack velocities.

INTRODUCTION

Michalske and Freiman have suggested a molecular model for crack growth in vitreous silica[1]. This model predicts that those molecules which can donate both electrons and protons, e.g. water (H_2O), ammonia (NH_3), hydrazine (N_2H_4), and formamide (CH_3NO), will undergo a chemical reaction with the highly strained Si-O bonds at a crack tip in silica, thereby promoting crack growth. This prediction was confirmed through experimental measurements of crack velocity as a function of the crack tip stress intensity factor, K_I. Tests conducted on vitreous silica in those aforementioned environments which were predicted to undergo a concerted reaction with a Si-O bond yielded log V-K_I curves which exhibited only one mechanism in the velocity range 10^{-9} to 10^{-3} m/s, confirming the fact that the bulk environment and not small quantities of water in the gas or liquid were responsible for the crack growth enhancement. In non-controlling environments, a typical Region 2 plateau occurred due to water diffusion rate limitations[2]. The purpose of the present study was to determine possible effects of modifier ions in the glass structure on the crack growth mechanism. Sodium is well known to produce non-bridging oxygen in the glass structure because of its tendency to ionically bind to the oxygen. A recent XPS study[3] indicates that Ca^{+2} exhibits behavior similar to Na^{+} in this respect.

EXPERIMENTAL PROCEDURE

Crack growth studies were conducted on a commercial soda lime silica glass (nominal composition (wt. %): SiO_2, 72; Na_2O, 14; CaO, 7.0; Al_2O_3, 2.0; MgO, 4.0; K_2O, 1.0). The glass was cut into double cantilever beam specimens, 50 x 12 x 1 mm^3, having a center groove of 1/2 the specimen thickness, annealed at 500 °C for 15 minutes, then

cooled at a rate of 2 °C/min. Aluminum arms were epoxied to the specimen after a crack had been introduced into it. Crack growth data was obtained by use of the applied moment technique[4] with dead weight loading. A 40X travelling microscope with a filar eyepiece was used to monitor crack motion. All tests other than those in water were conducted inside a plexiglas chamber which was purged with N_2 gas for 5-10 minutes prior to testing. In the case of ammonia, the gas was bled continuously into the chamber during the test. An N_2 overpressure was used for liquid environments to prevent H_2O pickup. No efforts were made to remove the H_2O prsent in the as-received environments.

RESULTS

Crack growth data for soda lime glass in water, ammonia, hydrazine, and formamide are plotted in Figure 1 as Log V versus K_I along with the water independent portion of the crack growth curve for soda lime glass in N_2 gas. The scatter in the data for each environment is typical of that obtained in the applied moment, double cantilever beam technique and represents a composite from three to five specimens. Slopes and intercepts determined from a linear least squares fit to segments of each of the curves are shown in Table I.

The crack growth curve for soda lime glass in water has the typical appearance reported by Wiederhorn and Bolz[5], namely a steeper portion at lower velocities, with a shallower portion at higher velocities. The curves for ammonia and hydrazine are essentially straight lines over the entire measured velocity range, while the data obtained in formamide exhibits the most complex shape, consisting of at least three portions. The slopes and positions of the curves for the four data sets are discussed in the next section. We should note here, however, that all

the environments found to enhance crack growth in vitreous silica also do so in soda lime glass, although, as discussed later, other factors can also be important.

$V\text{-}K_I$ behavior in environments which do not enhance crack growth is illustrated in Figure 2. The existence of a plateau in a $V\text{-}K_I$ curve indicates the presence of a minority constituent, e.g. water, in the environment which enhances crack growth rates above the levels which would be attained in the pure bulk environment[2]. As evidenced by the plateau in each of these curves, crack growth rates in the lower regime are controlled predominantly by the chemical activity of the water dissolved in these liquids, while the extremely steep slopes in the higher velocity regimes probably are indicative of a charge compensation mechanism of crack growth, which occurs in the absence of water.[2]

DISCUSSION OF RESULTS

The objective of this study was to determine how the presence of modifier ions, primarily Na^+, in a glass network affects the crack growth process of chemically enhanced Si-O bond rupture observed for vitreous silica. Figure 3 (a-d) compares the crack growth curves for soda lime glass with those for vitreous silica for each crack growth enhancing environment. Let us first consider the higher velocity portion of the curves, i.e. $> 10^{-6}$ m/s; this is the regime in which crack growth rates are governed by the reaction rate of the solid with the molecules of the bulk environment. There are three primary features to the $V\text{-}K_I$ curves in this regime. These features are (1) the shallower slope of the curve for soda lime glass in water than that for vitreous silica, (2) the fact that, excluding water, the $V\text{-}K_I$ curves for soda lime glass lie at larger values of K_I than those for vitreous silica and

(3) the trend to increasing slope of the $V-K_I$ curves for soda lime glass with a decreasing tendency of the environment to enhance crack growth, i.e. water < ammonia < hydrazine < formamide, as indicated by the progressive shift of the curves in each of these environments to higher K_I.

Crack Growth in Water

In comparing crack growth curves for soda lime glass and silica in water, it is important to remember that the aqueous solution at the crack tip will be quite different for the two glasses. Wiederhorn and Johnson[6] showed that the crack tip pH for vitreous silica in water is ≈5 while that for soda lime glass almost instantaneously reaches values of 10 to 12 due to ion exchange of Na^+ for H^+ (or H_3O^+). They also showed that the slope of the $V-K_I$ curve for soda lime glass approached (but did not equal) that for silica in very acidic solutions, e.g. 6N HCl. There are several possible reasons for the variation in slope with changes in pH. These include changes in the electronic structure of the crack tip Si-O bond due to the ion-exchange, the existence of tensile stresses arising because of the size difference between the Na^+ and the smaller H^+, or a change in the reacting species that controls crack growth i.e. H_2O to OH^- or vice-versa. At this time it is impossible to rule out the possibility that each of the three mechanisms described above contributes to the differences between the $V-K_I$ curves for soda lime glass and those for silica.

Position and Slope of Crack Growth Curves

In order to discuss either the shift in K_I between the soda lime and silica curves or the variation in $V-K_I$ slopes, it is necessary to make an assumption regarding the crack growth mechanism. We will assume that the reaction between the Si-O bridging bond and the environment molecule occurs spontaneously at a particular bond strain; that is, we will assume that the Si-O bond under consideration at the crack tip remains unaffected by the environment until the strain-aided "concerted" reaction takes place. While we cannot rule out hydrolysis of this bond prior to the "concerted" reaction, this assumption allows us to discuss the shifts in position and slope of the $V-K_I$ curves in a self consistent manner:

Note first that the $V-K_I$ curves for both vitreous silica and soda lime glass fall in the same order with respect to K_I for the four environments; i.e. water is the most effective crack growth agent and formamide the least for both glasses. However, as Fig. 3 (b-d) shows, the $V-K_I$ curves for soda lime glass lie at higher K_I values than those for vitreous silica in every environment. This shift suggests that the presence of Na^+ ionically bound to a non-bridging oxygen has a direct effect on the reactivity of the adjacent Si-O bridging bond. The decrease in reactivity in soda lime glass could result from changes in the non-bonding electron density on the oxygen coupled with a change in the silicon orbitals. Molecular orbital calculations have suggested that both of these effects will occur due to the presence of Na^+.[7]

However, a second possible reason for the shift in position involves our basic definition of K_I. According to linear elastic fracture mechanics, the stress intensity factor is defined as the slope of a stress versus $(\pi r)^{-1/2}$ curve, where r is the distance from the crack

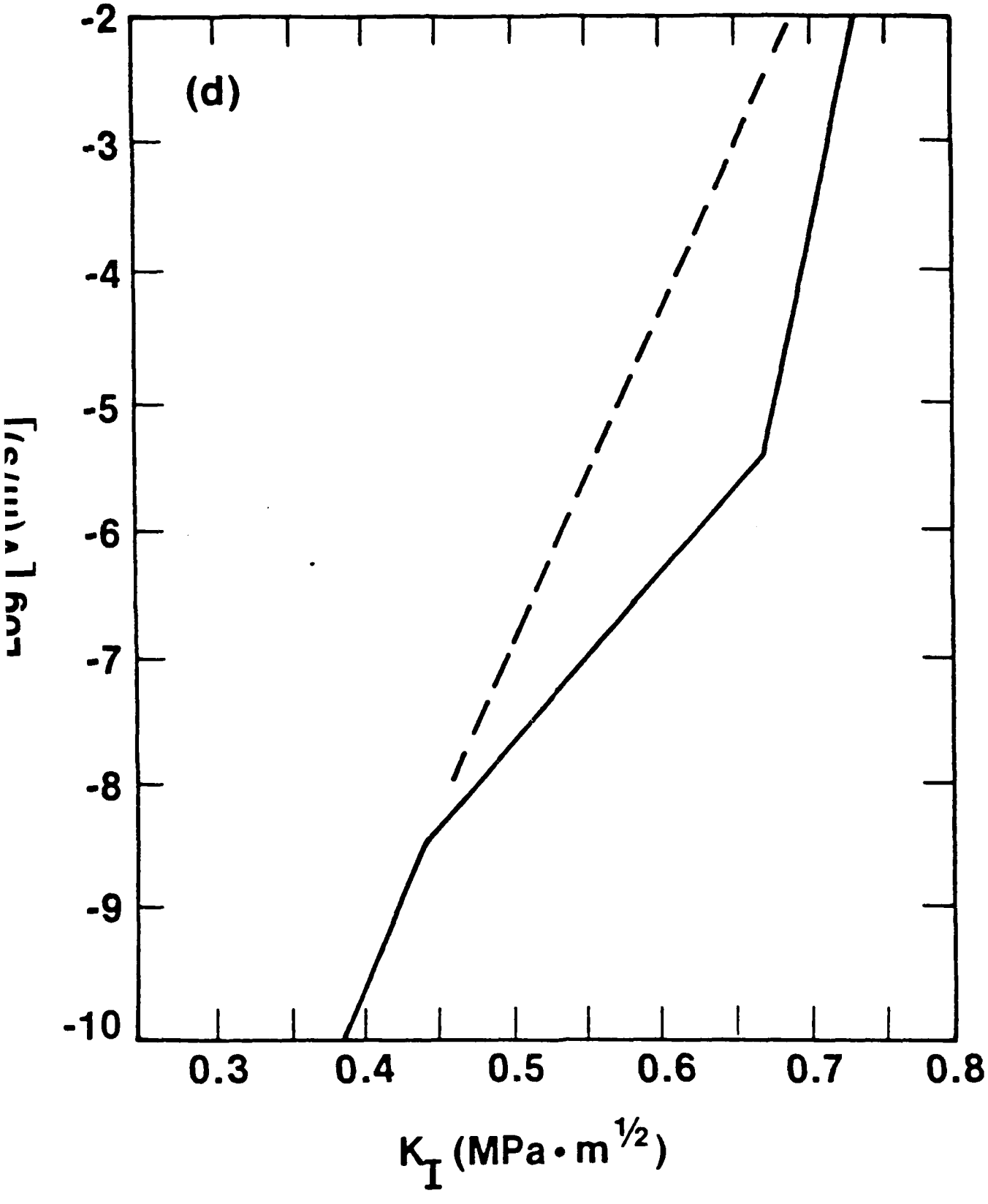
(d)
-2
-3
-4
-5
-6
-7
-8
-9
-10
0.3
0.4
0.5
0.6
0.7
0.8
K_I (MPa • $m^{1/2}$)
log [da/dN]

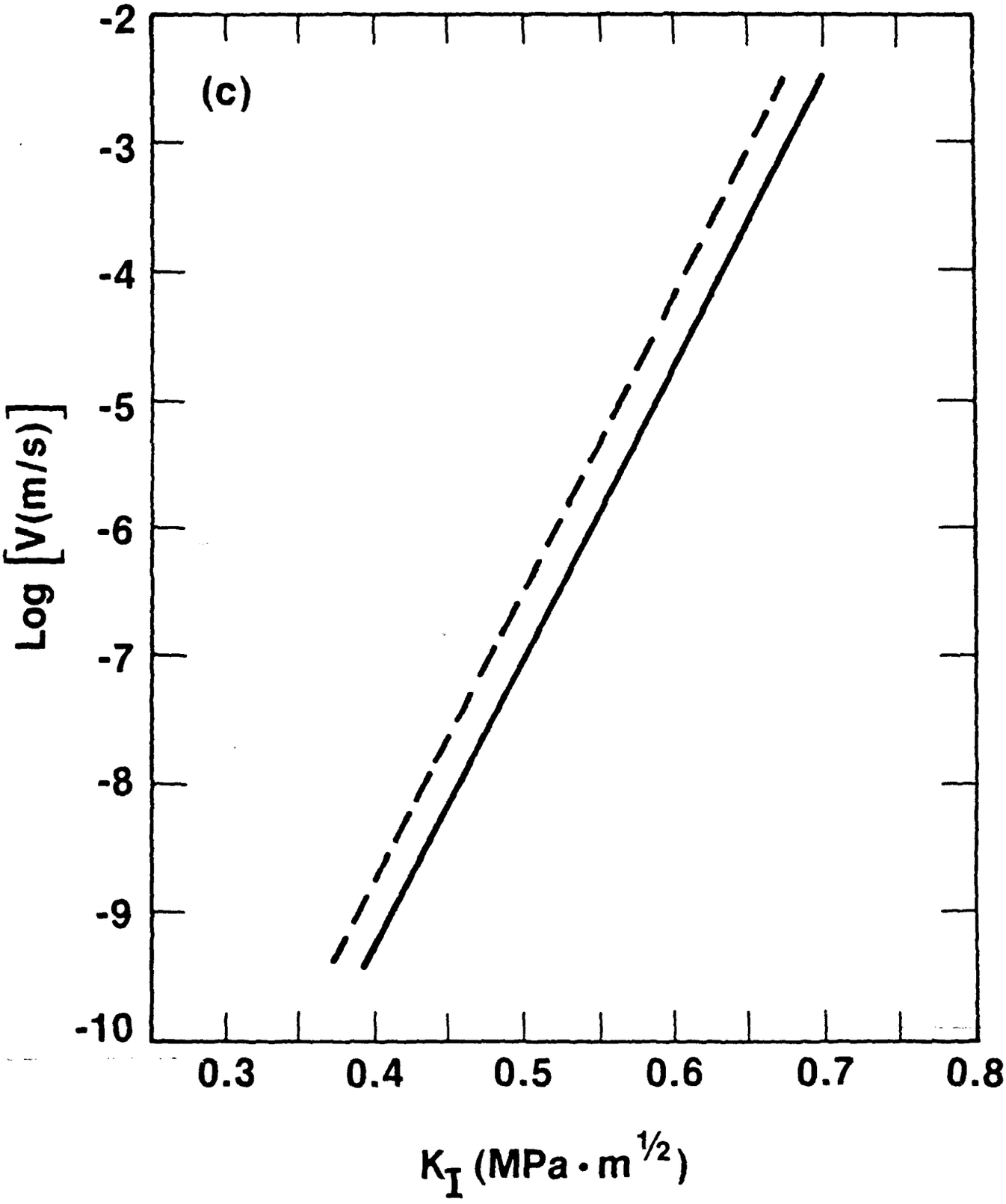

3.c.

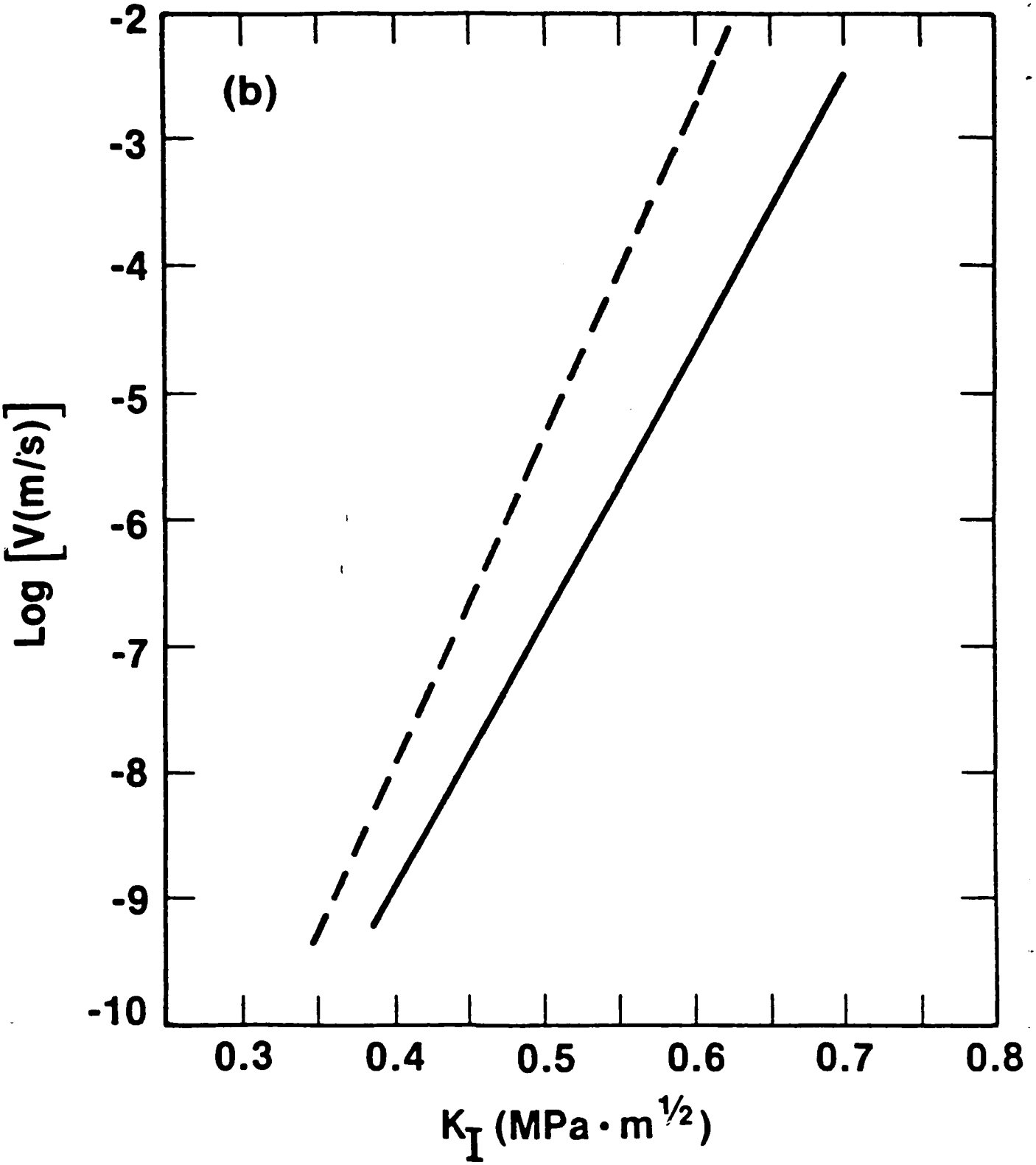
(b)
-2
-3
-4
-5
-6
-7
-8
-9
-10
Log [V(m/s)]
0.3
0.4
0.5
0.6
0.7
0.8
K_I (MPa · $m^{1/2}$)

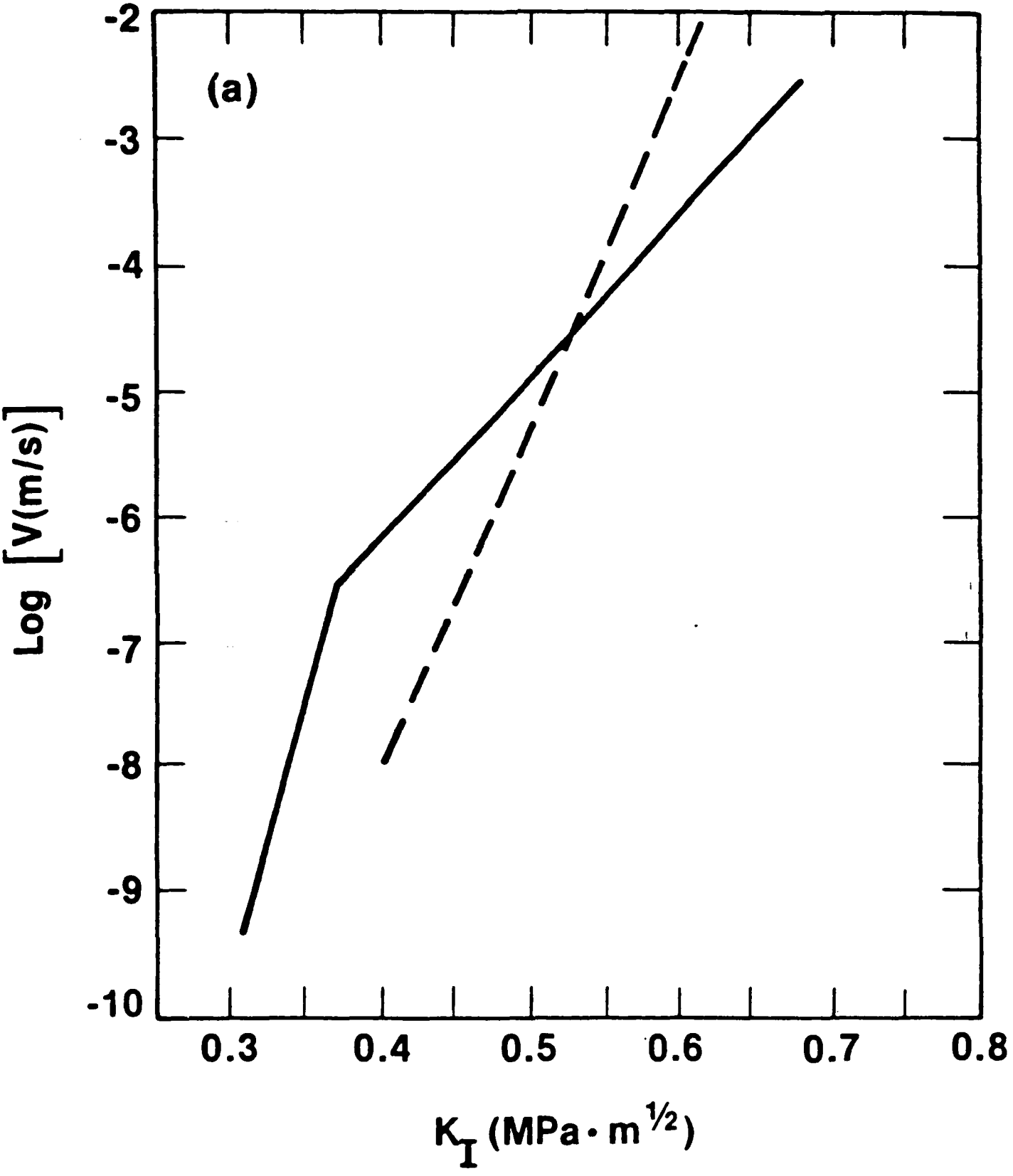
(a)
-2
-3
-4
-5
-6
-7
-8
-9
-10
Log [V(m/s)]
0.3
0.4
0.5
0.6
0.7
0.8
K_I (MPa · $m^{1/2}$)

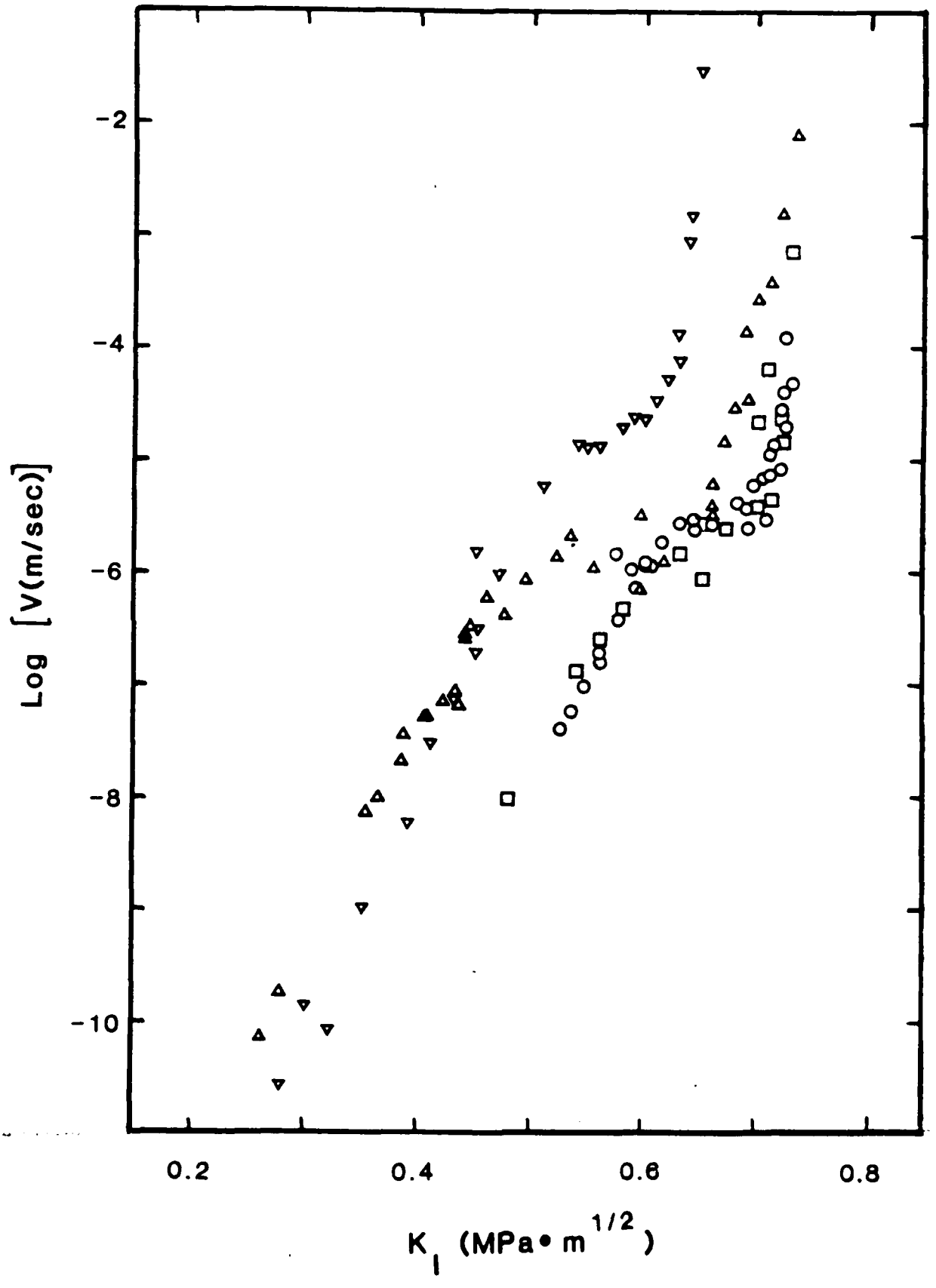

2.

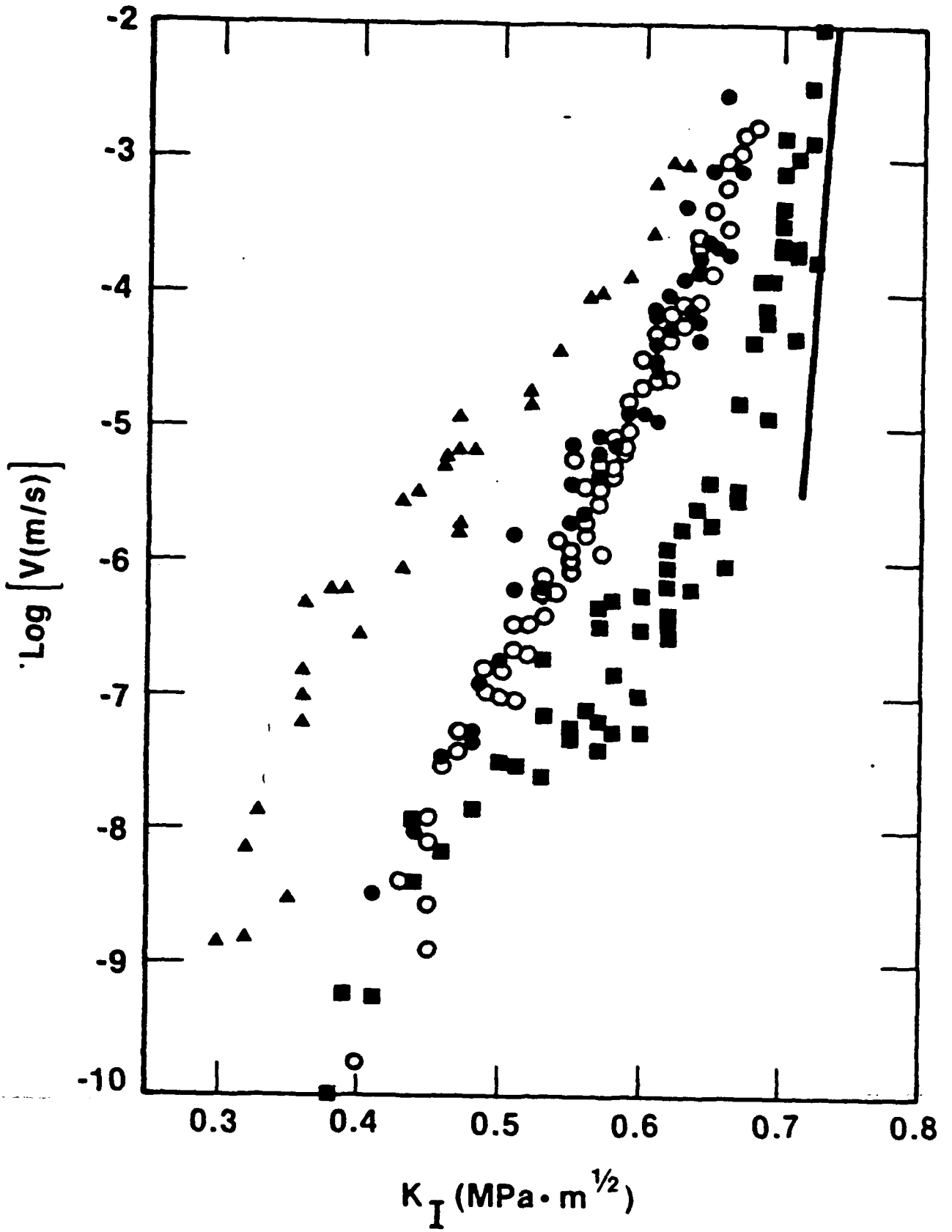

1.

Figure Captions

Fig. 1. Crack growth data for soda lime glass in water (▲), ammonia (●), hydrazine (○), and formamide (■). The solid line is the N_2 region III curve, shown for comparison.

Fig. 2. Crack growth curves for soda lime glass in nitrobenzene (△), acetonitrile (▽), diethyl ether (□), and pyridine (○). The plateaus in the curves indicate the presence of water impurities controlling crack growth in both region I and II.

Fig. 3. Comparison between crack growth behavior of vitreous silica (----) and soda lime glass (——) in (a) water, (b) ammonia, (c) hydrazine and (d) formamide.

Fig. 4. Crack growth data for soda lime glass in as-received formamide (■), 95% formamide-5% water (○), 90% formamide-10% water (▲) and 50% formamide-50% (●) water. The bent line is the least squares fit calculated for soda lime glass crack growth data in water. The straight line segment was drawn parallel to the upper water curve.

Table 1

Crack Growth Parameters for Soda Lime Glass in Environments which Promote Crack Propagation

Environment	[1] B	[1] Ln V_o	[2] N	[2] Log A	K_I Range
H_2O	105.1 ± 21.4	-53.6 ± 7.4	35.7 ± 7.5	9.03 ± 3.5	.25 - .38
	29.7 ± 1.7	-26.1 ± 0.88	15.9 ± .97	- .014 ± 3.1	.38 - .70
NH_3	49.9 ± 1.7	40.5 ± 0.97	27.4 ± .96	1.55 ± .23	all
Hydrazine	54.4 ± 1.0	-43.4 ± .6	29.8 ± .61	1.98 ± .15	all
Formamide	29.7	-31.1	15.9	-2.91	.45 - .66
	107.7 ± 10	-83.8 ± 7.6	74.9 ± 7.6	+7.9 ± 1.2	.66 - .75

(1) For $V = V_o \exp BK_I$

(2) For $V = AK_I^N$

6. S.M. Wiederhorn and H. Johnson, "Effect of Electrolyte pH on Crack Propagation in Glass," J. Am. Ceram. Soc. 56 [4] 192-97 (1973).

7. B.H.W.S. DeJong and G.E. Brown, Jr., "Polymerization of Silicate and Aluminate Tetrahedra in Glasses, Melts and Aqueous Solutions-II. The Network Modifying Effects of Mg^{2+}, K^{+}, Na^{+}, Li^{+}, OH^{-}, F^{-}, Cl^{-}, H_2O, CO_2 and H_3O^{+} on Silicate Polymers," Geochim. and Cosmochim. Acta, 44, 1627-42 (1980).

8. E.R. Fuller, Jr., G.S. White and S.W. Freiman, "Molecular Model for Stress-Assisted, Environmental Fracture of Silicate Glasses" To be published.

9. G. Kortvem and H. von Biedersee, Dampf/Flussigkeit-Gleichgewichte (Siedediagramme) Binarer Systeme Hoher Relativer Fluchtigkeit, Chem.-Ing.-Tech. 42, 552- (1970).

10. T.A. Michalske, "The Stress Corrosion Limit: Its Measurement and Implications," in Fracture Mechanics of Ceramics 5 (R.C. Bradt, A.G. Evans, D.P.H. Hasselman and F.F. Lane, eds.) Plenum Press, New York (1981), pp 277-290.

successful environments must be both electron and proton donors. The primary conclusion that we draw from this work is that crack growth rates in soda lime glass are governed by the stress enhanced rate of reaction between a crack tip Si-O bond and the environment. That is, the modifier ions, Na^+, Ca^+, etc., do not participate directly in the fracture process. However, the data suggest that the presence of these ionic species may change the reactivity of the adjacent Si-O bridging bond as well as affect the elastic properties of the network bond. A transition from crack growth controlled by a stress enhanced reaction with the bulk environment to one governed by reaction with dissolved water was observed. Ion exchange/dissolution mechanisms at the crack tip appeared to come into play at velocities below $\approx 10^{-8}$ m/sec.

ACKNOWLEDGEMENTS

The support of this work by the Office of Naval Research is gratefully acknowledged. The authors would also like to thank S. M. Wiederhorn and D. C. Greenspan for their helpful discussions.

REFERENCES

1. T.A. Michalske and S.W. Freiman, "A Molecular Mechanism for Stress Corrosion in Vitreous Silica," J. Am. Ceram. Soc. 66 (4) 284-288 (1983).

2. S.M. Wiederhorn, S.W. Freiman, E.R. Fuller, Jr., and C.J. Simmons "Effects of Water and Other Dielectrics on Crack Growth", J. Mat. Sci. 17, 3460-78 (1982).

3. B.W. Veal, D.J. Lam, A.P. Pavlikas, and W.Y. Ching, "XPS Study of CaO in Sodium Silicate Glass", J. Noncryst. Solids, 49 309-20 (1982).

4. S.W. Freiman, D.R. Mulville, and P.W. Mast, "Crack Propagation Studies in Brittle Materials," J. Mater. Sci. 8, 1527-33 (1973).

5. S.M. Wiederhorn and L.H. Bolz, "Stress Corrosion and Static Fatigue of Glass," J. Am. Ceram. Soc. 53 [10] 543-48 (1970).

Multislope Crack Growth Curve

Let us return to the complex shape of the log V-K_I curve for soda lime glass in "pure" formamide (Figure 4). If we make some fairly straight-forward assumptions regarding possible mechanisms, we can fit this multiregion curve with a series of straight line segments, each of which represents a different controlling reaction.

(A) At velocities > 10^{-6} m/sec, as discussed earlier, we assume that the controlling mechanism is the stress enhanced reaction between formamide and the Si-O bond at the crack tip. Clearly, the distinction between the lower end of this region and that due to water dissolved in the formamide is somewhat arbitrary, imposing an uncertainty in the slope of the curve.

(B) This line was drawn parallel to the curve for soda lime glass in water for the reasons discussed previously.

(C) The steeper, lower velocity of the V-K_I curve in formamide is nearly identical to that which appears in the curve for water. Michalske[10] convincingly demonstrated that this segment of the curve for soda lime glass in water leads to a crack growth limit. Whether the steeper curve in formamide also leads to crack arrest is not known at present. However, the similarity of this curve to the same portion in water suggests that in this region, the crack growth rate is controlled by the same mechanism.

SUMMARY AND CONCLUSIONS

It has been shown that those environments which enhance crack growth in vitreous silica also do so in soda lime glass. Similarly, environments which fail to enhance crack growth in vitreous silica are also ineffective in causing crack growth in soda lime glass. The

curve represents the same mechanism which occurs between formamide and the glass throughout the entire curve in vitreous silica. Based upon only the existing data, we cannot, however, rule out the possibility that a charge compensation mechanism as described by Wiederhorn et al.[2] rather than a true chemical reaction is occurring. We suggest that the lower curves represent crack growth controlled by a mechanism of stress induced reaction between water and the Si-O bond. Based upon its ability to donate its lone pair electrons, one would expect water to be a more active species for the stress enhanced crack tip reaction than formamide, so the trend to increasing velocity with increasing water content is to be expected. The lack of any water controlled region in the log V-K_I curve obtained for vitreous silica in "pure" formamide can be understood by the observation that the slopes of the curves in formamide and water are the same for silica and, therefore, the water controlled region would be virtually indistinguishable from the rest of the formamide curve.

One interesting point in soda lime glass is that crack growth data for a 50% water-50% formamide solution overlap the data for pure water. Solution data for a methyl formamide-water system[9] showed that at a mole fraction of 0.5 the activity of the water was ~0.95, clearly showing that activity can be much different from concentration. Since a model for chemically enhanced crack growth based on reaction kinetics[2] shows that crack velocity at any K_I should be directly dependent upon the activity of the reactive constituent (i.e. water, in this case), the data for the 50% formamide-50% water so'ution suggests that the activity of the water is ≈1.

to the slope of the bond stress strain curve, consistent with the increased slope of the $V-K_I$ curve for formamide compared to that for ammonia and hydrazine.

Water Effects in Bulk Liquids

One of the conditions specified with regard to whether a particular environment controls crack growth is that crack growth rates must be enhanced relative to those which would be produced by the activity of water in the gas or liquid. The linear curves for soda lime glass tested in ammonia and hydrazine have allowed us to eliminate the possibility that the water in each of these controls crack growth. The more complex curve in formamide (Fig. 3d) presents a different story. The middle portion of this $V-K_I$ curve is parallel to that in water and therefore suggests that crack propagation in this $V-K_I$ regime is controlled by the water in the formamide (~0.035% by weight). Crack growth data taken in solutions of 95-5%, 90-10%, and 50-50% solutions of formamide-water (Figure 4) bear out the hypothesis that water is the controlling species in this regime. Each of these formamide-water curves contains a region having approximately the same shape as the middle portion of that taken in "pure" formamide; each of these regions merges into the upper portion of the formamide-water curve. Since there is no Region 2 plateau in the "pure" formamide, i.e. no K_I independent region indicative of a transport controlled regime, water must still be reacting in small amounts at the crack tip at velocities corresponding to the junction of the two regions of the curve. We interpret this behavior to mean that the upper curve in formamide is due to a stress induced chemical reaction between formamide and the Si-O bond at the crack tip, and suggest that this steeper portion of the crack growth

tip measured into the unfractured solid. However, we know that in real materials, the bonds very near the crack tip are strained beyond their elastic limit, thereby placing an upper limit on the crack tip stress (or strain). The presence of non-bridging oxygen atoms introduced by the Na^+ may make the glass structure more compliant, thereby enlarging the zone of non-linear elastic behavior. Any increase in this zone size will produce a decrease in the actual crack tip stress which is the true reaction rate governing parameter. In other words, even though a higher K_I is required to produce the same reaction rate, the actual crack tip stress may be unchanged.

In addition to the shift in curve positions, we must also explain the increasing slopes of the $V-K_I$ curves for soda lime glass in going from water to formamide compared to the unchanging slopes for vitreous SiO_2 over this same range of environments. First, we have noted earlier that, in water, ion exchange of the soda lime glass would produce an extremely alkaline solution at the crack tip. Wiederhorn and Johnson,[6] showed that the slopes of $V-K_I$ curves for soda lime glass in alkaline solutions are less than those in acidic solutions, such as exist at a crack tip in vitreous silica. Also, it is possible that, besides affecting the reactivity of the bridging Si-O bond and the pH of the environment, the presence of Na^+ or Ca^{+2} in the glass structure causes the stress-strain relationship of the bond to be nonlinear. We have noted that the reactivity of the soda lime glass is reduced relative to the vitreous silica, resulting in a shift to higher K_I value. A lower bond reactivity suggests that a higher bond strain would be needed to produce the crack tip reaction, thereby possibly shifting the reactions to a nonlinear portion of the stress-strain curve. A recently developed model[8] predicts that the slope of a $V-K_I$ curve will be inversely related

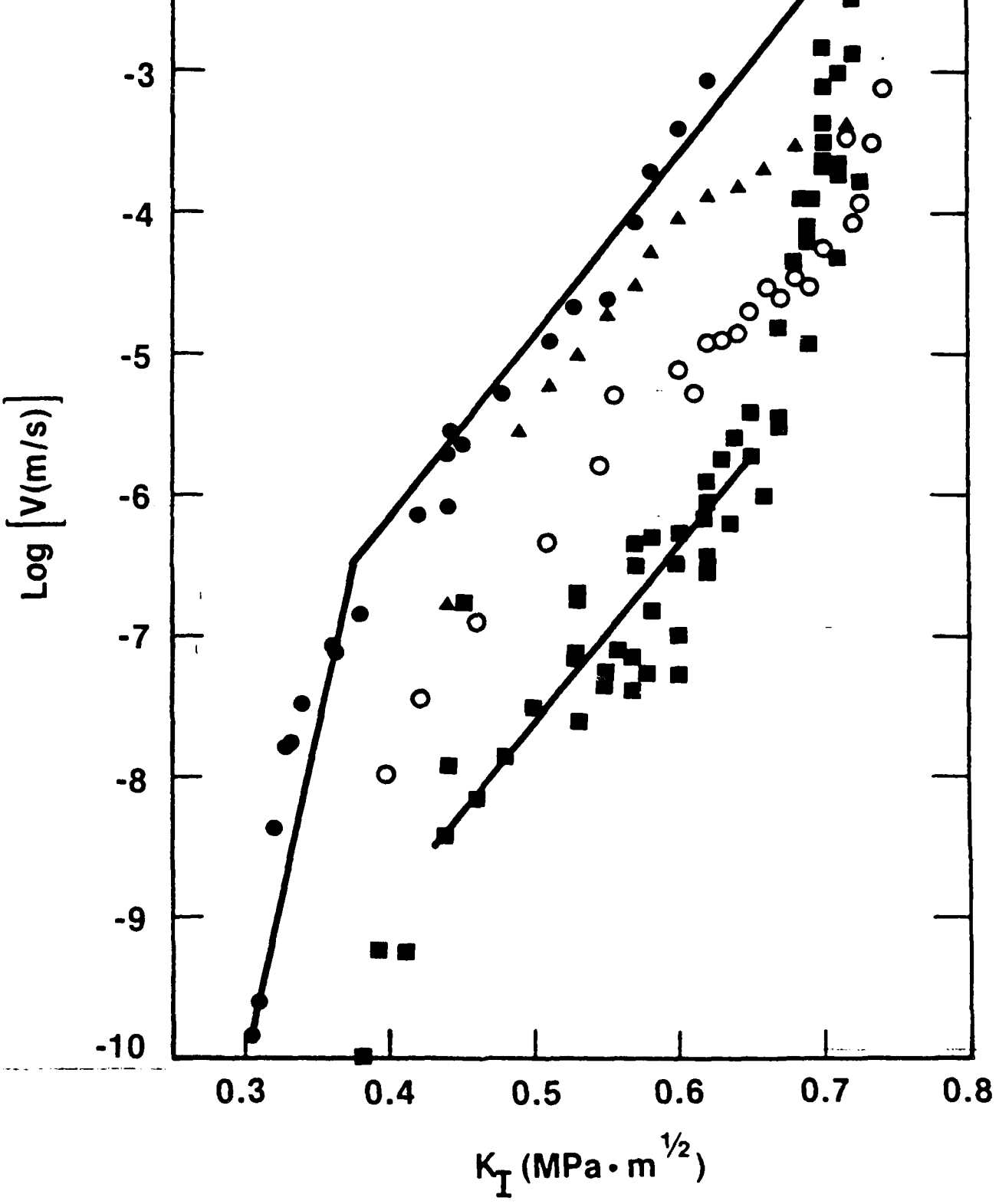
-2
-3
-4
-5
-6
-7
-8
-9
-10
Log [V(m/s)]
0.3
0.4
0.5
0.6
0.7
0.8
K_I (MPa · $m^{1/2}$)

RELATIONSHIP BETWEEN CORROSION AND CRACK GROWTH IN 33% Na_2O-67% SiO_2 AND 33% Li_2O-67% SiO_2 GLASSES

G.S. White, D.C. Greenspan[1]/ and S.W. Freiman
Inorganic Materials Division
National Bureau of Standards
Washington, DC 20234

INTRODUCTION

Recent papers have described effects of specific chemical environments on crack growth rates in vitreous SiO_2[1] and soda lime silica glass.[2] Michalske and Freiman proposed a model for the crack growth process which leads to specifications for the types of molecules which will participate in the crack tip reaction. In the case of the soda lime glass, it was also shown that dissolution/ion exchange processes at the crack tip due to either the bulk liquid or to small amounts of water in the liquid could modify the crack velocity (V) vs stress intensity (K_I) curves.

The objective of this work was to examine the relationship between crack growth and glass corrosion in more detail. The binary 33% Na_2O-67% SiO_2 (33N) and 33% Li_2O-67% SiO_2 (33L) glasses were chosen for this investigation because (1) they are relatively simple systems, (2) both SiO_2 dissolution and alkali-ion exchange should be enhanced over that in soda lime glass, and (3) fairly extensive data exists on the corrosion behavior of these glasses.[3-6] We will demonstrate, using infrared spectroscopy and atomic absorption spectroscopy, that "corrosion" and crack growth in these glasses are related. We will also show that at low velocities, dissolution/ion exchange dominates, while at higher velocities, crack growth is governed by the same crack tip reactions which govern in vitreous silica.

---

[1]/ Now at Accumetrix Corp., Arlington, VA

EXPERIMENTAL PROCEDURE

Glass Melting and Specimen Preparation

The 33N and 33L glasses employed in this study were melted in platinum crucibles at 1350°C and 1440°C respectively; the glasses were stirred during melting. The glasses were cast into blocks and annealed at 500 and 420°C, then cooled at 2°C/min until the temperature fell below the glass transition point, at which time the power to the furnace was turned off, and the glasses allowed to furnace cool. Double cantilever beam specimens (50 x 13 x 2 mm^3) were cut from the glass blocks. A groove 1 mm deep was placed down the center of each specimen to guide the crack. The specimens were then reannealed at 420°C. Because of their high rate of dissolution, even in air, all 33N specimens were stored in a dessicator prior to use. Pieces of the glasses 8 x 8 mm, were also cut from the blocks for use in the infrared spectroscopy and atomic absorption spectroscopy studies. These were polished through 600 grit SiC paper and stored in a dessicator.

Crack Growth

Cracks were introduced into the double cantilever beam specimens by pressing a pointed object into an end on the side opposite the groove. The applied moment technique[7] was used by hanging dead weight loads from aluminum arms epoxied to the specimen. Crack extension was monitored with an optical microscope containing a filar eyepiece. Tests in non-aqueous liquid environments were conducted inside a chamber which was purged with N_2 gas prior to the introduction of the liquid. Tests in continually flowing NH_3 gas were also conducted in this chamber.

Corrosion Analysis

The corrosion behavior of both 33N and 33L glasses was studied following techniques developed by Sanders et al.,[3-5] and D.E. Clark et al.[6] Samples polished to 600 grit were stored in a desiccator before being tested in either aqueous or non-aqueous environments. Prior to exposure, the samples were lightly abraded with 600 grit SiC paper to remove any surface films that may have formed due to atmospheric reactions. All samples were suspended in Teflon corrosion cells at room temperature for times ranging from 30 seconds to 15 minutes in each environment. The environments used in this study included distilled water, hydrazine, formamide, acetonitrile and methyl alcohol. The surface area/volume ratio was maintained throughout this study at 0.05 cm^{-1}.

Infrared reflection spectroscopy (IRRS) was performed in an N_2 atmosphere immediately after removal of the samples from the various solutions. The samples were scanned from 1500 cm^{-1} to 400 cm^{-1} utilizing an FTIR[2]/ instrument with a specular reflectance attachment at an incidence angle of 30°. Each spectra represents the average of 128 scans. The gain of the infrared signal was adjusted to maintain a reflection signal of at least 25% of the incident intensity for a freshly abraded control sample.

Ion analysis of the corrosion solutions was performed using a dual beam Atomic Absorption Spectrophotometer.[3]/ Na and Li analyses were determined by atomic emission using standards of the various non-aqueous

---

[2]/ Nicolet 60-SX, Nicolet Instrument Co.

[3]/ Model 460 Atomic Absorption Spectrophotomer Corp., Perkin Elmer Corp., Norwalk, CT

solutions used in the study. Si content was determined using a graphite atomization furnace.[4]/ Heating rates, atomization temperatures, and times were adjusted to account for the volatility of the various organic liquids. At least 5 separate determinations were averaged for each data point.

RESULTS

The results of this study will be presented in three parts, crack growth, infrared spectroscopy, and atomic absorption spectroscopy. The interrelation between these sections will be shown in the Discussion section.

Crack Growth

Log V-K_I for the 33N and 33L glasses tested in water (H_2O), ammonia (NH_3 gas), hydrazine (N_2H_4), and formamide (CH_3NO) are presented in Figures 1 and 2 respectively. The data for each environment was taken on 2 to 5 specimens. These environments were chosen because they possess necessary requirements i.e., electron and proton donating capability, to produce chemically enhanced crack growth in both vitreous SiO_2 and soda lime glass. The curves are considerably more complex than those obtained in vitreous SiO_2.[1] Notice, however, that except for the 33N glass at low velocities, there is no plateau indicative of a transport controlled crack growth regime. This low velocity plateau in the 33N glass previously has been interpreted as being related to the high rate of SiO_2 removal in this glass.[8] The absence of obvious transport controlled regimes suggests that each non-aqueous environment, rather than the known small amount of water

---

[4]/ Model 46A-2100 Graphite Furnace, Perkin Elmer Corp., Norwalk, CT

dissolved in it, controls crack growth rates in the higher velocity regime. However, we will show in the next section that the shallower slope curves at lower velocities represent a regime in which water in the liquid is the controlling factor. The absence of any diffusion controlled transition between the upper and lower velocity regimes indicates that water is still at the crack tip at the transition velocity. This transition simply reports the point at which the curve for the stress induced reaction with the nonaqueous liquid crosses that for the activity of water in the liquid. Crack growth curves for 33N and 33L taken in environments such as acetonitrile (CH_3CN), which can donate electrons but not protons, showed typical crack velocity plateaus (Figure 3) which occur when water transport to the crack tip becomes the rate controlling step[9] and which occur at the same velocity in the binary glasses as in SiO_2[1] and soda lime glass.[2]

The slopes and intercepts of the best fit straight lines to log V-K_I curves for both 33N and 33L glasses in all of the environments are listed in Table I and are charted for easier comparison in Figure 4. Where it was obvious that the curve consisted of more than one section, the parameters are given for each portion, although it should be pointed out that a determination of the junction of the curves was, at times, difficult. Based on previous evidence[1,2], the highest velocity portion of the curves is governed by the reaction rate of the bulk environment with the glass the lower portions will be shown to be controlled by ion exchange/dissolution processes due to water in the environment. The slope of the high velocity segments for 33L glass in H_2O ($N = 11.3$) is significantly shallower than those for either soda lime (($N = 16$) or 33N glass ($N = 21$). In fact, the value of N in H_2O for 33L is the lowest yet

observed for any glass or ceramic in a reaction rate controlled regime. By comparison, N values for 33N glass in all environments are significantly higher than the other two glasses. The differences in slopes for these glasses will be discussed in terms of specific reaction mechanisms in a later section.

IR Spectroscopy

The general spectra obtained for 33N and 33L glasses in the wavelength range of interest are shown in Figure 5 for as-ground surfaces and after immersion in H_2O. The two peaks of primary interest in both glasses, at 1060 cm^{-1} and 950 cm^{-1} have been assigned to Si-bridging oxygen (Si-O-Si) stretching vibrations and Si-non-bridging oxygen (Si-O-R) stretching vibrations respectively.[4,5] In the 33N glass notice that after a 5 min immersion in distilled water there is a sharpening of the Si-O-Si peak, and a shift to lower wavenumbers of the Si-O-Na peak. This behavior has been interpreted as due to ion exchange between H^+ (or H_3O^+) in the H_2O with Na^+ in the glass leaving a Na^+ depleted surface, coupled with SiO_2 removal from this surface.[5] Similar behavior is observed in the 33L glass. At longer reaction times, less change has occurred in the 33L glass spectrum however, because of the lower rates of ion exchange in this glass.[5,6] It is significant that a 5 min. immersion in hydrazine produces a sharp reduction in reflected IR intensity but little peak shift. We interpret this to mean that hydrazine produces more SiO_2 dissolution from the 33L glass, leading to surface roughening. Hydrazine produces the same effect in 33N glass. This difference in water and hydrazine will be reinforced by the atomic absorption data to be reported in the next section.

Quantitative shifts in the Si-O-Si and Si-O-Na peaks for 33N glass in a number of environments are shown in Figure 6. Notice that only those environments cause shifts which are known to enhance crack growth[5] (the apparent $\Delta 2cm^{-1}$ shift of acetonitrile is within the scatter of the system). All other environments produce no change in the spectra despite the fact that they are known to absorb physically on glass surfaces.[9,10] There is no evidence that the water dissolved in environments such as butanol or heptane produces any significant reaction on the glass surface.

Atomic Absorption Spectroscopy

Results obtained by atomic absorption spectroscopy of the solutions produced by immersion of the 33N and 33L glasses in the various liquids as a function of time compliment the IR spectroscopy data. The atomic absorption data were measured on ppm and converted to mole/liter.The concentration of Si and alkali in solution for the 33N and 33L glasses in the different environments are plotted mole/l as a function of immersion time in Figure 7. The following points are noted:

(1) Both the Si and alkali concentrations increase with time in solution.

(2) As would be predicted, the alkali ion exchange and SiO_2 dissolution rates for 33N glass are greater than those for 33L.

(3) Water is the most effect medium for removing alkali ions from both glasses, but hydrazine dissolves SiO_2 more readily, in agreement with the IR data given in the previous section.

---

[5] A similar observation has been made by Michalske and Bunker[13] for vitreous silica. Michalske also has obtained crack growth data for vitreous silica in methanol.

(4) Small quantities of alkali and SiO_2 were found to dissolve in formamide, but no dissolution occurred in acetonitrile within the detectability of the technique.

Examining the ratio of the alkali to Si removed from the glasses (Figure 8), we see that in H_2O, this ratio increases with time for both the 33N and 33L glasses, but remains constant in hydrazine. These results suggest that the ion exchange rate in these glasses has not reached steady state after 1 hour in water, but that simultaneous removal of alkali and Si is occurring after very short immersion times in hydrazine. However, the magnitude of the alkali/Si ratio being removed implies that the primary corrosion mechanism in both hydrazine and water is alkali ion exchange.

DISCUSSION OF RESULTS

As noted earlier, an examination of the slopes of the $V-K_I$ curves for the 33L and 33N glasses compared to those for soda lime glass and vitreous SiO_2 in the regime in which chemical reactions with the bulk environment control crack growth rates leads to two primary conclusions: (1) slopes in water are significantly lower for 33L, soda lime, and 33N than for vitreous SiO_2 and (2) slopes for 33N glass are consistently higher than those for 33L and deviate to progressively larger values as the reactivity of the environment decreases. With regard to the first point, the alkali containing glasses are capable of ion exchange with H^+ (or H_3O^+) from the water while SiO_2 is not. This ion exchange significantly increases the pH of the crack tip solution. Based on the work of Wiederhorn and Johnson,[11] pH values of ≥12 rapidly should be achieved. Wiederhorn and Johnson[12]

also showed that the slope of log V-K_I curves in high pH solutions are significantly smaller than those in acidic environments. There may also be effects of ion exchange upon the crack tip Si-O bond being ruptured.

The progressively increasing difference in slope between 33N and 33L glasses for environments of decreasing reactivity (Figure 4) presents a more complex problem. One possible explanation for this behavior is that a sodium atom bonded to a non-bridging oxygen atom in the glass has a much stronger effect on the reactivity of the adjacent bridging Si-O bond than does lithium. It would be likely that this difference in reactivity would in turn be reflected in a difference in the stress dependence of the reaction rate, which in turn is directly proportional to the slope of the V-K_I curve for the material.

Another possible explanation is that the different glasses transmit the externally applied forces to the crack tip in different degrees. It has been shown that based on the chemical rate theory, the rate of crack growth can be expressed as:[13]

$$V = V_o \exp(-E^* + bK_I/kT) \qquad (1)$$

where k is Boltzman's constant, T is temperature, E^* is the stress independent activation energy for the crack tip reaction, V_o is a constant and b, the slope of the ln V-K_I curve, is given by:

$$b = \Delta V^*/d^{1/2} \qquad (2)$$

ΔV^* is the activation volume for the reaction and d is a parameter with units of length. d can be thought of as the factor that transforms the stress intensity factor at the crack into the force on the crack tip bond. We can see, therefore, that the slope of a crack growth curve can change due either to a variation in the activation volume, i.e. a different stress dependence or due to a change in the mechanical response of the material to stress, which directly affects the strain on the crack tip bonds. At present, we do not feel that there is sufficient data to decide between these possibilities.

Let us now examine the possible relationship between crack growth and corrosion in these glasses. One indication that such a relationship exists is the fact that, with the environments investigated to date, only those environments which produce a significant material removal from the 33L and 33N glasses have been found to cause crack growth. Similarly, environments which were observed to cause shifts in the IR spectra enhanced crack growth in the binary glasses, while environments which failed to cause such shifts also failed to enhance crack growth. Although these observations do not constitute proof, they suggest the possibility that similar processes might be occurring on the surface of the binary glasses as occur at the crack tip during fracture. Michalske and Bunker[14] have made a similar suggestion based upon the correlation they found between environments causing enhanced crack growth and environments which bonded to the surface of the de-hydroxylated vitreous silica. It is known that a distribution of bond angles exists in the glasses and that the various angles require different energies to form. It is not unreasonable to expect the more highly strained bonds to react with the environment similarly to the strained bonds at the crack tip.

Finally, looking back at the crack growth curves in Figures 1 and 2, we see that the lower velocity portions of the 33N curves in hydrazine and formamide are essentially parallel to the 33N curve in H_2O, the same being true of the 33L glass. This behavior suggests that at these crack growth rates, the H_2O in the hydrazine (~5%) and formamide (~.035%) controls crack growth. To further investigate this possibility, crack growth rates in the 33L glass were obtained in a formamide - 10% H_2O solution. The shift in the lower portion of the formamide curve (Figure 9) is consistent with the concept that the H_2O in solution is the governing factor. At the higher velocities, the formamide and formamide-10% H_2O curves merge indicating control by formamide. This type of shift is in agreement with similar data obtained on soda lime glass in the same environments.[2]

CONCLUSIONS

The combination of AA, FTIR spectroscopy and crack growth data in the binary alkali glasses studied lead to three conclusions:

1. Those environments that enhance crack growth in vitreous SiO_2 also do so in alkali silicate glasses, and vice versa.

2. Chemically enhanced crack growth in binary alkali-silicate glasses consists of two regimes:

   a. Higher velocities - stress assisted concerted reaction controls growth rate.

   b. Lower velocities - ion exchange/dissolution dominates.

3. Those environments, e.g. water, hydrazine, which produce the largest changes in the I.R. spectra and which dissolve the most material, show the largest effect on crack growth in alkali-silicate glasses.

ACKNOWLEDGEMENTS

We would like to thank David Cronin and Dale Kaufman for making the ghlasses used in this work. This work was performed under a contract from the Office of Naval Research. Their support is gratefully acknowledged.

REFERENCES

1. T.A. Michalske and S.W. Freiman, "A Molecular Mechanism for Stress Corrosion in Vitreous Silica," J. Am. Ceram. Soc. 66 [4] 284-288 (1983).

2. S.W. Freiman, G.S. White and E.R. Fuller, Jr., "Environmentally Enhanced Crack Growth in Soda Lime Silica Glass, submitted to J. Am. Ceram. Soc.

3. D.M. Sanders, W.B Pearson and L.L. Hench, "New Method for Studying Glass Corrosion Kinetics," Appl. Spectroscopy, 26 [5] 530-536 (1972).

4. D.M. Sanders and L. L. Hench, "Mechanisms of Glass Corrosion," J. Am. Ceram. Soc. 56 [7] 373-77 (1973).

5. D.M. Sanders and L.L. Hench, "Environmental Effects on Glass Corrosion Kinetics," Amer. Ceram. Soc. Bull. 52 [9].(1973).

6. D.E. Clark, M.F. Dilmore, E.C. Ethridge and L.L. Hench, "Aqueous Corrosion of Soda-Silica and Soda-Lime-Silica Glass," J. Am. Ceram. Soc. 59 [1-2]] 62-65 (1976).

7. S.W. Freiman, D.R. Mulville and P.W. Mast, "Crack Propagation Studies in Brittle Materials," J. Mater. Sci. 8, 1527-33 (1973).

8. C.J. Simmons and S.W. Freiman, "Effect of Corrosion Processes on Subcritical Crack Growth in Glass," J. Am. Ceram. Soc. 64 [11] 683-86 (1981).

9. R.S. McDonald, "Surface Functionality of Amorphous Silica by Infrared Spectroscopy," J. Phys. Chem. 62, 1168-1178 (1958).

10. M.L. Hair, Infrared Spectroscopy in Surface Chemistry, Marcel Dekker, N.Y. (1967).

11. S.M. Wiederhorn and H. Johnson, "Effect of Electrolyte pH on Crack Propagation in Glass," J. Am. Ceram. Soc. 56]4] 192-97 (1973).

12. S.M. Wiederhorn and H. Johnson, "Tinfluence of Sodium-Hydrogen Ion Exchange on Crack Propagation in Soda-Lime Silicate Glass," J. Am. Ceram. Soc. 56 [2] 108-09 (1973).

13. S.M. Wiederhorn, S.W. Freiman, E.R. Fuller, Jr. and C.J. Simmons, "Effects of WAter and Other Dielectrics on Crack Growth," J. Mater. Sci. 17, 3460-78 (1982).

14. T.A. Michalske and B.C. Bunker," A Fracture Model Based on Strained Silicate Structures," Accepted for publication by J. Appl. Phys.

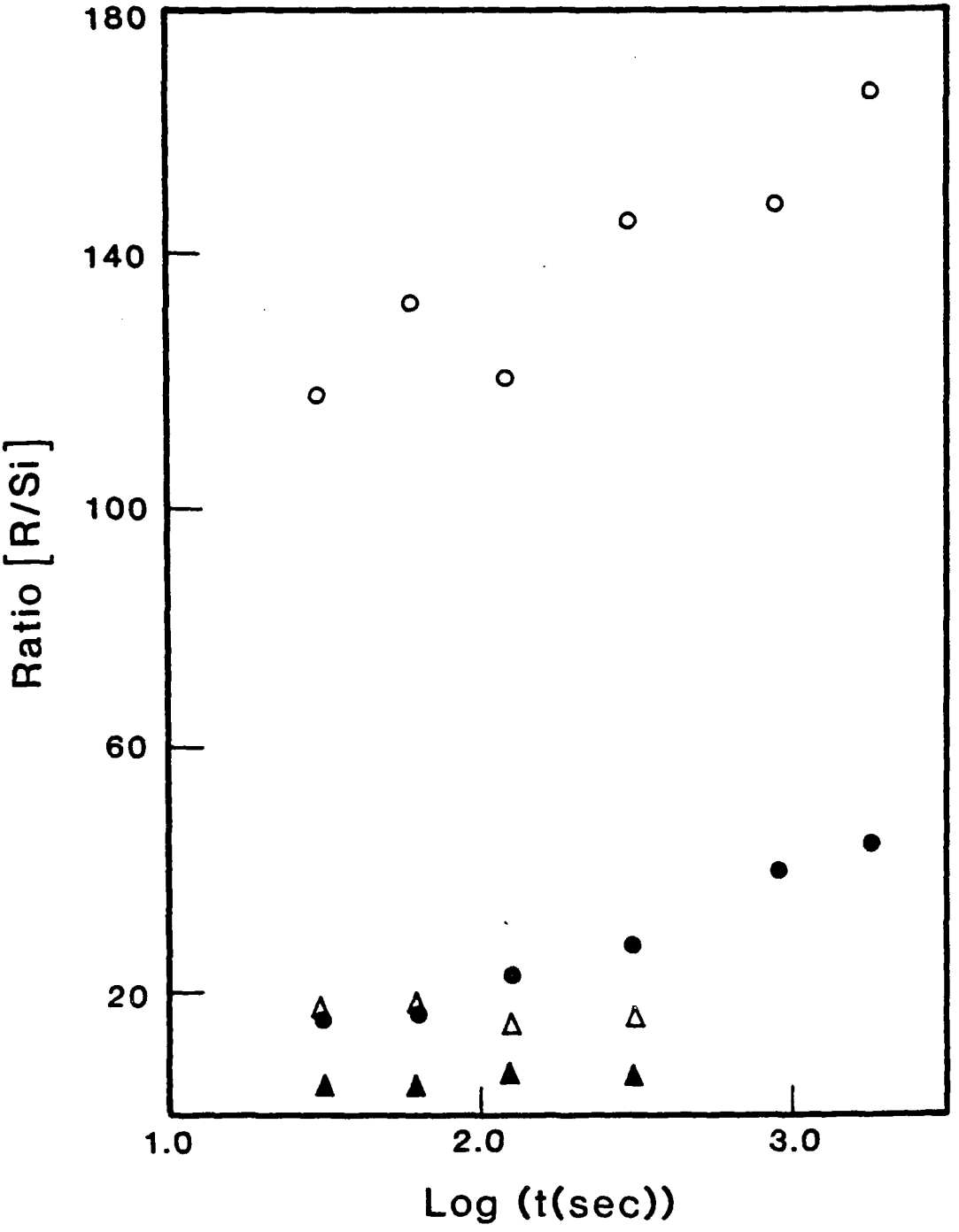

8.

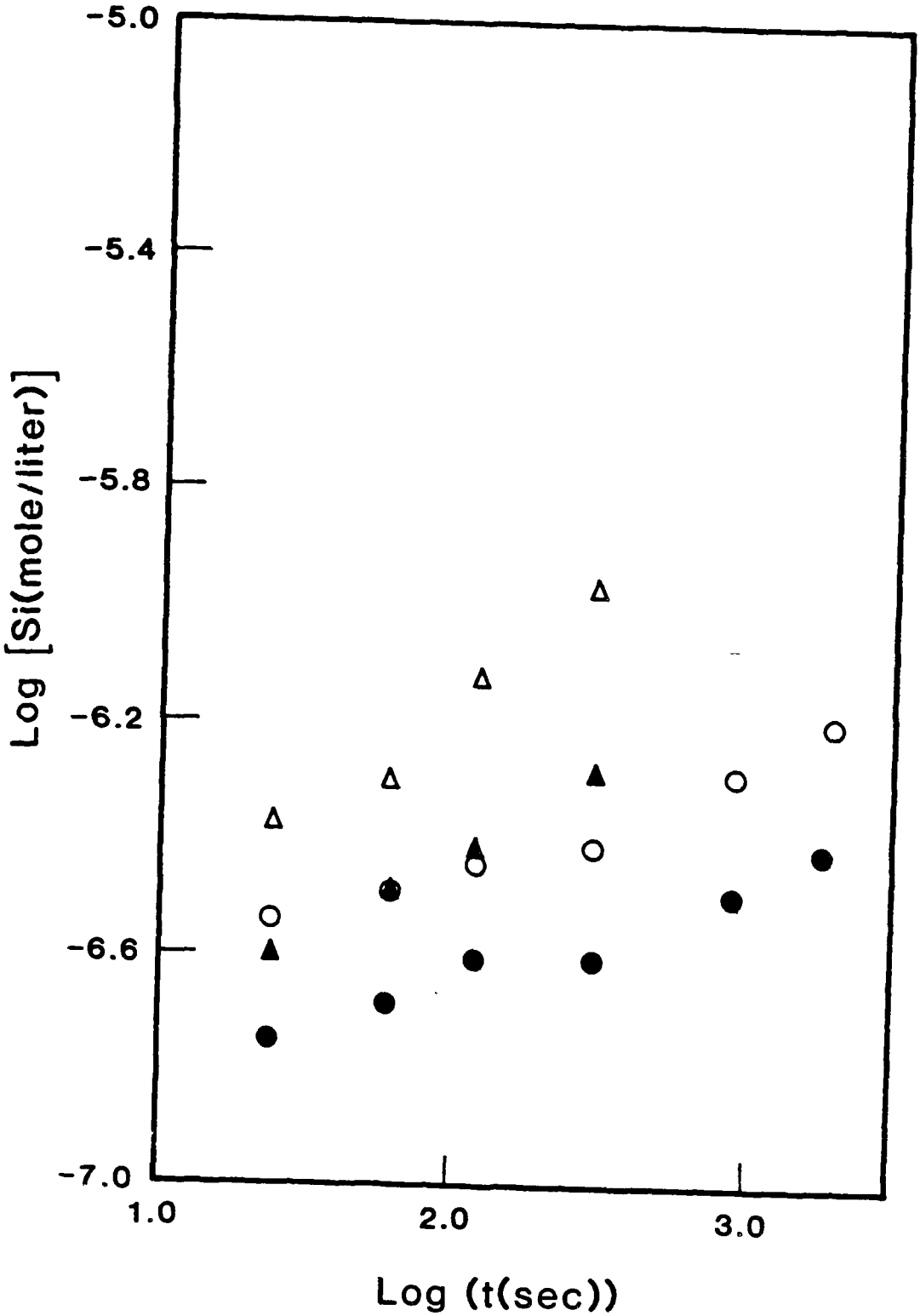
-5.0
-5.4
-5.8
-6.2
-6.6
-7.0
Log [Si(mole/liter)]
1.0
2.0
3.0
Log (t(sec))

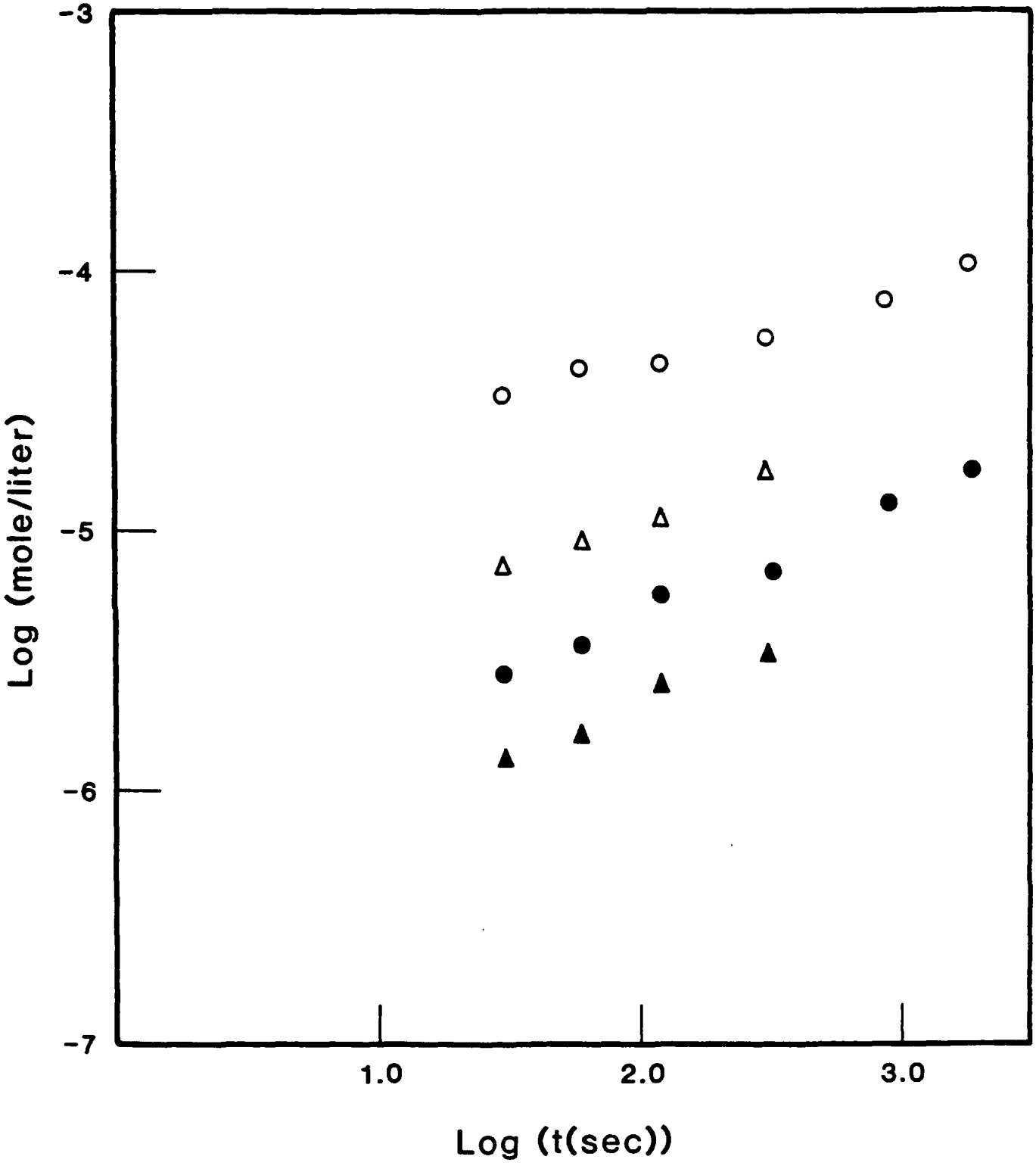
-3
-4
-5
-6
-7
Log (mole/liter)
1.0
2.0
3.0
Log (t(sec))

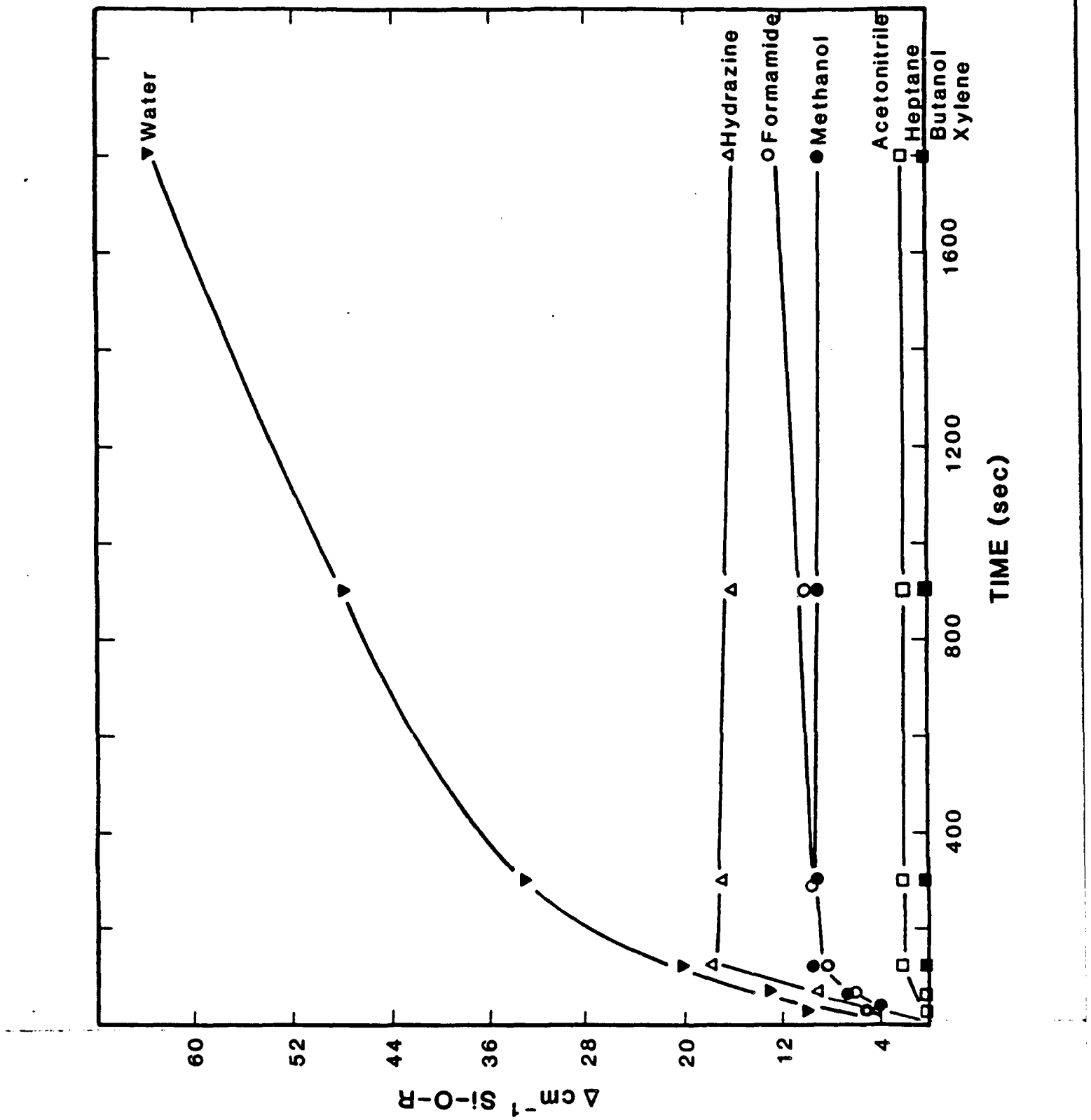
Water
Hydrazine
Formamide
Methanol
Acetonitrile
Heptane
Butanol
Xylene
TIME (sec)
400
800
1200
1600
Δ cm⁻¹ Si-O-R
4
12
20
28
36
44
52
60

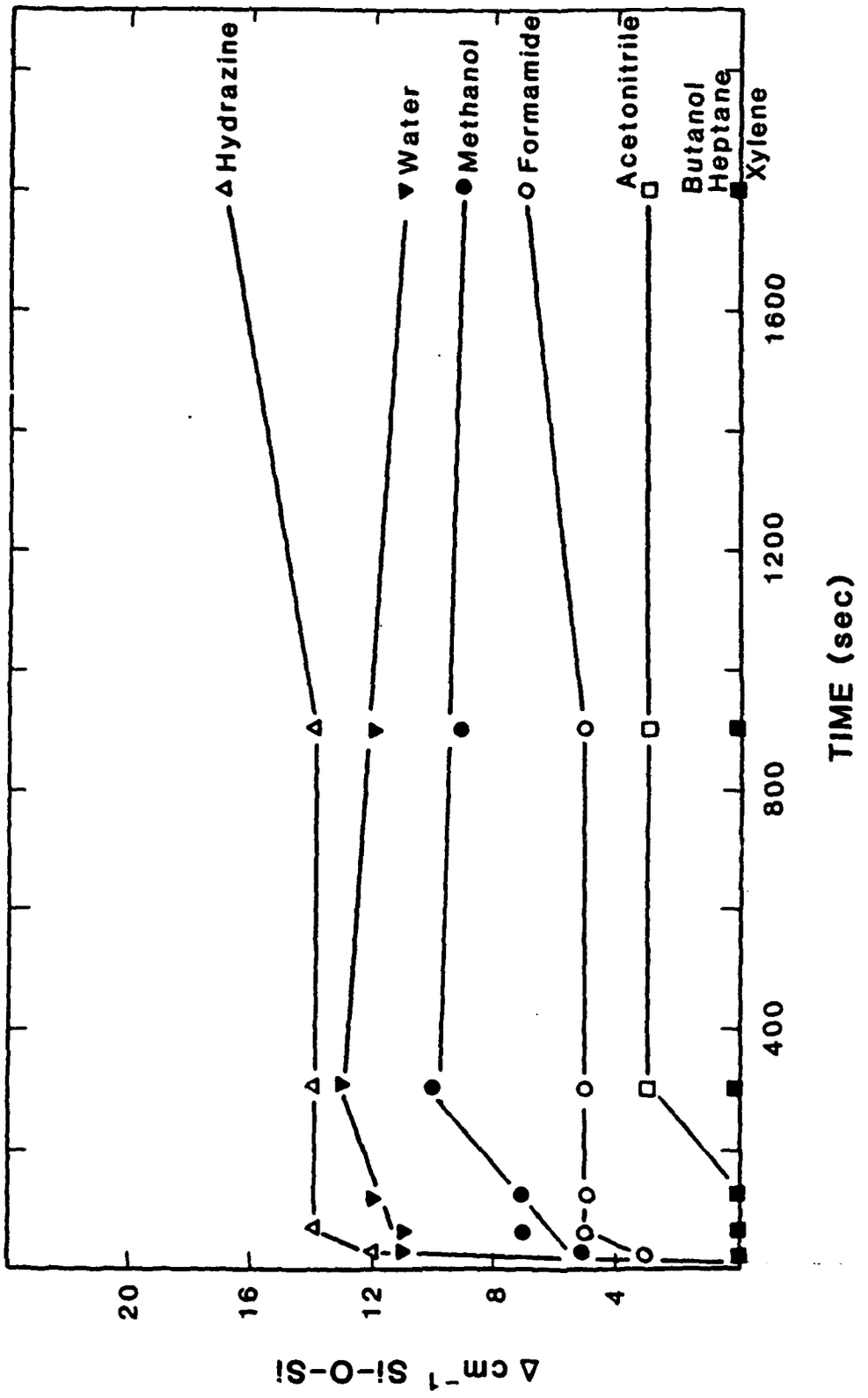
Hydrazine
Water
Methanol
Formamide
Acetonitrile
Butanol
Heptane
Xylene
TIME (sec)
400
800
1200
1600
Δ cm⁻¹ Si-O-Si
4
8
12
16
20

6.a.

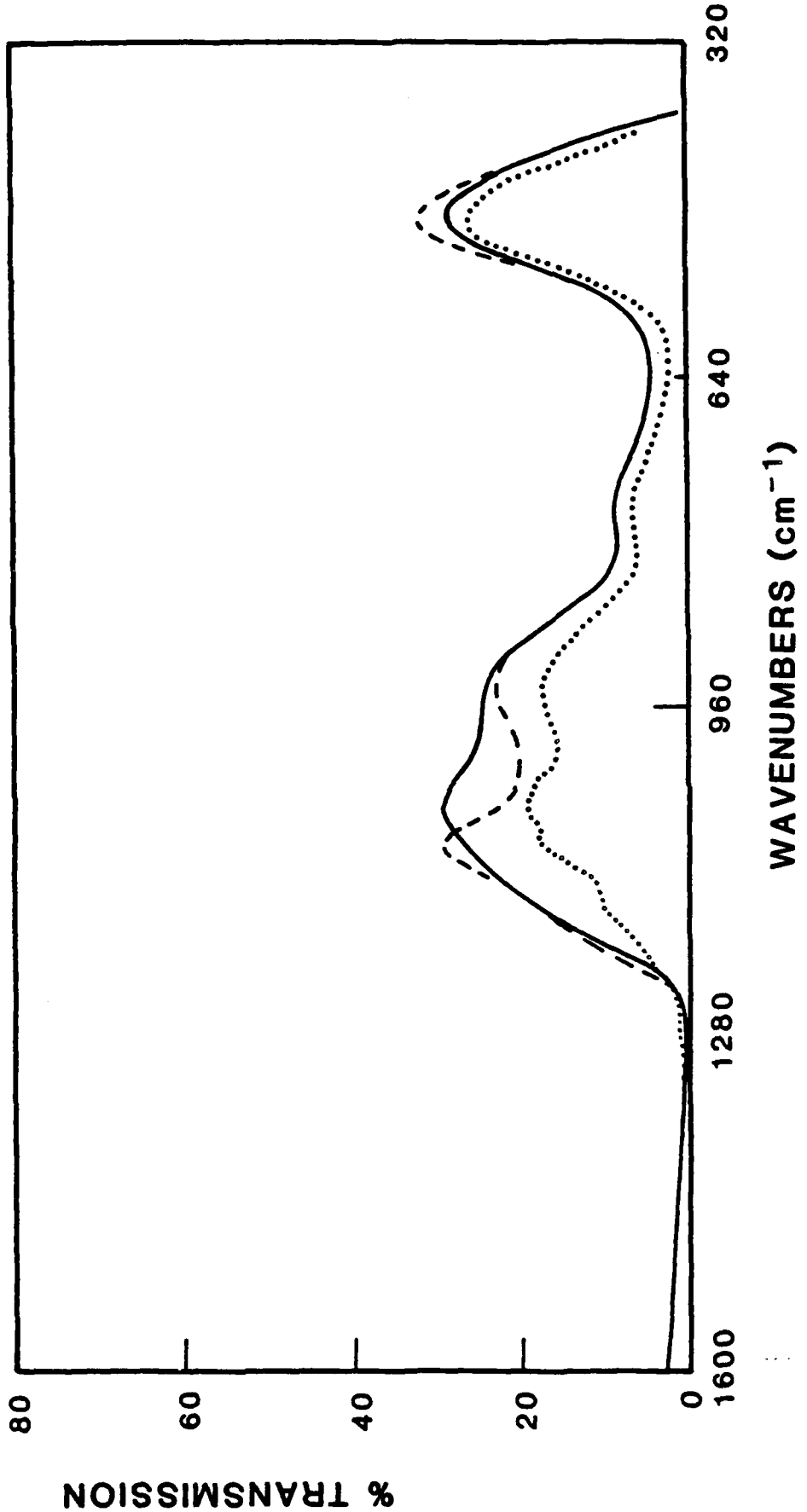
% TRANSMISSION
80
60
40
20
0
1600
1280
960
640
320
WAVENUMBERS (cm^{-1})

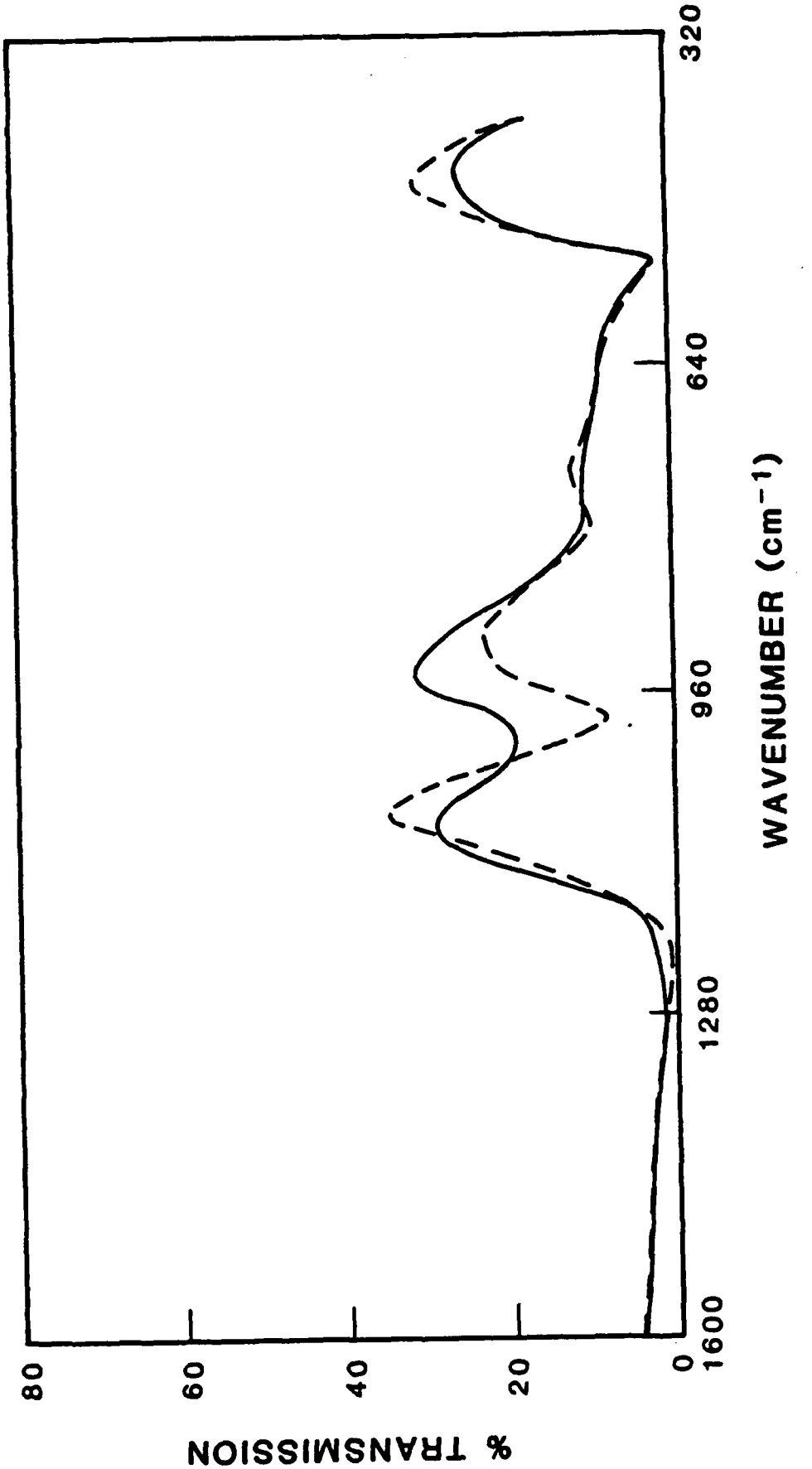
% TRANSMISSION
80
60
40
20
0
1600
1280
960
640
320
WAVENUMBER (cm⁻¹)

5. a.

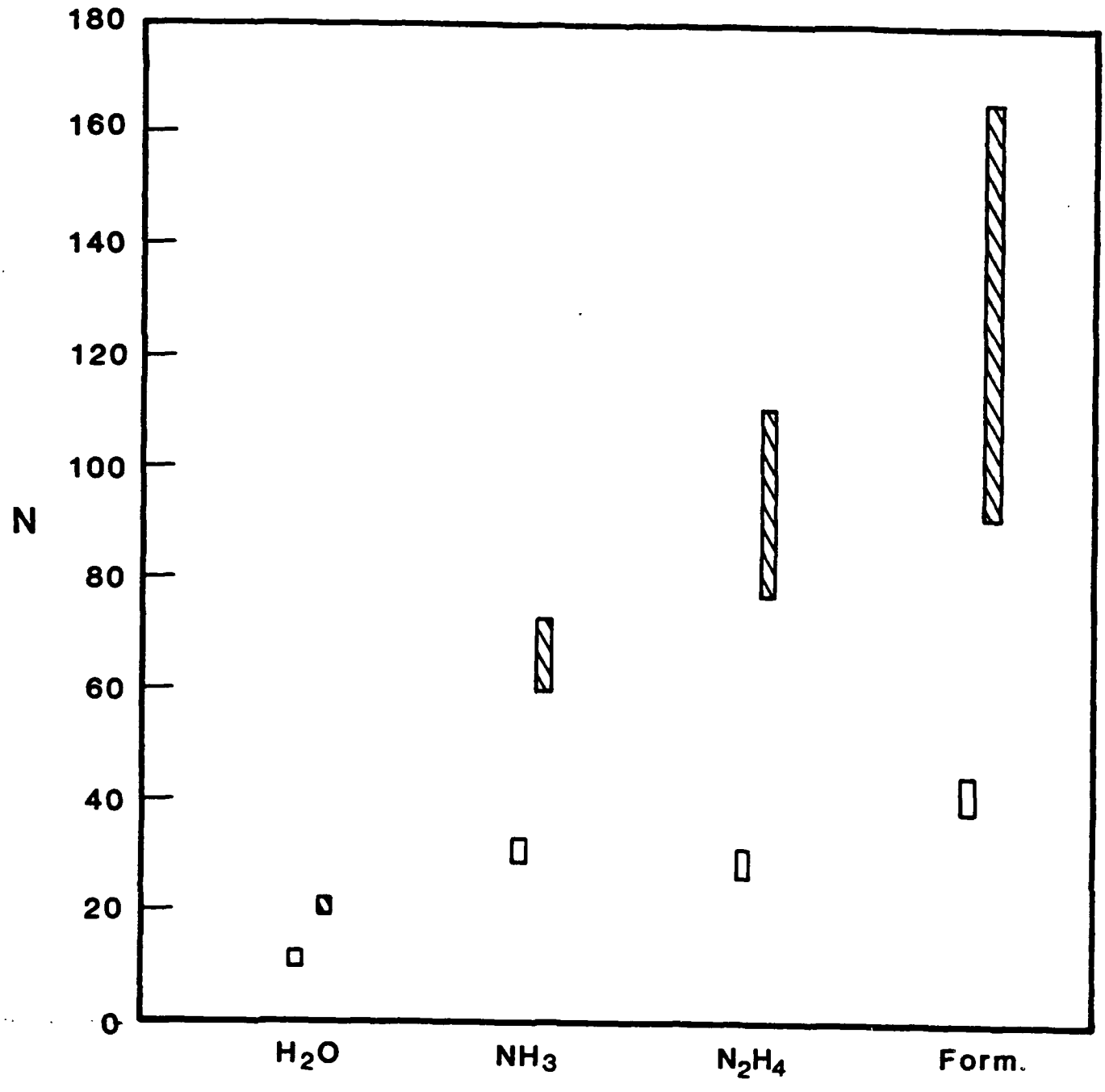
180
160
140
120
100
80
60
40
20
0
N
H_2O
NH_3
N_2H_4
Form.

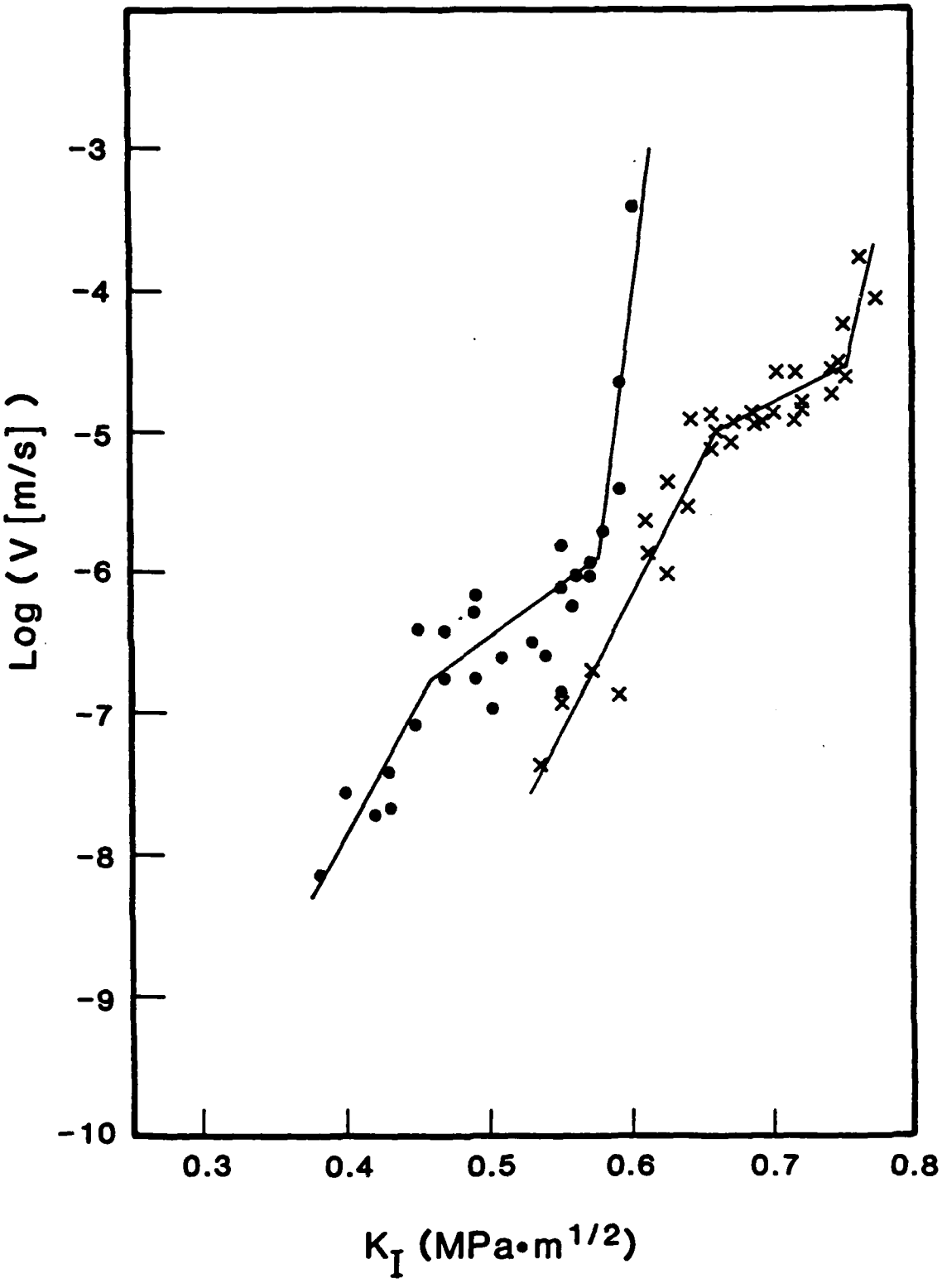

Fig 3

3.

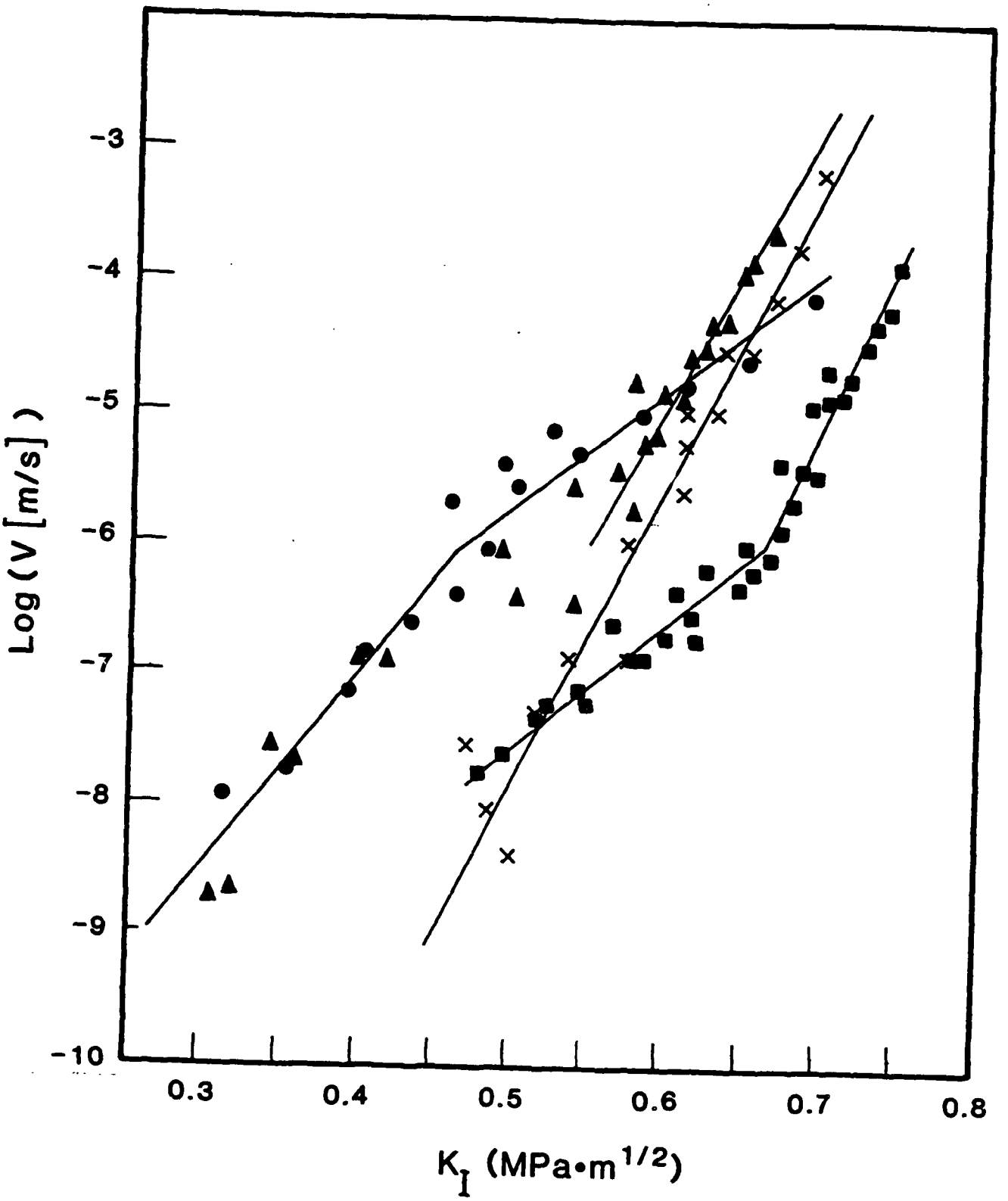

2.

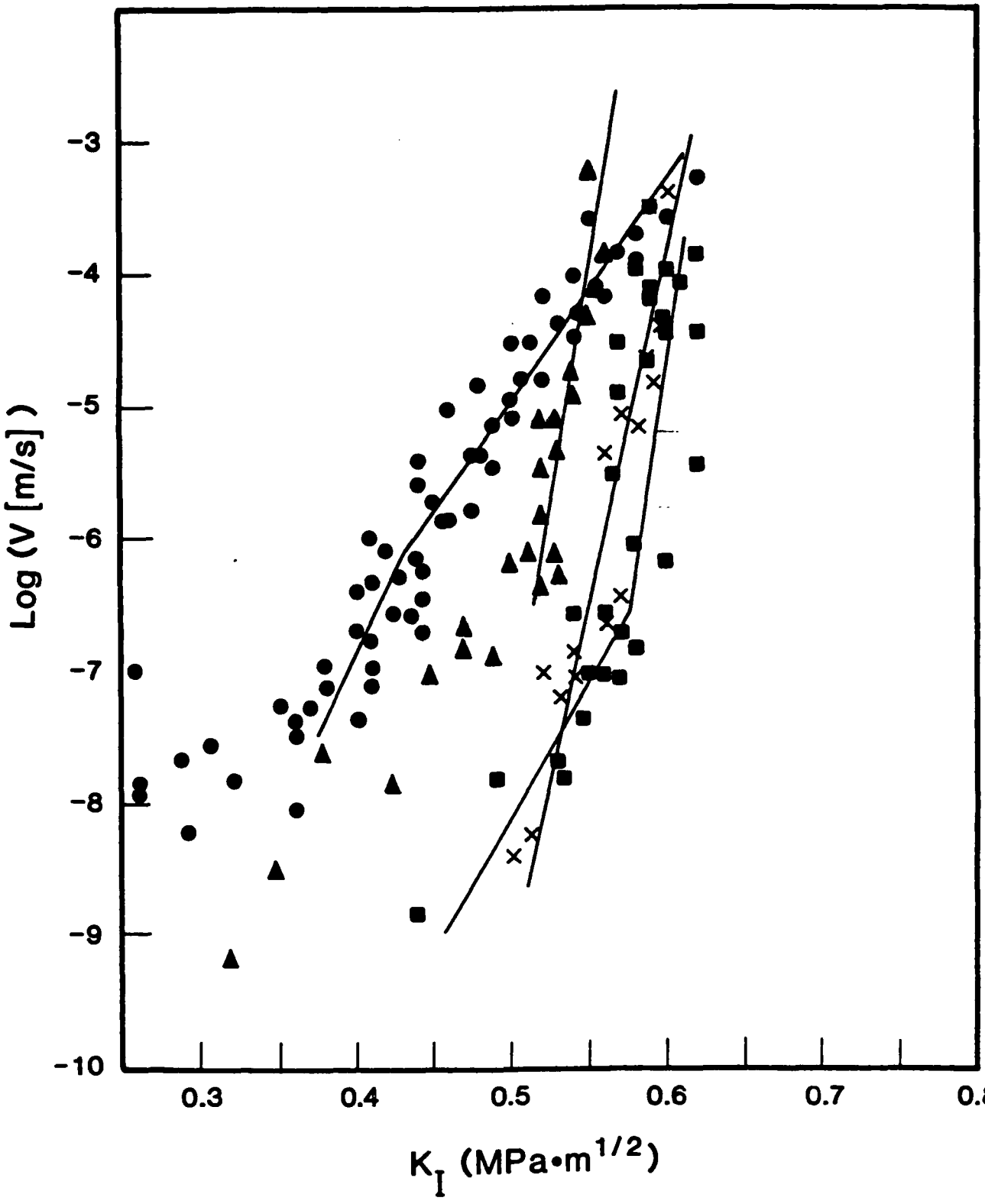

1.

Figure Captions

1. Log V vs K_I crack growth data for 33N glass in four environments: water (●), ammonia (x) hydrazine (▲), and formamide (■). Straight line segments are calculated least square fit to the data.

2. Log V vs K_I crack growth data for 33L glass in water (●), ammonia (x), hydrazine (▲), and formamide (■). Straight line segments are calculated least square fit to the data.

3. Log V vs K_I crack growth data for N33 (●) and L33 (x) taken in acetonitrile. Each set of data evidences a plateau, indicating that water impurity rather than the bulk environment, controls crack growth.

4. Comparison of N values for N33 (hatchmarked) and L33 (open) glasses in water, ammonia, hydrazine, and formamide. The indicated ranges are the standard deviation values.

5. (a) FTIR spectra of N33 glass before (-) and after (---) 5 minutes immersion in distilled water. (b) FTIR spectra of L33 glass before interaction with environment (-) after 30 minutes in water (--) and after 5 minutes in hydrazine (...).

6. Plot of the position shifts in various environments of the (a) Si-O-S, and the Si-O-R IR peaks in 33N glass.

7. (a) Log of the concentration of Si from 33N glass in water (o) and hydrazine (Δ) and from 33L glass in water (●) and hydrazine (▲). (b) Log of alkali (Na or Li) concentration obtained from soaking N33, glass in water (o) or hydrazine (Δ) or soaking L33 glass in water (●) or hydrazine (▲).

8. Ratio of alkali to Si in solution: (o) Na/Si in water (Δ) Na/Si in hydrazine, (●) Li/Si in water, and (▲) Li/Si in hydrazine.

Acetonitrile	31.1 ± 3.6	+ 0.81 ± .78	52.1 ± 5.9	-19.7 ± 1.6	.5 - .66
	66.8 ± 22.	+ 4.0 ± 2.7	88.8 ± 29.3	-33.3 ± 9.6	.73 - .80
Hydrazine	29.2 ± 2.5	+ 1.6 ± 0.6	49.0 ± 4.2	-17.6 ± 1.1	.53 - .7
NH_3	30.8 ± 2.1	+ 1.4 ± 0.5	53.2 ± 3.3	-19.3 ± 0.8	all
Formamide	44.8 ± 4.5	1.7 ± .5	59.5 ± 5.7	-23.3 ± 1.9	.72 - .8
+10% H_2O	14.9 ± .4	-2.3 ± .08	24.1 ± .7	-11.9 ± 1.8	.5 - .72
	5.6 ± .9	-4.7 ± .3	13.0 ± 1.9	- 9.3 ± .3	.3 - .55

(1) Where plotting is $V = AK_I^N$

(2) Where plotting is $V = V_o \exp(BK_I)$

Table 1. Crack Growth Parameters for the Binary Alkali Silicate Glasses

33N

Environment	(1) N	Log A	(2) B	Log V_o	K_I Range
NH_3	66.1 ± 6.6	10.9 ± 2.8	119.77 ± 11.6	-34.9 ± 2.8	all
Water	24.0 ± 3.8	2.7 ± 1.5	59.9 ± 9.5	-17.3 ± 1.7	.35 - .45
	21.0 ± 1.5	1.4 ± 0.4	40.1 ± 2.9	-13.7 ± .65	.45 - .70
Formamide	23.8 ± 6.5	- 0.80 ± 1.9	48.2 ± 13.2	-18.5 ± 3.0	.43 - .55
	128.7 ± 37.4	24.5 ± 8.7	220.5 ± 64.6	-61.5 ± 16.5	.55 - .65
Hydrazine	26.0 ± 2.9	+ 1.9 ± .9	36.3 ± 4.1	-14.2 ± .77	.3 - .5
	94.3 ± 16.6	+20.6 ± 4.6	176.3 ± 30.5	-46.0 ± 7.0	.5 - .6

33L

NaOH-HCl	6.9 ± .6	- 3.03 ± .3	18.3 ± .9	- 0.0 ± .2	all
H_2O	11.3 ± 1.4	- 2.2 ± .4	20.3 ± 2.7	-10.1 ± 3.6	.45 - .8
	13.7 ± 1.4	- 1.42 ± .5	33.7 ± 3.2	-12.8 ± .6	.25 - .5
N_2	23.1 ± 2.1	- 1.68 .4	38.1 ± 3.5	-16.8 ± 1.0	.5 - .7
Formamide	12.8 ± 1.0	- 3.76 ± .23	22.6 ± 1.7	-12.5 ± 0.4	.45 - .66
	41.4 ± 3.3	+ 1.4 ± .5	59.4 ± 4.7	-23.1 ± 1.4	.65 - .75

Environmentally Enhanced Crack Growth in Glasses

S.W. Freiman
Inorganic Materials Division
National Bureau of Standards
Washington, DC 20234

ABSTRACT

This paper reviews our current understanding of environmentally enhanced crack growth in glasses. This process is shown to lend itself to analysis by chemical reaction rate theory. The environmental dependence of the lower end of the crack velocity regime, Region I, is shown to fit a recent molecular model for a stress induced chemical reaction in SiO_2. Crack growth in Region II is shown to be transport rate controlled, while above Region II, a recently proposed electrostatic model is shown to fit the data for soda-lime-silica glass. Effects of experimental variables such as pH and temperature on the slope and portion of crack growth curves are discussed.

INTRODUCTION

The objective of this paper is to provide a current view of the mechanisms of environmentally enhanced crack growth in glasses. Because of its homogeneity and relatively simple structure, particular attention is given to vitreous SiO_2 as a model material, but data will be presented for other glass compositions as well. This review will concentrate on recent models for stress aided physical and chemical processes which appear to govern crack growth.

All of the materials discussed will be considered to be completely brittle, i.e. any inelastic deformation zone at the crack is considered to be negligibly small. While standard linear elastic fracture mechanics is assumed to be applicable, possible limitations in its use to understand the details of the crack growth process will be discussed.

The majority of the data presented in this paper was collected using double cantilever beam specimens, either by applying a constant load or a constant bending moment, although some double torsion data is included. Crack growth rates from 10^{-10} to 10^{-2} m/sec were generally obtained by optically measuring crack extension as a function of time on a travelling microscope equipped with a filar eyepiece. The stress intensity factor, K_I, was calculated from the load and the specimen dimensions, using standard expressions.

GENERALIZED CRACK GROWTH DIAGRAMS

Before considering the details of crack growth mechanisms, let us first examine a schematic of the various possible segments that can contribute to a $V(K_I)$ diagram. Figure 1 shows a plot of Log (Velocity) versus K_I. The reasons for the choice of the semilogarithmic form will be made clear later. Each segment of this curve can be ascribed to a different rate controlling mechanism, as follows:

Region I.

This is the crack growth region of primary interest, since the time to fracture of glass structures which undergo delayed failure is controlled by flaws which spend most of their growth period in this regime. Slopes of $V\text{-}K_I$ curves vary from low ($Li_2O\text{-}SiO_2$, N = 11)) to moderate (SiO_2 N = 35)).*

---

* For a relationship $V = AK_I^N$.

Wiederhorn (1967) showed that for a given K_I, crack velocities in Region 1 were related to the relative humidity, i.e. partial pressure of water, through an expression of the form:

$$V = a \left[\frac{P_i}{P_o}\right]^n \exp(bK_I) \qquad (1)$$

where a and b are constants, P_o is the vapor pressure of pure water at the temperature of interest, and P_i is the vapor pressure of water in the gas or the equilibrium vapor pressure over the solution, and n is the order of the chemical reaction between the water and the glass (Figure 2).* Wiederhorn's data suggested a possible change in the chemical reaction from first order to one-half order at low relative humidities, as does data taken in straight chain alcohols (Freiman (1974)). Freiman's data reinforced the concept that when the major constituent in the environment does not enhance crack growth, then the water in solution becomes the dominant factor. Because it is the partial pressure, i.e. relative humidity, of this water that is important, the fact that a liquid dissolves only minute quantities, i.e. <50 ppm, is not important. It is the partial pressure of water relative to that at saturation that is the primary factor. This is a very significant point since it means that liquids such as silicone oil and fluorinated hydrocarbons cannot be considered inert just because their solubility for water is small. A further piece of evidence for the importance of activity rather than concentration is

*It will be shown in a later section that an expression of this form can be derived from chemical rate theory.

the fact that the crack growth curves for vitreous silica in liquid H_2O or in N_2 gas at 100% relative humidity overlap, even though the H_2O concentration differs by orders of magnitude.

Region IA.

It is not clear that the mechanism of crack growth in this steeper regime of the V-K_I diagram is radically different than that in Region I. Under some conditions, e.g. soda-lime silica glass in H_2O, this regime ends in a stress corrosion limit, as was demonstrated convincingly by Michalske (1983). Based upon the time required to achieve a steady state velocity and fracture surface markings, Michalske showed that some change in the crack tip geometry or structure occurred during 16 hour holds at K_I's below 0.25 MPa $m^{1/2}$. Whether this is crack tip blunting as suggested by the model of Charles and Hillig (1962), or due to the formation of corrosion products at the crac tip, is not clear at this time. Except for some data on borosilicate glasses Wiederhorn and Johnson (1973) and Simmons and Freiman (1980), observations of a stress corrosion limit have not been made on other glass compositions. In the latter two, the occurrence of phase separation in the glass may be a significant factor.

Region IB.

The extremely shallow curve in the velocity range of 10^{-10} to 10^{-8} m/sec has been observed only in binary Na_2O-SiO_2 glasses tested in aqueous environments (Simmons and Freiman, 1981) (Figure 3) and in a binary Li_2O-SiO_2 glass (Freiman, 1983). It is hypothesized that, because of the high rate of solubility of these glasses, the crack is growing at the rate at which SiO_2 is dissolving. The crack shape is maintained because of the tendency of the

small applied stress to preferentially remove corrosion products at the crack tip, so that dissolution occurs there more rapidly. However, effects of tensile stresses generated due to an exchange of H^+ for Na^+ or Li^+ cannot be ruled out.

Region II.

This regime appears when crack growth takes place in an environment in which the minor constituent controls the crack tip reaction. Although, the Region II velocity is shown in Figure 1 to be completely stress independent, slopes in the range of 2 to 6 have been measured experimentally. Crack growth in Region II was shown by Wiederhorn et al. (1982) to be transport rather than reaction rate limited. Because diffusion can also take place from the sides of a fracture mechanics specimen as well as from behind the crack, all parts of the crack front may not be in the same regime. Both Richter (1977a) and Quackenbush and Frechette (1978) showed that the crack velocity at which Region II is observed is specimen thickness dependent. This mixed mechanism may explain the small but definite K_I dependence in Region II.

The onset of the transport controlled mechanism of crack growth has been modeled by Wiederhorn et al. (1982) as follows. As the crack grows, the species in the environment which reacts with the highly strained bonds, e.g. H_2O, is depleted at the crack tip. As the crack velocity increases, the size of the depleted zone, δ, also increases, thereby creating a diffusion gradient. At some critical velocity, the rate at which the active species can diffuse through the depleted zone to the crack tip becomes slower than the crack tip reaction rate, and hence becomes the controlling step in the crack growth process. Through the use of the Stokes-Einstein relation for the

diffusivity of a molecule in a liquid, it was shown that the velocity at which the change in mechanism occurs is given by: (Wiederhorn et al. 1982)

$$V = \frac{0.0275\ kT}{6\pi r\delta}\left(\frac{C_o}{\eta}\right) \qquad (2)$$

where k is the Boltzman constant, T is the temperature, r is the size of the diffusing molecule, C_o is the bulk concentration, and η is the viscosity of the solution. Experimental data for alcohol-water solutions has verified the applicability of Eq. 2. (Figure 4).

Region III.

Crack growth in Region III has been least understood. The curves are quite steep, i.e. 5-10 times the slope in Region I. Wiederhorn (1967) showed that crack growth rates for soda-lime glass in Region III were stable and were independent of the relative humidity in the N_2 gas in which the tests were conducted. He suggested the possibility that a chemical process internal to the glass controlled crack velocity. Freiman (1974) later showed that while crack growth in Region III was not affected by water, in agreement with Wiederhorn, there were shifts in both the position and slope of the Region III $V\text{-}K_I$ curves for soda lime glass with the chain length of the alcohol in which the tests were conducted (Figure 5). Similar data was subsequently reported by Richter (1977). A recent model for Region III crack growth based on an electrostrictive interaction between the solid and the environment at the crack tip (Wiederhorn et al. 1982) will be discussed in a later section.

CRACK GROWTH KINETICS

While reductions in the surface energy of a glass due to the attachment of surface groups can be considered to be the thermodynamic driving force for crack growth, as suggested by Orowan (1944) and Parks (1983), crack growth

rates are determined by a kinetic process. If we assume that crack growth is controlled by a stress enhanced chemical reaction between the glass and the environment, as is suggested by the experimental data; then chemical reaction rate theory can be used to derive a model for growth rates. A synopsis of such a derivation for the SiO_2-H_2O reaction (Wiederhorn et al. 1982) is given as follows:

A general expression for the chemical reaction between H_2O and an Si-O bond is given by:#

$$[Si\text{-}O\text{-}Si] + H_2O \rightleftharpoons \chi^* \longrightarrow 2[SiOH] \qquad (3)$$

where χ^* is the activated complex. In reaction rate theory (Laidler, 1965) the decomposition of the activated complex to the products is assumed to be rapid compared to the reverse reaction. Then the rate of reaction can be expressed as:

$$\text{Rate} = \kappa\left(\frac{kT}{h}\right)\exp\left(-\Delta G^*/RT\right)\left(\frac{a\ (H_2O)}{f}\right) \qquad (4)$$

where κ is the transmission coefficient (usually assumed equal to 1), k is the Boltzman constant, T is temperature, h is Planck's constant, ΔG^* is the Gibbs free energy of activation, $a(H_2O)$ is the activity of water, and f is the activity coefficient for the activated complex. Combining terms and assuming that the crack velocity is directly proportional to the reaction rate, we obtain:

#This assumes a 1st order reaction between H_2O and SiO_2 at a crack tip, which is justified on the basis of the experimental results (Wiederhorn 1967).

$$V = V_o\, a(H_2O)\, \exp\,(-\Delta G^*/RT) \qquad (5)$$

Note that the crack velocity is directly proportional to the activity rather than the concentration of water, as is indicated by the experimental results of Wiederhorn (1967) and Freiman (1974). The stress dependence of the reaction is contained in the ΔG^* term. It has been shown (Wiederhorn et al. 1980) that this term can be expanded as follows:

$$\Delta G^* = - T\Delta S^* + \Delta E^* - (\pi d)^{-1/2} K_I \Delta V^* - (\gamma V^* - \gamma V)/\rho \qquad (6)$$

where ΔS^*, ΔE^* and ΔV^* are the activation entropy, activation energy and activation volume respectively; d is a dimensional parameter depending on the structure of the crack tip.[#] The last term is included following the approach of Charles and Hillig (1962) and accounts for changes in the surface energy of the crack tip during the reaction. The effect of stress on the crack tip reaction rate is included in the $(\pi d)^{1/2} K_I \Delta V^*$ term. d must have units of $(\text{dimension})^2$ so that $d^{-1/2} K_I$ has units of stress. The use of the activation volume in this context assumes that the tensile stress dependence of the reaction rate can be expressed as the negative of the pressure dependence. Equations 5 and 6 can be combined to yield

$$V = V_o\, a(H_2O)\, \exp\,[(-E^* + b\, K_I)/RT] \qquad (7)$$

[#]Wiederhorn et al. (1982) use the crack tip radius, ρ, but for values of ρ approximately that of the network spacing in the solid, this term probably has little meaning.

where all of the non-stress dependent terms are included in E^*. This equation will be used later to explain certain aspects of crack growth behavior.

MECHANISM OF CHEMICAL REACTION ENHANCED CRACK GROWTH

The derivation of the kinetics of crack growth in the previous section was completely general. No details of the chemical reaction between the environment and the glass were discussed. One important question is why H_2O is such an effective crack growth agent for glasses, when the corrosion rate of a material such as vitreous SiO_2 is extremely low? A second question is what are the properties of other environments which would make them crack growth enhancers? Finally, can we predict changes in stress corrosion susceptibility with changes in glass composition?

Michalske and Freiman (1983) described a specific chemical mechanism by which strained Si-O bonds in vitreous silica react with molecules of a gas or liquid. This model for the H_2O-SiO_2 reaction is shown in Figure 6 as a three step process:

Step 1. An H_2O molecule orients itself with respect to an Si-O-Si bond at the strained crack tip such that one set of the lone electron pair orbitals on the oxygen are aligned toward the Si; hydrogen bonding occurs between the O (silica) and the H.

Step 2. Electron transfer from the O (water) to the Si take place simultaneous with proton transfer to the O (silica), forming two new bonds. It is hypothesized that the strain on the bridging Si-O bond (>20%) enhances the tendency for this reaction by making the electron distribution in the Si-O bond more favorable for electron transfer.

Step 3. The weak hydrogen bond between O (water) and the transferred hydrogen breaks to form two Si-OH surfaces.

Note that in this mechanism no reaction products are removed from the solid. Hence the term "stress corrosion" may be something of a misnomer. However, as will be discussed later, the formation of corrosion products at the crack tip may alter the rate of crack growth by influencing the accessibility of the crack tip to the reactive environment. Also note that the model does not require prior dissociation of the water molecule. Although as will be shown later, such dissociation may affect reaction rates.

Of prime importance is the fact that the model predicts that the other environments which would enhance crack growth in SiO_2 should have structure and bonding similar to water, namely, lone pair orbitals available on one portion of the molecule and proton donor sites on another. There may be size limitations as well since the Si-O bond distance is only 1.63Å.

Figure 7 shows crack growth curves for vitreous silica in water, ammonia, hydrazine, formamide and N_2 gas. Ammonia, hydrazine and formamide can each donate electrons and protons. As pointed out earlier, the plateau in the N_2 gas curve occurs when crack growth is controlled by the rate of diffusion to the crack tip of the small quantity of dissolved water. The absence of this plateau in the curves for ammonia, hydrazine and formamide leads to the conclusion that their reaction with the crack tip bonds governs crack growth rates in preference to the reaction of the water present in these environments. Other environments such as carbon monoxide, acetonitrile and nitrobenzene did not control crack growth (Figure 8). This would be predicted by the above model, since each of these molecules does not meet all of the required bonding specifications. Although each contains lone pair orbitals, none can donate protons. It should also be noted that no direct correlations

were found to exist between dielectric constant or dipole moment alone and an environment's ability to cause crack growth in preference to water. The direct participation of proton transfer is shown by two pieces of data. First, Figure 9 shows the V-K_I curves for tests carried out in H_2O and D_2O. In order to eliminate specimen to specimen variations, the same sample was used to obtain data in both environments. The reduction in crack velocity at the same K_I obtained in D_2O is approximately that predicted for a primary isotope effect. Second, experiments were carried out in pyridine, C_5H_5N, whose electron donating ability is equal to that of H_2O, but which cannot donate protons. No evidence was seen that pyridine enhanced crack growth in SiO_2.

Crack growth data obtained on a commercial soda-lime-silica glass (Figure 10) shows the same general environmental sensitivity as does SiO_2 (Freiman and White, 1982). The positions of the curves for these environments which control crack growth in soda-lime glass are in the same order as those for SiO_2. A major difference, however, is the relatively shallow slope of the upper curve in H_2O compared to that in the other environments or for SiO_2. We speculate that there is a true corrosion phenomena that occurs in soda lime glass in H_2O which involves ion exchange of Na^+ in the glass for H^+.

ELECTROSTATIC MODEL FOR CRACK GROWTH

A discussion of the proposed mechanism of crack growth in Region III is included as a separate section because it is only at velocities above the Region II plateau that the dominating effect of H_2O in most environments can be eliminated. We will see that certain features of the proposed mechanism are similar to those for the chemical reaction model described in the last section.

The model developed by Wiederhorn et al. (1982) is based on the concept that positive and negative charges are formed on the Si and O atoms respectively during bond rupture. The formation of these charges produces an electrostrictive force which contributes to the activation volume for the reaction. In fact, this electrostatic contribution to normal chemical reactions is usually 3 to 10 times that due to changes in bond length. Since for a given glass, the activation volume is directly proportional to the slope of the crack velocity curve (see Equation 6) any environment at the crack tip which modifies these charges and thereby the activation volume will produce a change in the slope of the $V\text{-}K_I$ curve.

In this model it is assumed that the Si and O lie at a stressed surface of the glass. It is also assumed that the electrostatic contribution to the activation volume results entirely from charging the Si and O atoms during bond fission. That is, no contributions due to bond stretching are considered. Finally, it is assumed that the process is slow enough so that the static component of the dielectric constant can be used.

By treating both the glass and the environment as a continuum, the following expression was derived for the stress (i.e. negative pressure) dependence of the activation volume.

$$\Delta V^*_{ES} = \frac{Ne^2}{r}\left[(3B)^{-1}(\varepsilon_1+\varepsilon_2)^{-1} - (\varepsilon_1+\varepsilon_2)^{-2}\frac{\partial\varepsilon_2}{\partial P}\right] \qquad (8)$$

where N is Avogadro's number, ε is the unit of electric charge, r is the radius of an atom (contributions of Si and O are calculated separately), B is the bulk modulus of the glass, and ε_1 and ε_2 are the dielectric constants of the liquid and glass respectively.

As noted previously, the stress dependent term to the crack velocity can be expressed as:

$$\text{Log } V = (\pi d)^{-1/2} \Delta V^{*} K_I \qquad (9)$$

ΔV^{*} can therefore be calculated from the slope of the log V-K_I plot and related to that determined from Equation 7 provided that we have a value for d. d can be thought of as a dimensional parameter that defines the size of a zone extending out from the crack tip within which non-linear elastic deformation occurs. In this sense it is analogous to the concept of a plastic zone around crack tips in metals. d will probably differ from one glass to another because of changes in glass structure.

ΔV^{*}_{ES} calculated from the electrostatic model, Equation 8, is plotted in Figure 11 versus that determined from measured slopes of V-K_I curves for soda lime glass in environments of varying dielectric constant. Despite the experimental scatter, a definite correlation exists between ΔV^{*}_{ES} and the total ΔV^{*}. The dependence of the slope of the V-K_I curves on the dielectric constant of the environment is apparent, supporting the idea that electrostatic interactions between the environment and the strained bonds at the crack tip are important. Evidence to the effect that it is the dielectric constant of the environment and not the molecule's dipole moment was obtained by determining the crack growth curves in both liquid and vapor. For an environment such as acetone, the liquid dielectric constant is 21, but in the vapor phase for any chemical $\varepsilon' = 1$. The fact that the V-K_I curves differ under these conditions (Wiederhorn et al. 1983) is indicative of the importance of dielectric constant.

EXPERIMENTAL OBSERVATIONS

In this section we will discuss a number of the features of experimental $V\text{-}K_I$ data for various glass systems and relate those observations to the crack growth models.

$V\text{-}K_I$ Slopes

As noted in the section on crack growth kinetics, the slope of a semi-logarithmic $V\text{-}K_I$ plot in Region I is directly related to the activation volume for the chemical reaction. Why then are the slopes of these curves in H_2O dependent on glass composition, when the reaction should involve only the Si-O network? One possible answer is that the crack growth rate controlling step is a corrosion type process such as exchange of Na^+ in the glass for H^+ ions in the H_2O. This process would tend to produce a compositional gradient at the crack tip as well as lead to possible tensile stresses due to the difference in volume occupied by the different ions. Work reported by Simmons and Freiman (1981) supports the hypothesis that ion exchange reactions can be important. This work showed that both the positions and the slopes of 33% Na_2O - 67% SiO_2 and 25% Na_2O - 75% SiO_2 glasses varied depending on whether experiments were carried out in aqueous solutions containing IM Li^+ or IM Cs^+ ions (Figure 3). No such effect of Li^+ or Cs^+ ions was observed for soda-lime glass however, possibly because rates of exchange are much slower for this glass.

It has also been observed that the slope of the $V\text{-}K_I$ curve for soda lime glass is the same in liquid water as in N_2 gas of varying relative humidity (Wiederhorn, 1967). This would be predicted from Equation 5, since the activity of the H_2O appears only in the pre exponential term. This same trend

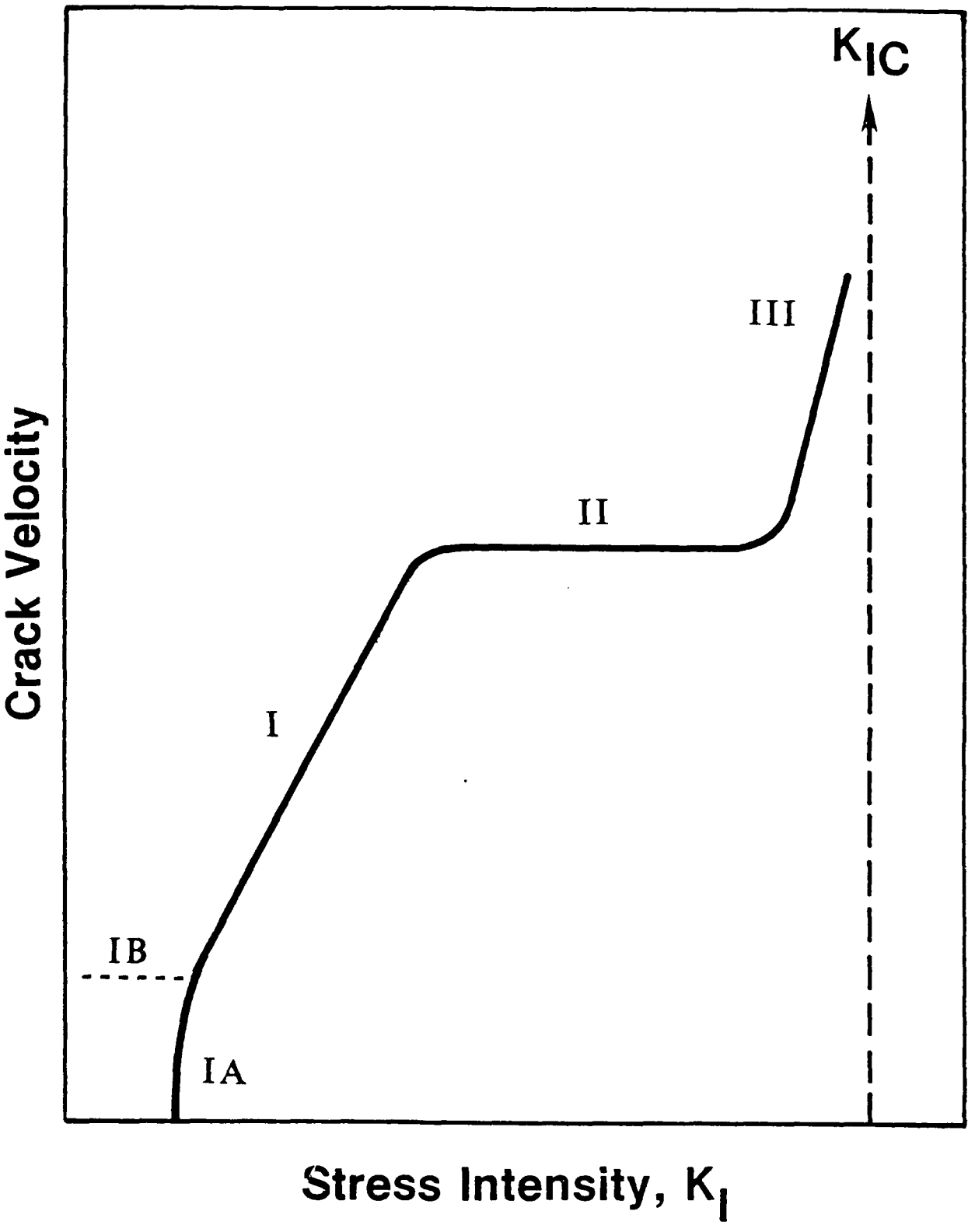
K_{IC}
III
II
I
IB
IA
Crack Velocity
Stress Intensity, K_I

Figure 8. $V\text{-}K_I$ curves for vitreous SiO_2 in environments which do not enhance crack growth. Plateaus are due to the fact that velocity is controlled by the H_2O in the environments. (after Michalske and Freiman, 1983).

Figure 9. $V\text{-}K_I$ curves for vitreous SiO_2 in H_2O and D_2O. The same specimen was used to obtain points on each curve. (after Michalske and Freiman, 1983).

Figure 10. Crack growth curves for soda lime silica glass in environments which undergo a stress enhanced reaction. Slopes of curves for ammonia, hydrazine and formamide are similar to those for SiO_2. (after Freiman and White, 1982).

Figure 11. Activation volume for soda lime silica glass determine from the Region III slope of the $V\text{-}K_I$ curves in liquids of various dielectric constant (Eq. 9) plotted versus the activation volume, ΔV^*_{ES}, calculated from Equation 8. (after Wiederhorn et al. 1982).

Figure 12. Comparison of positions of $V\text{-}K_I$ curves for various glasses.

Figure 13. Effect of pH on crack growth curves in glass. (a) Vitreous SiO_2. (b) Soda-lime-silica glass (after Wiederhorn and Johnson, 1973).

FIGURE CAPTIONS

Figure 1. Schematic of the different possible segments of a crack velocity - K_I curve for glasses, all of which have been observed in experiment.

Figure 2. Relative humidity dependence of crack velocity in Region 1 for soda lime silica glass (after Wiederhorn, 1967).

Figure 3. Crack growth curves for $33Na_2O$-$67SiO_2$ glass tested in H_2O, 1M Li^+ solution, 1M Cs^+ solution, and air. The data in H_2O overlaps that in 1M Cs^+. (After Simmons and Freiman, 1981).

Figure 4. Crack velocity for soda lime glass in Region II as a function of (conc./viscosity), as suggested by Equation 2. Data was obtained in straight chain alcohols containing various concentrations of water.

Figure 5. Position of the Region III crack growth curves for soda lime silica glass tested in alcohols containing varying partial pressures, i.e. differing relative humidity of H_2O (after Freiman, 1974).

Figure 6. Model for the reaction sequence between H_2O and the strained Si-O bond at a crack tip (after Michalske and Freiman, 1983).

Figure 7. Crack growth curves for vitreous SiO_2 in environments whose molecular structure is favorable for stress enhanced reactions, compared to that in N_2 gas at a relative humidity of 2%. (after Michalske and Freiman, 1983).

If the assumption is valid that crack propagation in region I can be directly correlated with the rate of dissolution of a glass, going from the deuterated system to the hydrogenated system would increase the crack propagation in a soda lime silica glass by a factor of five in neutral and basic solutions and no effect will observed in acid solutions. For SiO_2, where the pH at the crack tip can't deviate markedly from the pH of the solution $\surd H_2O/\surd D_2O$ 2.2.

REPLY: Evidence suggests that crack growth rates do not correlate directly with dissolution rates of glasses, e.g. the binary Na_2O-SiO_2 system (Simmons and Freiman, 1981). However, I agree that the variations in dissociation constant that you discuss, may explain the isotope data of Wiederhorn (1983) as well as that of Michalske and Freiman (1983). Experiments which could determine whether dissociation or reaction rates control crack growth have not yet been performed.

REPLY: I agree. H_2O in SiO_2 would tend to change the acceptor/donor capabilities of the Si-O bond, thereby possibly changing its susceptibility to stress enhanced reactions.

COMMENTS BY: B. M. Smets

In my opinion an alternative explanation can be given for the isotope effect observed with your SiO_2 data and Wiederhorn's glass data. Following Boksay (Phys. Chem. Glasses, Vol. 21, 110-113) the rate of dissolution of glass at low pH values would be proportional to the H_3O^+ concentration. At intermediate pH values the rate of dissolution is proportional to $[OH^-]$ and at pH values higher than 10 it is proportional to $[H_3O^+]\ [OH^-]/[Na^+]$. Consequently it is to be expected that in deuterated systems at low pH values (i.e. 1 N DCl in D_2O) the rate of dissolution will be the same as for the hydrogenated system. At high pH values the rate of dissolution would be lower by a factor of five in NaOD with respect to NaOH in view of the fact that $K_H = [H_3O^+]\ [OH^-] = 10^{-14}$ and $[D_3O^+]\ [OD^-] = K_D = 2.6 \times 10^{-15}$. In neutral solution

$$\mathcal{J} = k_1\ [H_3O^+] + k_2\ [OH^-]$$

$$= K_H\ (k_1 + k_2)$$

Consequently in D_2O the rate of dissolution will be lowered by a factor of $\sqrt{K_D}/\sqrt{K_H}$ 2.2.

COMMENTS BY: J. R. Varner

I would like to comment on Region II behavior. Prof. Frechette, at Alfred University, is now of the opinion that, in a fundamental sense Region II does not exist. In Region II, part of the crack is moving in Region III and part is moving in Region I. Therefore, Region II shows up in experiments, because of this combined effect. In other words, it is an artifact of the experiment, and is, as you pointed out, heavily dependent on specimen geometry and the test itself.

REPLY: I would tend to agree with your comments regarding the specimen experiment dependence of Region II. However, I do believe that at some velocity, crack growth rates become transport limited. The velocity at which Region II occurs and the V-K_I slope in Region II has been shown to be different for small flaws compared to that for fracture mechanics specimens (Wiederhorn et al., ASTM STP, to be published).

COMMENTS BY: J.J. Mecholsky

Joe Wysocki of Hughes Research Laboratories recently reported delayed failure in aluminum coated fibers at high (loaded at 90% of breaking) stresses. The interpretation is that the breaking of the fibers is due to Region III behavior because the aluminum has kept the external environment from the silica glass. However, different batches of fiber behaved differently which indicates it could be the internal water in the glass governing Region III behavior. Obviously, we need more experiments in this region to determine the time effects.

DISCUSSION

COMMENTS BY: Helmut Schaeffer

I am surprised the that K-v-curves of Wiederhorn (low pH values) do not exhibit an isotopic effect (DCl versus HCl). In leaching experiments this isotopic effect shows up (Scholze's work). Does this mean that the hydrogen ion (or hydrogen-related species) is not diffusion-controlling, or in other words that the actual leaching process is irrelevant for the advancement of the crack tip?

REPLY: I am not familiar with Scholze's work. However, I would expect to see effects of isotopes on diffusion rates. In the case of crack growth, a reaction between Si and the O_{water} must also occur. If this is the slow step in the crack growth process, then it will be rate controlling. I think this is why there is only a minimal effect of low pH variations on crack growth, e.g. Figure 13.

COMMENTS BY: M. Tomozawa

You stated that crack velocity of SiO_2 in region I in NH_3 is the same as that in H_2O. Is static fatigue of SiO_2 observed in NH_3?

REPLY: These experiments have not yet been performed.

Wiederhorn, S.M. and Bolz, L.H., Stress Corrosion and Static Fatigue of Glass, J. Am. Ceram. Soc. 53, 543-48, 1970.

Wiederhorn, S.M. and Johnson, H., Effect of Electrolyte pH on Crack Propagation in Glass, J. Am. Ceram. Soc. 56, 192-197, 1973.

Wiederhorn, S.M., Fuller, E.R., Jr. and Thomson, R., Micromechanisms of Crack Growth in Ceramics and Glasses in Corrosive Environments, Metal Science, 14, 450-458 1980.

Wiederhorn, S.M., Freiman, S.W., Fuller, E.R., Jr. and Simmons, C.J., Effects of Water and Other Dielectrics on Crack Growth, J. Materials Science, 17, 3460-3478 (1982).

Wiederhorn, S.M., Freiman, S.W. and Kravitz, D., unpublished data, 1983.

REFERENCES

Charles, R.J. and Hillig, W.B., Symposium on Mechanical Strength of Glass and Ways of Improving It, p. 511, Union Scientifique Continentale du Verre, Charleroi, Belgium, 1962.

Freiman, S.W., Effect of Alcohols on Crack Propagation in Glass, J. Am. Ceram. Soc. 57, 350-353, 1974.

Freiman, S.W., unpublished data, 1983.

Freiman, S.W. and White, G.S., Effects of Chemical Environments on Crack Growth in Soda-Lime Glass, Bull. Am. Ceram. Soc. 61, 414, 1982.

Kennedy, C.R., Bradt, R.C., Rindone, G.E., Fracture Mechanics of Binary Sodium Silicate Glasses, Fracture Mechanics of Ceramics, Vol. 2, 883-93, 1974.

Laidler, K.J., Chemical Kinetics, McGraw Hill, New York, 1965.

Michalske, T.A., Crack Arrest in Glass: The Blunt Truth, to be published in Fracture Mechanics of Ceramics, V-VI, 1983.

Michalske, T.A. and Freiman, S.W., A Molecular Interpretation of Stress Corrosion in Silica, J. Am. Ceram. Soc. 66, April 1983.

Orowan, E., The Fatigue of Glass under Stress, Nature, 154, 341-343, 1944.

Parks, G.A., The Surface and Interfacial Free Energies of Quartz, this volume.

Quackenbush, C.L. and Frechette, V.D., Crack Front Curvature and Glass Slow Fracture, J. Am. Ceram. Soc. 61, 402-06, 1978.

Richter, H., Proceedings of Eleventh Int. Congress on Glass, Vol 2, Prague, 1977a.

Richter, H., The Effect of Different Liquids on the Transition from Slow to Fast Crack Growth Propagation in Soda-Lime Glass, Physics of Non-Crystalline Solids, Ed. by G.H. Frischat, Trans. Tech. Pub., Aedermannsdorf, Switzerland, 1977.

Simmons, C.J. and Freiman, S.W., Effects of Phase Separation on Crack Growth in Borosilicate Glass, J. Non. Cryst. Solids, 38-39, 503-508, 1980.

Simmons, C.J. and Freiman, S.W., Effect of Corrosion Processes on Subcritical Crack Growth in Glass, J. Am. Ceram. Soc. 64, 683-686, 1981.

Wiederhorn, S.M., Influence of Water Vapor on Crack Propagation in Soda-Lime Glass, J. Am. Ceram. Soc. 50, 407-414, 1967.

Wiederhorn, S.M., Effect of Deuterium Oxide on Crack Growth in Soda-Lime Silica Glass, J. Am. Ceram. Soc. 65, C202-C203, 1982.

TABLE I.

Crack Growth Parameters for Glasses in H_2O*

Glass	E^* KCal/mole	b MKS units	ln V_o
Silica	33.1 ± 1.0	0.216 ± 0.006	-1.32 ± 0.6
Aluminosilicate 1	29.0 ± 0.7	0.138 ± 0.003	5.5 ± 0.4
Aluminosilicate 2	30.1 ± 0.6	0.164 ± 0.003	7.9 ± 0.3
Borosilicate	30.8 ± 0.8	0.200 ± 0.006	3.5 ± 0.5
Lead Alkali	25.2 ± 1.2	0.144 ± 0.006	6.7 ± 0.6
Soda-lime silica	26.0 ± 1.1	0.110 ± 0.004	10.3 ± 0.5

*After Wiederhorn and Bolz (1970)

SUMMARY

Depending on the chemical environment in which the data is obtained, crack velocity - K_I curves for glasses can consist of a number of segments of differing slope. Each segment represents a different controlling crack growth mechanism. These mechanisms can be summarized as:

I. Stressed enhanced chemical reaction between Si-O bonds and the active ingredient in the environment.

IA. Same as 1, except that changes in crack tip structure are taking place.

IB. SiO_2 dissolution rate.

II. Diffusion rate of the active ingredient to the crack tip.

III. Electrostatic reactions between polar molecules and the rupturing Si-O bond.

It has been shown that chemical rate theory can be used to explain crack growth kinetics both in Regions I and III. A molecular model for the chemical reaction between highly strained Si-O bonds and various environments has been described. This model allows one to predict whether a given chemical environment will cause enhanced crack growth in silicate glasses. In addition it was shown that electrostatic interactions between the environment and the glass determine the slope of the crack growth curve in the higher velocity, Region III, where the normally dominant effects of H_2O are absent.

tip solution is basic, i.e. where the rate is controlled by the rate of reaction of the H_3O^+ ion. However, there are still a number of unanswered questions regarding effects of pH.

Temperature Dependence

In concept, the measurement of the temperature dependence of the V-K_I curves for a glass should allow us to determine the stress free activation energy, E^* in Equation 7, and should provide information regarding the activated process. E^* can be calculated from experimental data in three ways; (1) V-K_I curves are fit to the data points at each temperature. Each curve is then extrapolated to the point $K_I = 0$, and the velocity at which this point occurs plotted versus 1/T. The slope of such a curve yields a value of E^*. Extrapolating the V-K_I curves over such long distances, however, can lead to large uncertainties. (2) The entire set of data points can be fit to Equation 7, yielding values of E^*, b, and V_o. Wiederhorn and Bolz (1970) chose to fit the V-K_I curves for various glasses in H_2O to over the temperature range of 2°-90°C, in this way obtaining the parametrs shown in Table 1. As we can see, the activation energies range between 25 and 35 KCal/mole. Whether these values of E^* are indicative of the fundamental crack growth processes is open to question, however. (3) The third technique is to assume that the stress dependence of the crack growth section is not temperature dependent (i.e. all the curves have the same slope). Then at any K_I, a plot of velocity versus 1/T yields a value of activation energy. In all cases one must be careful that the activity of the reacting environment remains constant.

SiO_2 at the same applied K_I. In addition there is the possible formation of a corrosion layer in various glasses, which would also lead to a different crack tip stress.

pH EFFECTS

As noted earlier, there is no requirement in the model for the reaction of H_2O with vitreous SiO_2 that prior dissociation of a H_2O molecule occur. This is not to say, however, that effects of variations in H_3O^+ or OH^- activity would not be expected. If the activity of one species, i.e. electron donor or proton donor, is very small compared to the other then the rate of reaction of this species should control the overall reaction rate. Figure 13a shows a V-K_I plot for vitreous SiO_2 in various acidic and basic solutions (Wiederhorn and Johnson, 1973). The slopes of these curves can be placed into two categories; those for pH of H_2O and lower (i.e. <6) are approximately the same as H_2O; those for pH >6 are shallower. The data for soda lime glass taken by the same authors (Figure 13b) shows a similar behavior. One difference is that the slope in H_2O more closely resembles that in basic solutions, probably because ion exchange produces a crack tip pH higher than that of the bulk solution. One can argue that at low pH (i.e. large values of the H_3O^+ activity) the rate of reaction at the crack tip is controlled by the activity of the OH^- species with the Si, since this would be the slowest step. Conversely, at high pH (larger activity of OH^-) the rate would be controlled by the H_3O^+ activity. This concept is supported by recent results of Wiederhorn (1982) who showed an observable effect of D_2O on the position of the V-K_I curves for soda lime silica glass only for cracks in which the crack

is not observed in the binary soda-silica system, however, (Figure 3) (Simmons and Freiman, 1981). The slope of the curve for 33% Na_2O - 67% SiO_2 in 30% r.h. air is steeper than that in H_2O. This behavior may again point to exchange mechanisms which could occur in liquid H_2O.

Position of V-K_I Curve

Even though the position and slope of a V-K_I curve are not independent of each other, as long as the slopes are not too different one can roughly compare the positions of the curves. One might predict that as the number of bridging Si-O bonds is reduced, by the addition of Na_2O for instance, that the structure would be weakened proportionally. The data in Figure 12 suggests that this is not the case. There is little if any difference between the curve for vitreous SiO_2 and that for a glass having 33% Na_2O. In addition, the critical fracture toughness of binary Na_2O-SiO_2 glasses has been shown to increase with increasing Na_2O concentration (Kennedy et al. 1975).

A possible explanation for this trend involves our use of stress intensity factor to characterize the crack tip stress field. By comparing everything in terms of K_I, an implicit assumption is that all crack tips are identical in structure. Actually, since a real material will exhibit some non linear elastic behavior below the stress at which fracture occurs, we clearly cannot use K_I to calculate stresses at distances very near the crack tip. Further, the distance from the crack tip at which breakdowns occurs, and probably the crack tip stress, will be a function of glass composition and network structure. Because of their more open structure, one might predict that glasses containing large quantities of Na_2O could reach an elastic limit at lower stresses so that the actual crack tip strain is lower than that for

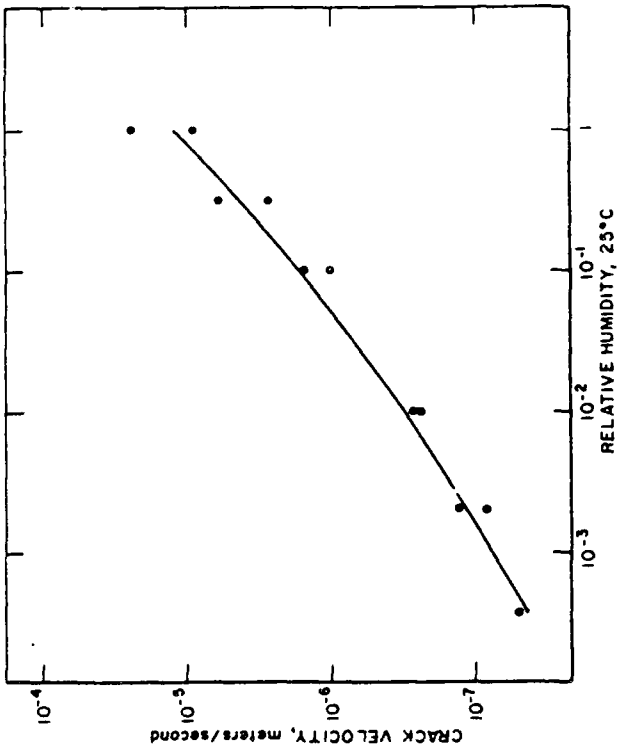
CRACK VELOCITY, meters/second
10^{-4}
10^{-5}
10^{-6}
10^{-7}
RELATIVE HUMIDITY, 25°C
10^{-1}
10^{-2}
10^{-3}

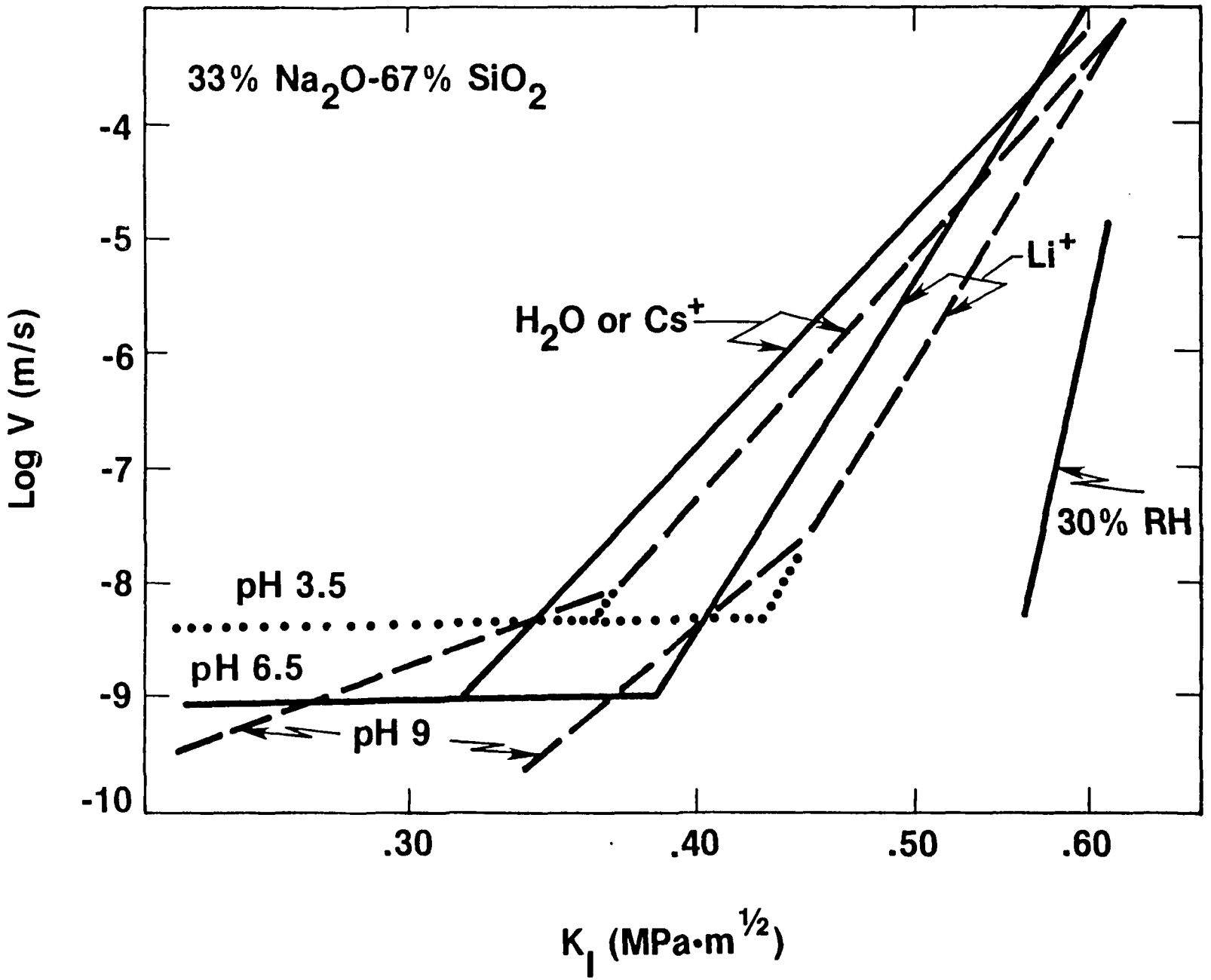
33% Na_2O-67% SiO_2
-4
-5
-6
-7
-8
-9
-10
Log V (m/s)
H_2O or Cs^+
Li^+
30% RH
pH 3.5
pH 6.5
pH 9
.30
.40
.50
.60
K_I (MPa·$m^{1/2}$)

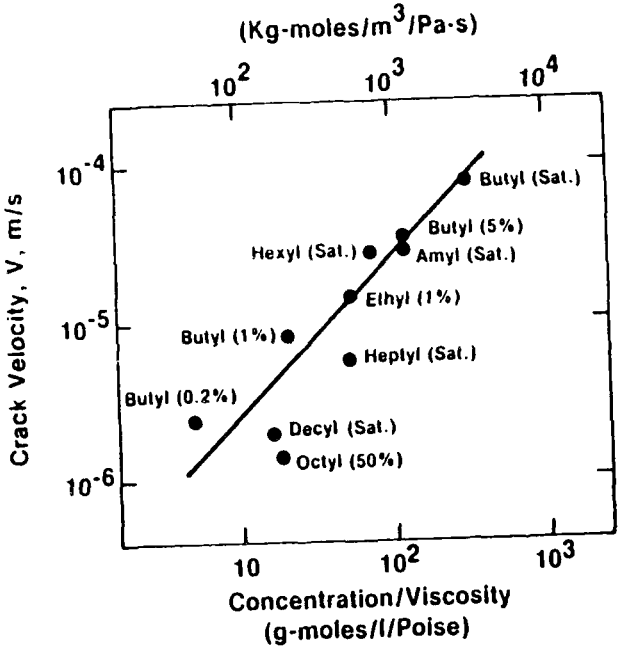
(Kg-moles/m^3/Pa·s)
10^2
10^3
10^4
10^{-4}
10^{-5}
10^{-6}
Crack Velocity, V, m/s
Butyl (Sat.)
Butyl (5%)
Hexyl (Sat.)
Amyl (Sat.)
Ethyl (1%)
Butyl (1%)
Heptyl (Sat.)
Butyl (0.2%)
Decyl (Sat.)
Octyl (50%)
10
10^2
10^3
Concentration/Viscosity
(g-moles/l/Poise)

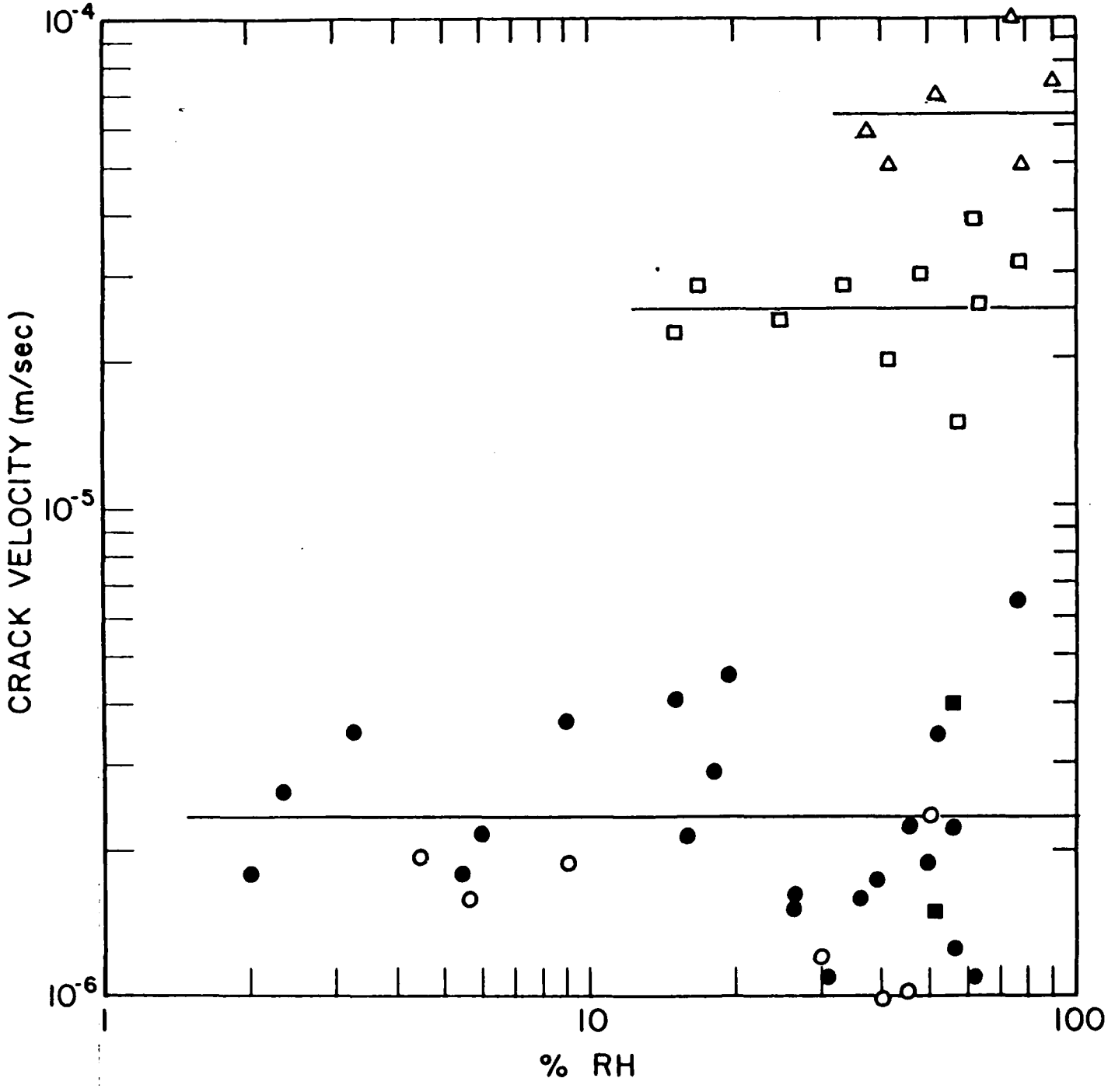
10^{-4}
10^{-5}
10^{-6}
CRACK VELOCITY (m/sec)
1
10
100
% RH

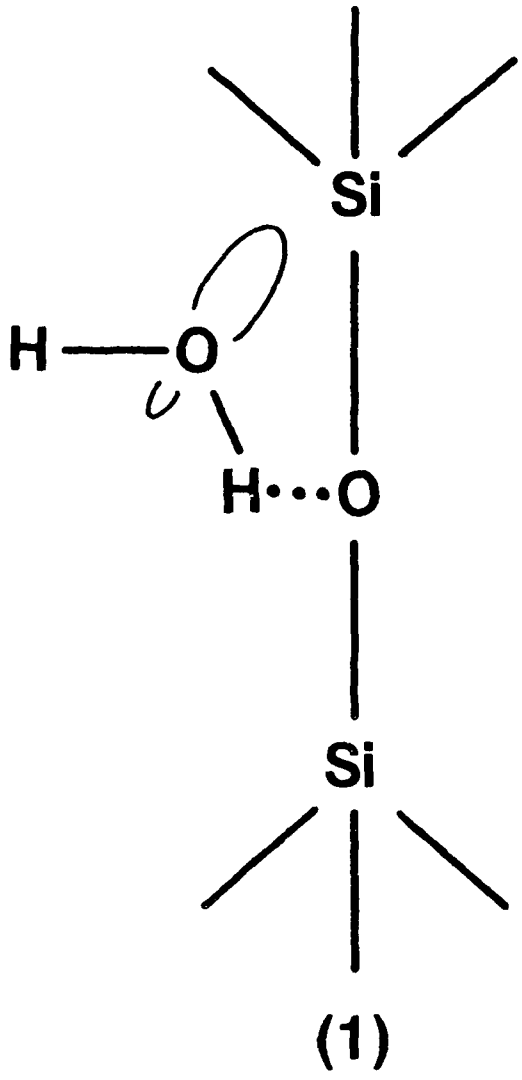

(1)

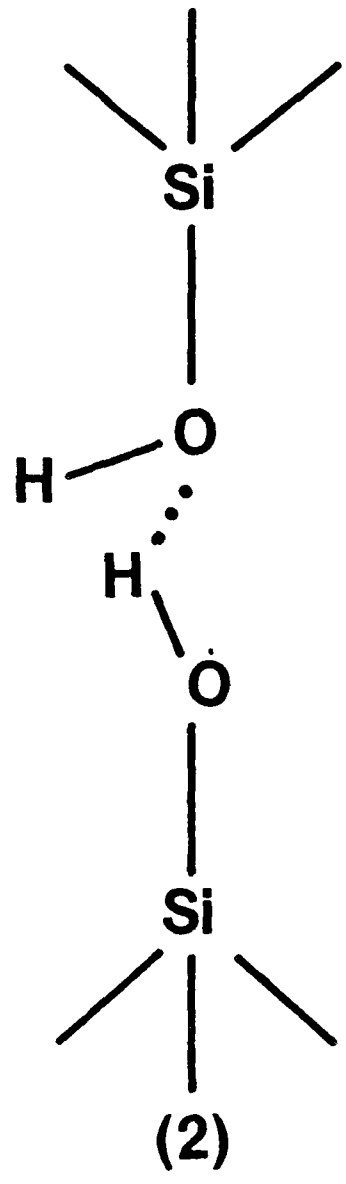

(2)

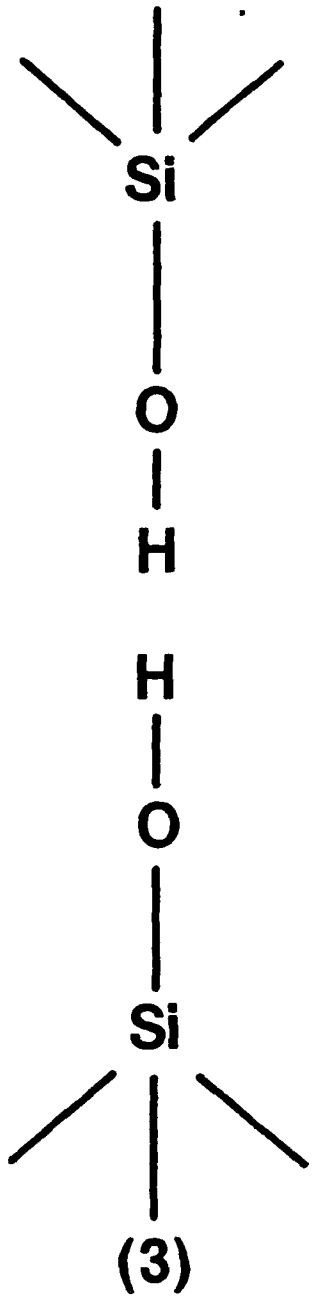

(3)

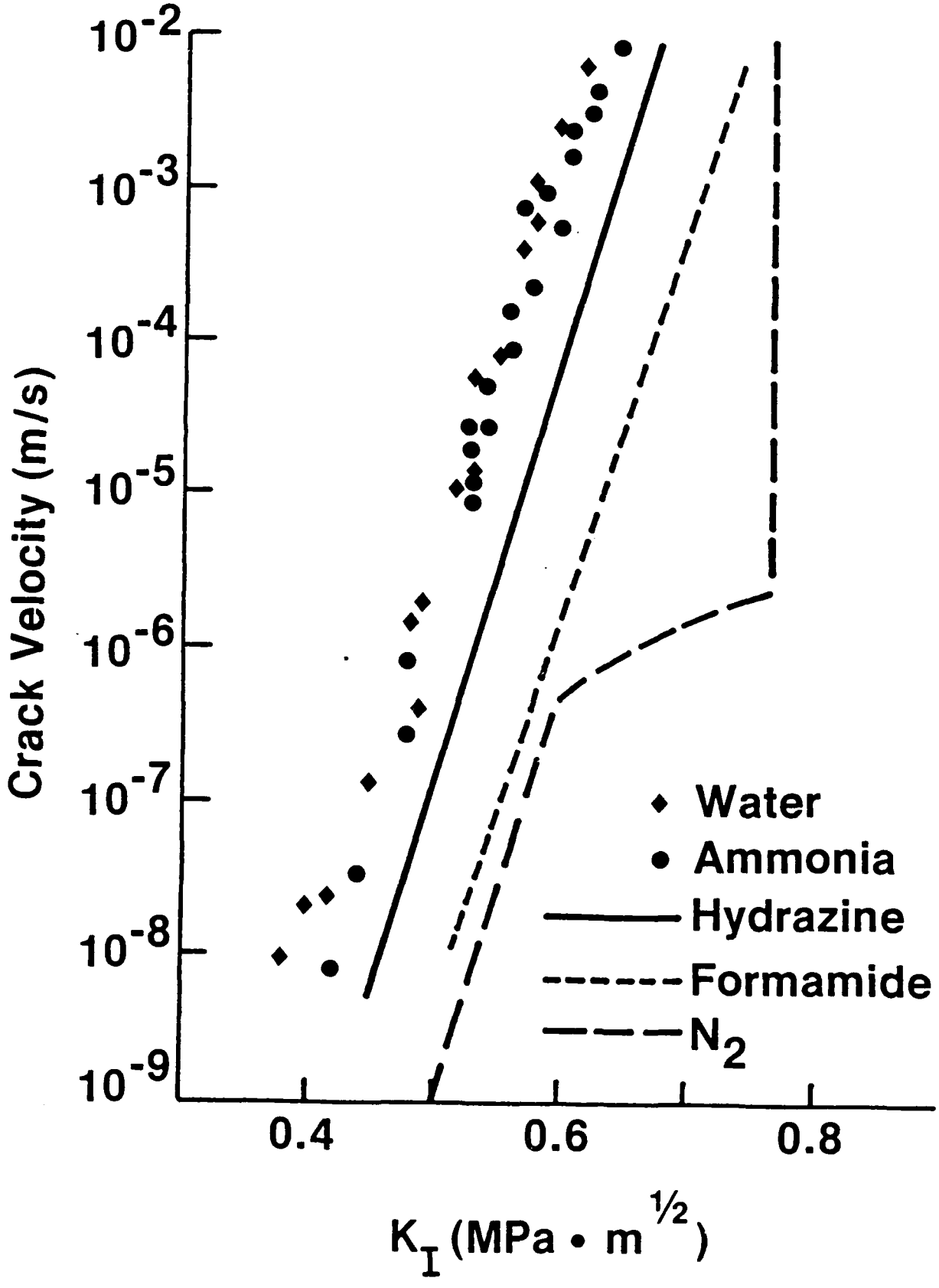
Crack Velocity (m/s)
10-2
10-3
10-4
10-5
10-6
10-7
10-8
10-9
0.4
0.6
0.8
KI (MPa • m1/2)
Water
Ammonia
Hydrazine
Formamide
N2

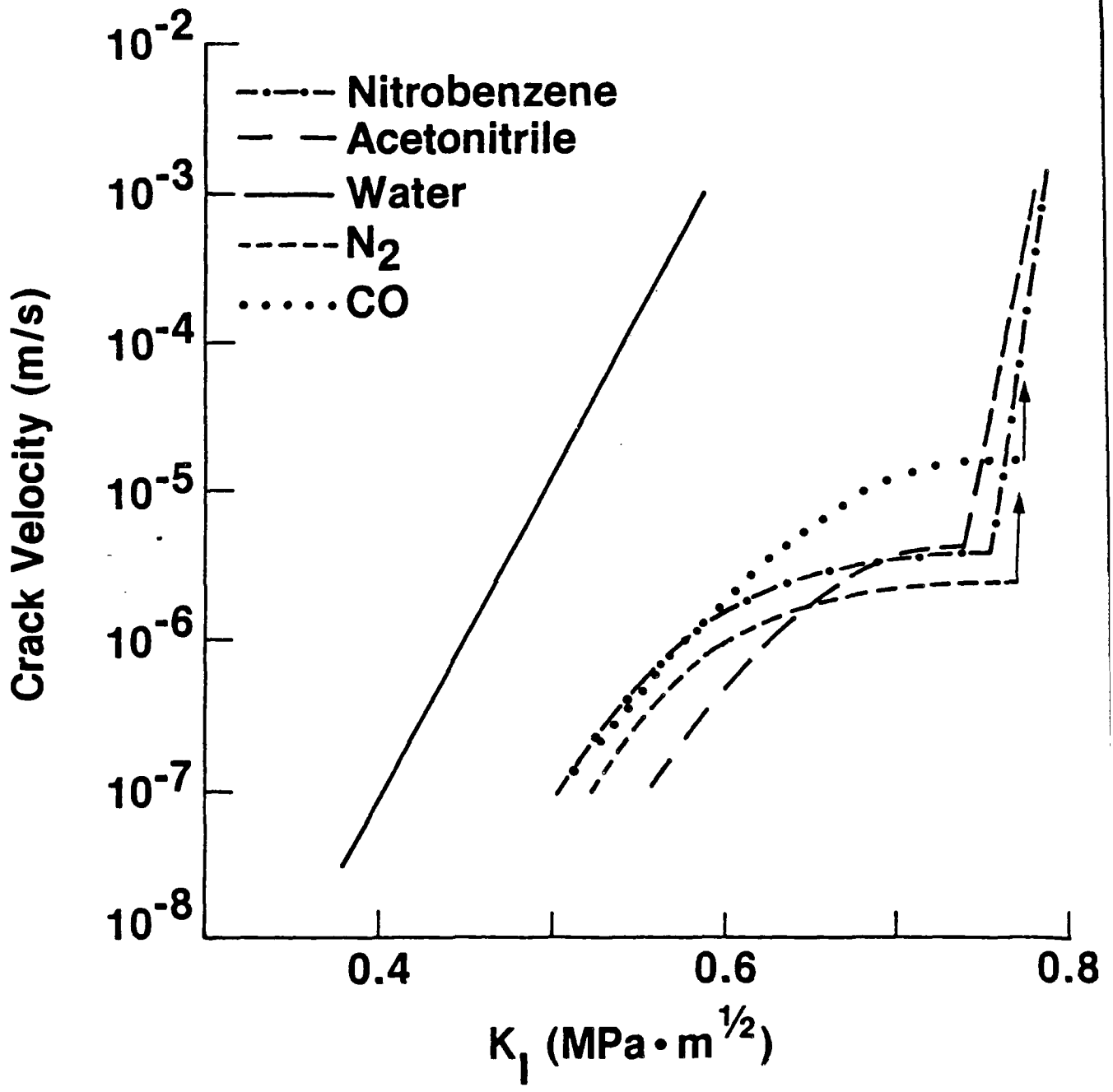
Nitrobenzene
Acetonitrile
Water
N_2
CO
Crack Velocity (m/s)
10^{-2}
10^{-3}
10^{-4}
10^{-5}
10^{-6}
10^{-7}
10^{-8}
0.4
0.6
0.8
K_I (MPa • $m^{1/2}$)

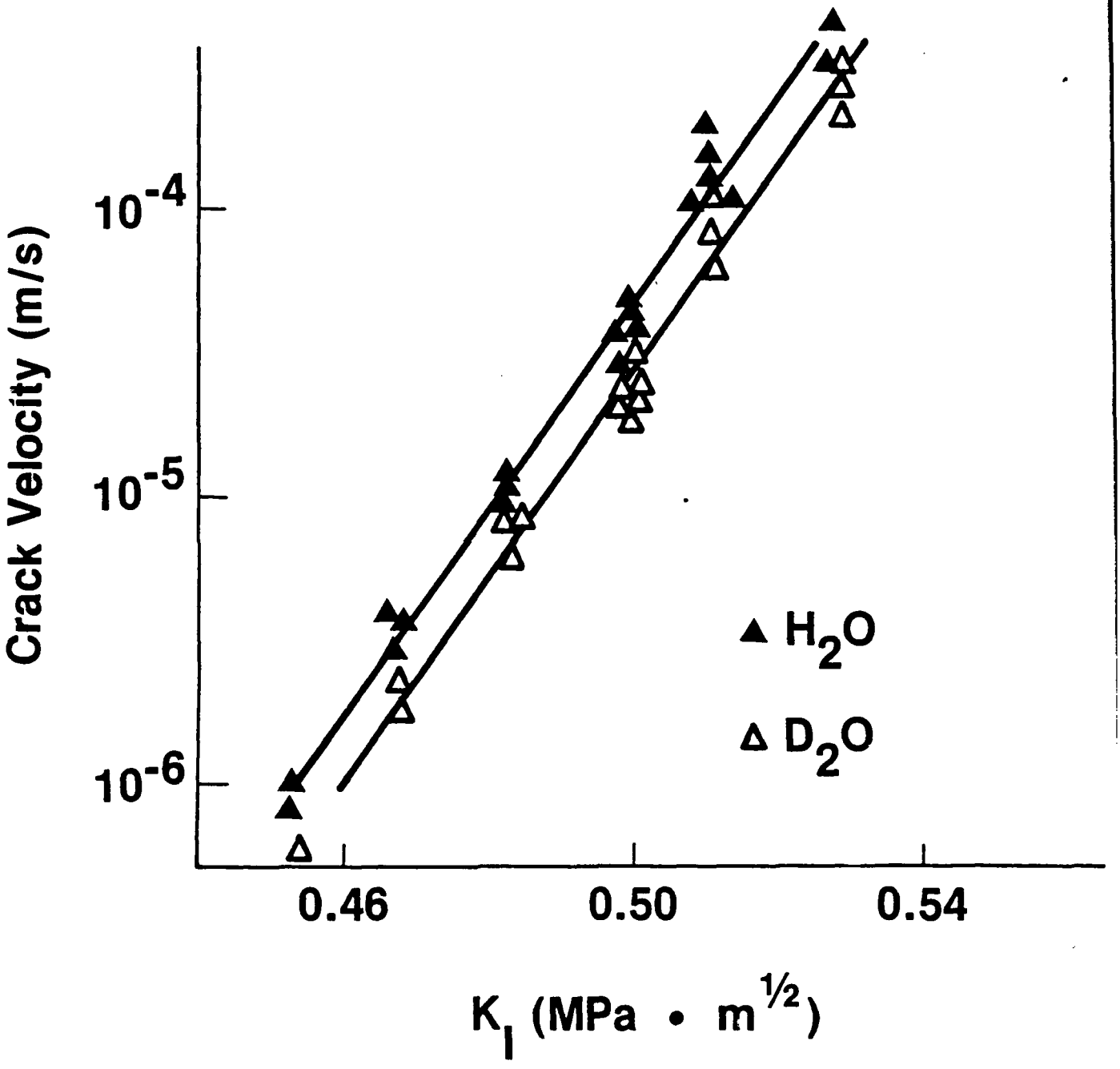
Crack Velocity (m/s)
10-4
10-5
10-6
0.46
0.50
0.54
K1 (MPa • m1/2)
▲ H2O
△ D2O

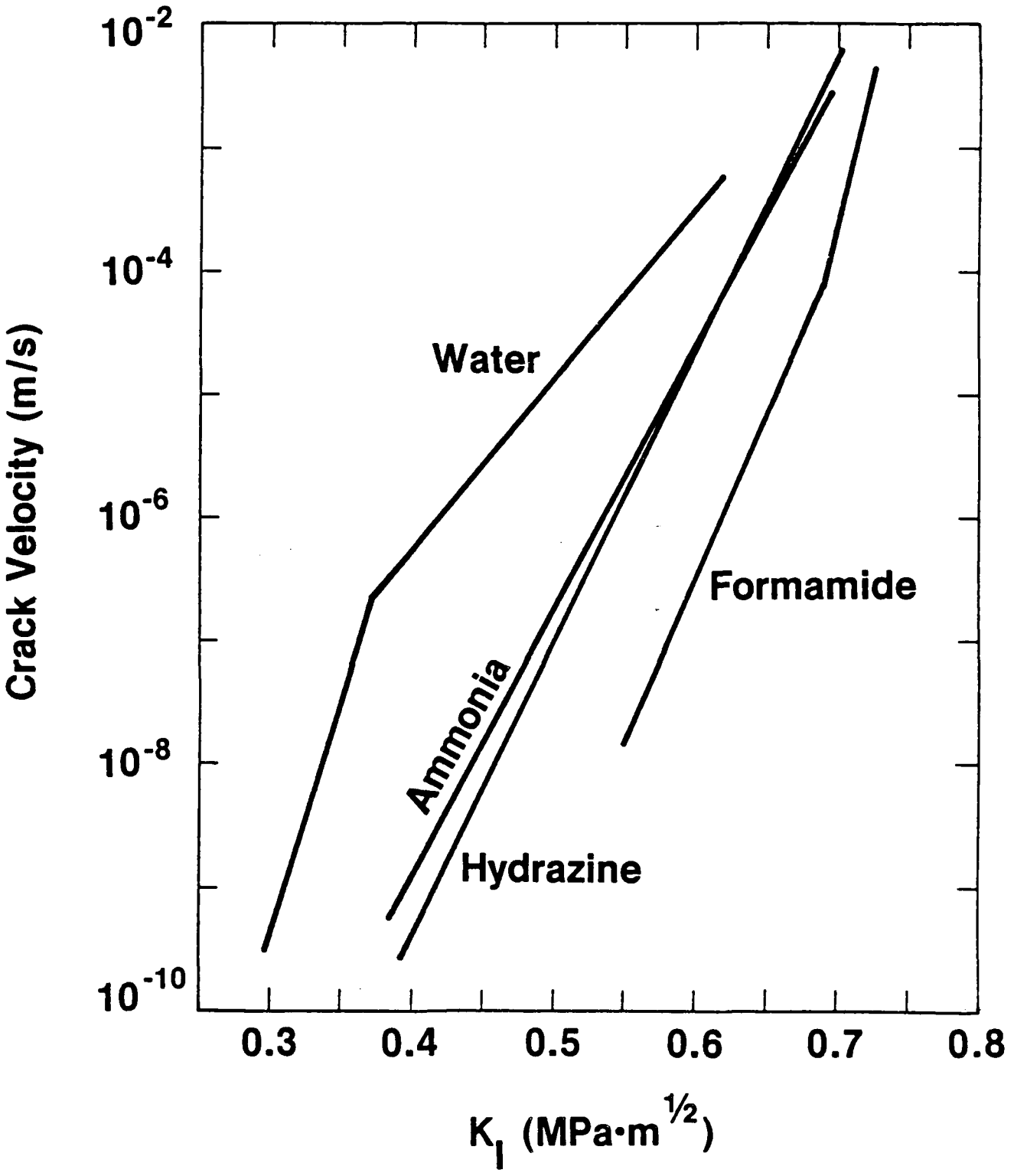
Crack Velocity (m/s)
10^-2
10^-4
10^-6
10^-8
10^-10
Water
Ammonia
Hydrazine
Formamide
0.3
0.4
0.5
0.6
0.7
0.8
K_I (MPa·m^1/2)

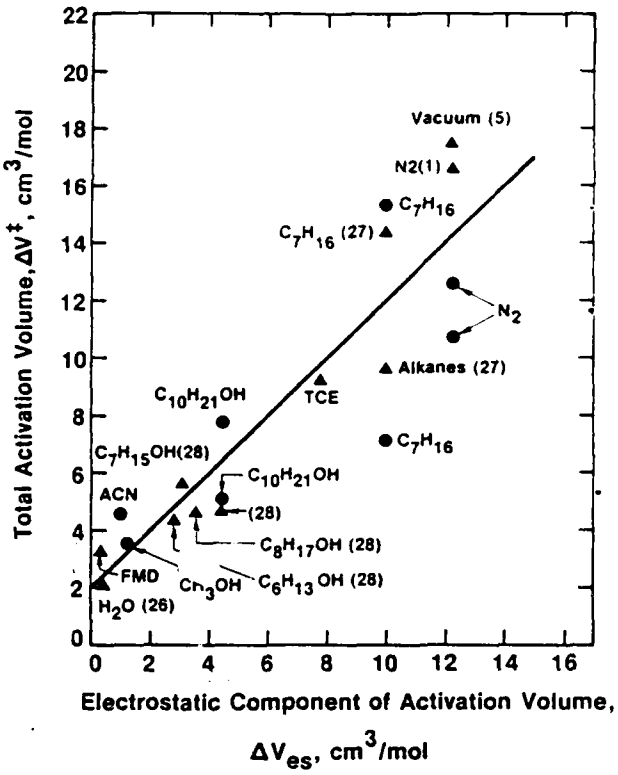
Total Activation Volume, $\Delta V^{\ddagger}$, cm^3/mol
Electrostatic Component of Activation Volume, ΔV_{es}, cm^3/mol
Vacuum (5)
N2(1)
C_7H_{16}
C_7H_{16} (27)
N_2
Alkanes (27)
$C_{10}H_{21}OH$
TCE
C_7H_{16}
$C_7H_{15}OH$(28)
$C_{10}H_{21}OH$
ACN
(28)
$C_8H_{17}OH$ (28)
FMD
Cn_3OH
$C_6H_{13}OH$ (28)
H_2O (26)

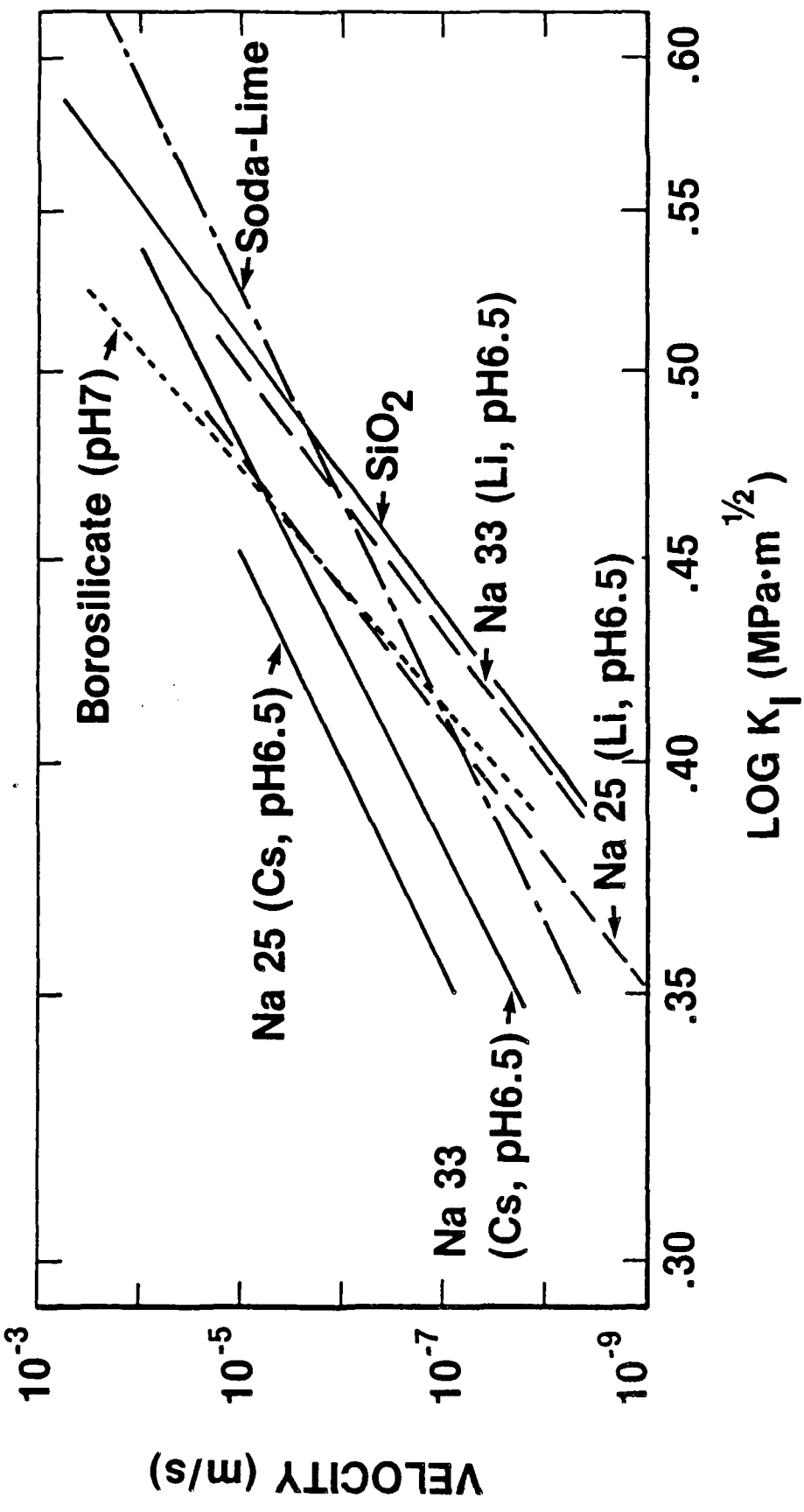
VELOCITY (m/s)
10^{-3}
10^{-5}
10^{-7}
10^{-9}
.30
.35
.40
.45
.50
.55
.60
LOG K_I (MPa·m$^{1/2}$)
Borosilicate (pH7)
Soda-Lime
SiO_2
Na 25 (Cs, pH6.5)
Na 33 (Li, pH6.5)
Na 25 (Li, pH6.5)
Na 33 (Cs, pH6.5)

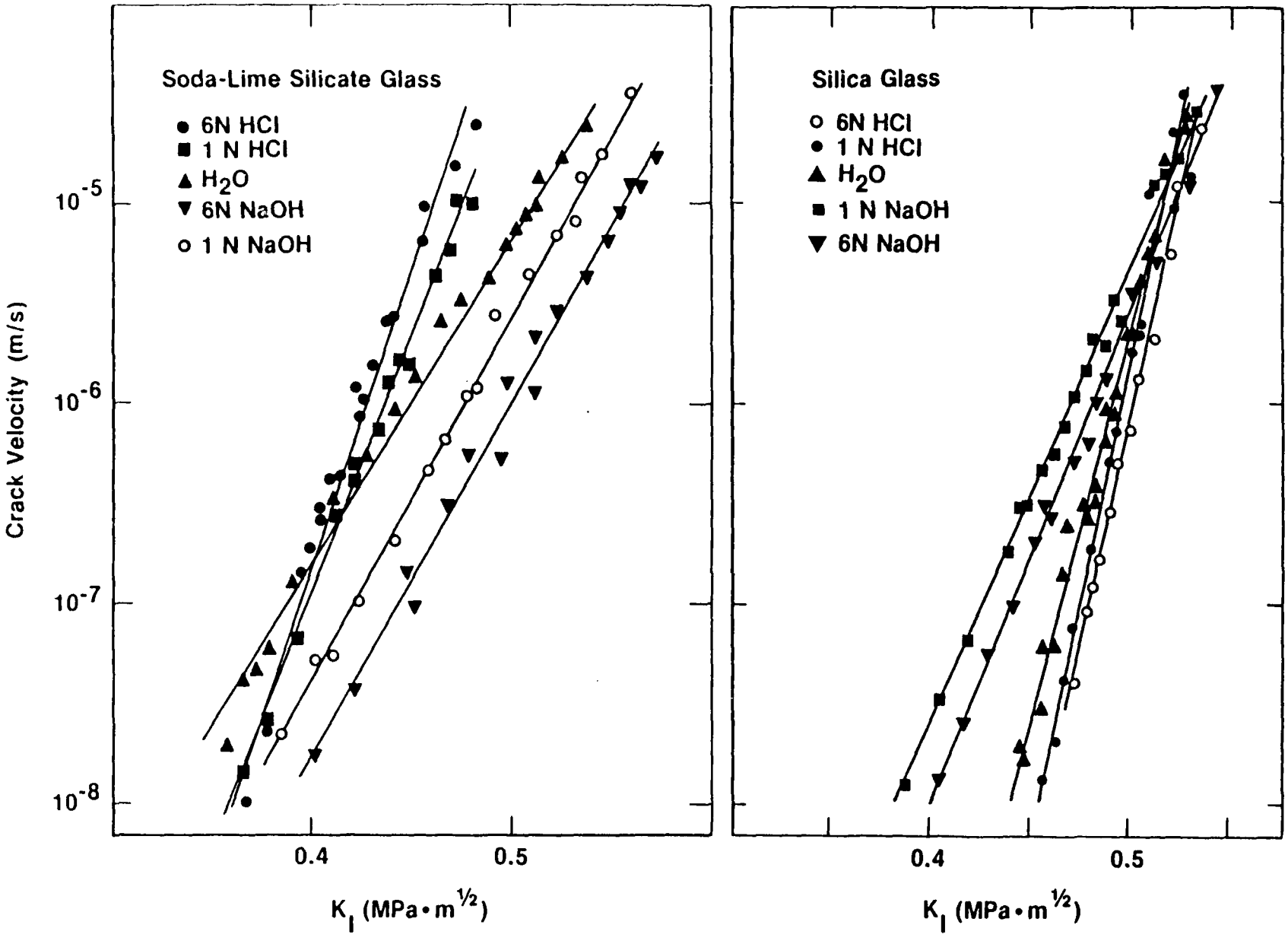
Soda-Lime Silicate Glass
6N HCl
1 N HCl
H_2O
6N NaOH
1 N NaOH
Crack Velocity (m/s)
10^{-5}
10^{-6}
10^{-7}
10^{-8}
0.4
0.5
K_I (MPa • $m^{1/2}$)
Silica Glass
6N HCl
1 N HCl
H_2O
1 N NaOH
6N NaOH
0.4
0.5
K_I (MPa • $m^{1/2}$)

Electrical Failures Due to Cracks in Multilayer Ceramic Capacitors

S.W. Freiman and A.C. Gonzalez
Inorganic Materials Division
National Bureau of Standards
Gaithersburg, MD 20899

INTRODUCTION

Cracks can occur in multilayer ceramic capacitors due to a number of factors. One of the most prevalent causes of crack formation is thermal stresses generated during the process of soldering the capacitor to a substrate. A finite element analysis[1] has shown that the differing thermal expansion coefficients of the capacitor and the substrate can lead to tensile stresses in the capacitor of the order of 55 MPa. The type of cracks that can be produced by these stresses is shown in Figure 1; these cracks frequently occur near or under the metal end caps and often extend from one electrode layer to the outside surface or to another electrode. Sources of stress other than due to soldering, e.g. evolution of gases during firing or the introduction into the green ceramic of impurities having a different thermal expansion coefficient than the bulk material, can also produce cracks[2].

A primary question is, when does a crack act as a source of electrical failure? Clearly, one way in which this can happen is for the crack to provide a shorting path. It has been suggested[3] that at low operating voltages (i.e. <5V) electrode material can diffuse down the crack producing a highly conducting short between two electrodes. If the voltage is increased to ~50 volts, the capacitor again behaves normally.

It has been hypothesized that the conducting path is vaporized by the current passing through it at the higher voltage. If the field on the capacitor is reduced again, the shorting process will be repeated.

The purpose of the current study was three-fold, (1) to establish the crack growth parameters for ceramic materials used in multilayer capacitors, (2) to determine under what conditions a crack would cause electrical failure of a capacitor and (3) to investigate the possibility that fracture mechanics models could be used to predict the lifetime of a capacitor which is subject to mechanical stresses.

EXPERIMENTAL PROCEDURE

Materials

The materials used in this study consisted of both actual commercial capacitors and ceramic material especially prepared with and without particular electrode configurations.[1] The latter were supplied as square plates (25 mm x 1.8 mm) of ceramic (composition comparable to that in a capacitor having a Z5U designation) with no included metal electrode layers or as bars (30 x 5 x 2 mm) having one metal layer located 60 μm from each 5 x 30 mm surface.

Indentation Procedures

A Vickers diamond pyramid indenter was used to introduce controlled cracks into the capacitors and capacitor materials. Critical fracture toughness measurements were made on both NPO and X7R type capacitors in air by placing an indentation between the electrode layers in a sectioned

---

[1]Specimens were prepared for this study by AVX Corporation.

AD-A155 020 STRESS CORROSION OF CERAMIC MATERIALS(U) NATIONAL BUREAU OF STANDARDS GAITHERSBURG MD INORGANIC MATERIALS DIV S W FREIMAN ET AL. MAY 85 N00014-84-F-0019 2/2

UNCLASSIFIED F/G 11/2 NL

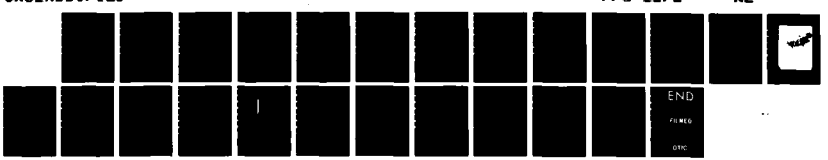

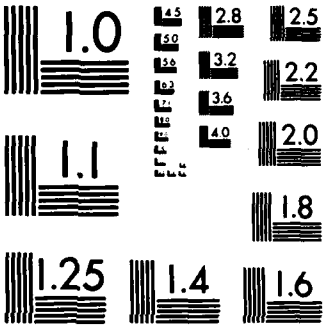

capacitor as shown schematically in Figure 2a. Crack lengths both parallel and perpendicular to the electrodes were measured in an optical microscope. The other procedure was to introduce the indentation into one face of the capacitor as shown in Figure 2b. In both cases, crack lengths were measured in an optical microscope. Values of critical fracture toughness, K_{IC}, were determined using the expressions of Anstis et al.[4]

Strength and Crack Growth Tests

Both inert strengths and subcritical crack growth behavior of the capacitor ceramic material (independent of the influence of electrodes) were determined using indentation procedures[5-7]. A Vickers indentation was placed in the center of the 25 mm squares of ceramic. These indented specimens were then fractured in bending on a universal test machine using a piston and three ball arrangement.[8] Inert strengths were measured by placing a drop of oil on the indentation site and rapidly loading the specimen to failure (<2 sec loading time). The subcritical crack growth exponent, N, was determined by performing dynamic fatigue tests in water on the indented (P = 5N) squares over ≈6 orders of magnitude in stressing rate. The failure stresses, σ, in both the inert and dynamic fatigue tests were calculated using the following expressions[8]

$$\sigma = -0.2387\ P(X-Y)/d^2 \qquad (1)$$

where

P = load at fracture

$X = (1 + \nu) \ln (B/C)^2 + [(1-\nu)/2] (B/C)^2$

$Y = (1 + \nu) [1 + \ln (A/C)^2] + (1 - \nu) (A/C)^2$

ν = Poisson's ratio = 0.21

A = radius of support circle = 10 mm

B = radius of ram = mm

C = radius of specimen = 12.5 mm (half of one side of a square)

d = specimen thickness at fracture origin

Electrical Measurements

The leakage current through a capacitor was used as a measure of the effect of any defects on its operation. A picoammeter was placed in series with the capacitor under particular applied D.C. fields (usually 50 V). The current was monitored continuously after application of the field. Some capacitance measurements were also made by placing a capacitance gauge across the capacitor.

RESULTS AND DISCUSSION

Crack Growth

Anstis et al.[4] have shown that the critical fracture toughness of single phase glasses and ceramics can be calculated from the indentation load, P, and the resulting crack length, C_o, based on the following expression:

$$K_{IC} = \xi_v^R (E/H)^{1/2} (P/C_o)^{3/2} \qquad (2)$$

where E is the elastic modulus (100 GPa), H is the hardness (8 GPa), and ξ_V^R is an empirical constant, calculated from a fit to K_{IC} data for many ceramics to be .016.[4] Based on Equation 2, a logarithmic plot of crack length versus indentation load should be a straight line of slope 3/2 as shown by the dashed line in Figures 3a and 4a, along with the crack lengths measured on the NPO and X7R capacitors. At crack lengths less than 1/2 the electrode spacing, good agreement between the indentation model and the data is achieved. At higher indentation loads, the measured values of crack lengths both parallel and perpendicular to the electrode layers deviate from those predicted in both type of capacitors. The cracks parallel to the electrodes are somewhat longer than predicted, while those perpendicular to the electrode layers, are actually stopped by these layers up to fairly large values of indentation load. In some cases they did not pop through the electrode at the point at which they entered, but reinitiated into the ceramic at some other location along the electrode. The increased length of the set of cracks parallel to the electrodes can be ascribed to relaxation of the stress rate of the crack because of the presence of the free surfaces.

The values of K_{IC} calculated from Equation 2 will reflect these deviations from normal indentation behavior, Figures 3b and 4b. However, when there is interaction between the crack and the second phase electrodes, there is question whether the absolute value of K_{IC} has any meaning, since the assumptions regarding linear elasticity at the crack tip are probably no longer valid. However, the relative values of K_{IC} are indicative of the ability of the metal layers in the capacitor to impede crack growth.

In order to determine the role of cracks in electrical breakdown, the leakage current was monitored for as-received NPO type capacitors as well as for those in which a 30N indentation load had been placed in the surface perpendicular to the electrode layers (Figure 2b). An indentation load of 30N was chosen because this load would produce a crack sufficiently large to cut through two electrode layers.

The leakage current at a 50V imposed field for a typical unindented capacitor varies with time as shown in Figure 5a. There was no measurable effect of introducing a 100% R.H. environment into the test chamber during the test. In contrast, Figure 5b shows that for capacitors containing a 30N indentation, introduction of a 100% R.H. environment produces a small but measurable increase in leakage current. In order to determine whether a more highly conductive path would cause more significant changes in current, a drop of 1M NaCl solution was placed on the indentation while the test was in progress. The presence of this solution produced an almost instantaneous five orders of magnitude increase in current Figure 5b). Removal of the solution from the surface and reintroduction of a dry N_2 atmosphere did not reduce the current levels over times up to hours.

Because of the strong effect of this NaCl solution on the leakage current, it was thought that the use of this solution might provide a means of discriminating between cracked and uncracked capacitors. A blind study was conducted in which one person indented 3 of 10 capacitors with a 30N load. The 10 capacitors were then randomized, soaked in 1M NaCl solution for one minute, washed sequentially in water, alcohol and acetone, dried, then placed in the electrical test chamber. The individual making the electrical measurements picked out the three

indented specimens based on their significantly increased leakage current as shown in Figure 6. The use of the "methanol test" which has been reported to discriminate between cracked and uncracked capacitors[9], produced no difference in current between indented and unindented capacitors.

In order to determine whether the presence of a highly conducting medium is a requirement to produce large current increases, a set of fifty capacitors were indented using a 30N load and placed in the chamber at 100% R.H. under a 3V DC applied field. After one week the leakage current on ten of the capacitors was greater than 10^{-4} A. The currents on the remaining forty capacitors had not risen above 10^{-11} A.

Crack Growth and Electrical Failure

The subcritical crack growth characteristics for a capacitor ceramic (Z5U) were obtained by performing dynamic fatigue tests on indented (5N) plates of the material in water. A plot of strength as a function of stressing rate is shown in Figure 7. The slope of this curve yielded a value of N of 43.7, where N is the exponent in the empirical relationship

$$V = V_o \left(\frac{K_I}{K_{IC}}\right)^N \qquad (3)$$

in which V is crack velocity, K_I is stress intensity factor and A is a constant. Based on Equation 3, an expression can be derived which can be used to predict the times to failure, T_f, of capacitor materials held under a constant applied stress, σ_a.

$$T_f = B\, S_i^{N-2}\, \sigma_a^{-N} \qquad (4)$$

where B is a constant and S_i is the initial strength of the material, i.e. the strength measured under conditions where no subcritical crack growth will occur. The data from Figure 7 is transformed into a such a time to failure plot in Figure 8. It should be recognized that the presence of electrodes in an actual capacitor may change the position of the curve in Figure 8, because of the crack-electrode interactions noted earlier, but the value of N should not be affected.

One of the objectives of this study was to determine whether the growth of cracks could be detected through changes in the electrical properties of the capacitor. The specimen design and electrical arrangement used to perform these tests are shown in Figure 9a. The circuit was designed so that the growth of a crack from the indentation to the electrode located 60 μm below the surface would produce a short. The drop of NaCl solution at the indentation assured that a conducting path would form as the crack grew. A 3N indentation load was chosen and the applied field was 50V DC. The 3N load was chosen in order to insure that the crack was shorter than 60 μm but long enough so that mechanical failure would not occur before the crack reached 60 μm in length. The specimens were loaded at a rate of .03 MPa/sec. Because there is some variability in the crack length produced by an indentation, some specimens exhibited immediate shorting while others broke before any change in current occurred. The data shown in Figure 9b represents the thirteen tests in which a change in current was measured before failure took place. It is not clear why the data is so noisy. Nevertheless, there is a

definite increase in current beginning between 1000 and 2000 sec. One can hypothesize that this time represents that needed for the crack to grow from its initial size, ≈45 μm, to the electrode, ≈60 μm.

Calculations of crack extension were performed using the model developed by Fuller et al.[10] for dynamic fatigue of indentation induced cracks. A numerical integration was performed for the expression:

$$\frac{dC}{dT} = [.25C^{3/2} + .75\ S_a\ TC^{1/2}]^N \qquad (5)$$

where $C = C/C_m$, $S_a = \frac{\sigma_a}{\sigma_m}$, and $T = t\ V_o/C_m$

in which C is crack length, σ_a is applied stress, t is time, and C_m and σ_m represent the strength and corresponding crack size measured under inert conditions.

The following values for the crack growth parameters needed for the time prediction were used in the calculations:

$$N = 43.7,\ K_{IC} = .75\ MPa{\cdot}m^{1/2},\ \sigma_m = 63\ MPa,\ V_o = 0.1$$

C_m was calculated from the expression[11]

$$C_m = \left(\frac{K_{IC} + 0.68}{2.02\ \sigma_m}\right)^2 \qquad (6)$$

$$= 1.1 \times 10^{-4}\ m$$

Using these values, Equation 5 was numerically integrated over the range from 45 μm to 60 μm for a stressing rate of .03 MPa/sec. This integration yielded a time of 800 sec. which is within a factor of 3 of the time in which the current use occurs in Figure 9. Because of the extreme sensitivity of the calculation to the crack growth parameters this agreement should be considered to be quite good.

SUMMARY

Electrical breakdown of multilayer ceramic capacitors has been demonstrated to occur when both a crack long enough to intersect two electrodes and an environment which can provide a conducting path are present. Based on this premise, it was shown that a test could be developed which would discriminate between good capacitors and those which were already cracked.

Fracture mechanics data was taken on Z5U capacitor material. This data was used to predict the time required for a crack in a capacitor to grow to a length sufficient to cause a significant rise in the leakage current.

ACKNOWLEDGEMENTS

This work was performed under a contract to the Office of Naval Research (Contract No. N00014-84-F-0019). The support of our contract monitor, Dr. R.C. Pohanka is gratefully acknowledged. We would also like to express our appreciation of Lisa Kelley of the AVX Corp. who supplied

many of the specimens, without which this work could not have been performed. The helpful advice of G.S. White during the course of this work is also appreciated.

REFERENCES

1. Draper Report.
2. S. Ropiak, "Characteristics of Low Voltage Ceramic Capacitor Failures", pp. 231-37, The Reliability of Multilayer Ceramic Capacitors, National Materials Advisory Board, Publication NMAB-400, National Academy Press, Washington, DC (183).
3. K. Sato, Y. Ogato, K. Ohno, and H. Ikeo, "Mechanisms of Ceramic Capacitor Leakage Failures Due to Low Stress", Proceedings of the 18th International Reliability Physics Program, 212-217 (1980).
4. G.R. Anstis, P. Chantikul, B.R. Lawn, and D.B. Marshall, "A Critical Evaluation of Indentation Techniques for Measuring Fracture Toughness: I, Direct Crack Measurements", J. Am. Ceram. Soc. 64 [9], 533-38 (1981).
5. P. Chantikul, G.R. Anstis, B.R. Lawn, and D.B. Marshall, "A Critical Evaluation of Indentation Techniques for Measuring Fracture Toughness: II, Strength Method", J. Am. Ceram. Soc. 64 [9], 539-43 (1981).
6. B.R. Lawn, D.B. Marshall, G.R. Anstis and T.P. Dabbs, "Fatigue Analysis of Brittle Materials Using Indentation Flaws: I", J. Mater. Sci. 16 [10], 2846-54 (1981).
7. R.F. Cook, B.R. Lawn, and G.R. Anstis, "Fatigue Analysis of Brittle Materials Using Indentation Flaws: II", J. Mater. Sci. 17 [4], 1108-16 (1982).

8. J.B. Wachtman, Jr., W. Capps and J. Mandel, "Biaxial Flexure Tests of Ceramic Substrates", J. of Materials, JMLSA, 7 [2], 188-94 (1972).

9. R.C. Chittick, E. Gray and J.H. Alexander, "Non-destructive Screening for Low-Voltage Failure in Multilayer Capacitors", Proc. of the 3rd Annual Capacitor and Resistor TEchnology Symposium (1983).

10. E.R. Fuller, Jr., B.R. Lawn, and R.F. Cook, "Theory of Fatigue for Brittle Flaws Originating from Residual Stress Concentrations", J. Am. Ceram. Soc. 66 [5] 314-20 (1983).

11. R.F. Cook and B.R. Lawn, "A Modified Indentation Toughness Technique", J. Am. Ceram. Soc. 66 [11], C200-C201 (1983).

FIGURE CAPTIONS

Figure 1. Typical crack found near the end cap in capacitors (30X). Photograph supplied by W.L. Robbins of C.S. Draper Lab.

Figure 2. Schematics of indentation locations in capacitors:
(a) Side face of sectioned capacitor; cracks will grow either parallel or perpendicular to electrode layers.
(b) Top face; cracks always cut electrodes.

Figure 3. Indentation crack length data for NPO type capacitors.
(a) Crack length as a function of indentation load for cracks parallel (●) and perpendicular (●) to the electrodes. The dashed line represents the crack lengths predicted from Equation 2.
(b) Hardness (□) and K_{IC} both parallel (●) and perpendicular (0) to the electrodes.

Figure 4. Indentation crack length data for X7R type capacitors.
(a) Crack length as a function of indentation load for cracks parallel (●) and perpendicular (0) to the electrodes. The dashed line represents the crack lengths predicted from Equation 2.
(b) Hardness (□) and K_{IC} both parallel (●) and perpendicular (0) to the electrodes.

Figure 5. Leakage current measured as a function of time for NPO type capacitors both with and without indentations in different environments.
(a) Unindented capacitor measured in dry N_2 gas followed by introduction of N_2 gas saturated with H_2O.
(b) Indented capacitor measured in same environments as in (a) followed by contact with 1N NaCl solution. Note that removal of NaCl solution from the surface and reintroduction of dry N_2 did not cause any lowering of the current.

Figure 6. Comparison of leakage current for indented and unindented capacitors in 1N NaCl solution.

Figure 7. Dynamic fatigue curve for Z5U ceramic. A crack growth exponent, N = 43.7, was calculated from this data.

Figure 8. Translation of data from Figure 7 into a time to failure versus stress plot via Equation 4.

Figure 9. Electrical degradation of model capacitors under stress.
(a) Schematic of experimental set-up.
(b) Leakage current from the model capacitor as a function of increasing load and time. Stressing rate = .03 MPa/sec.

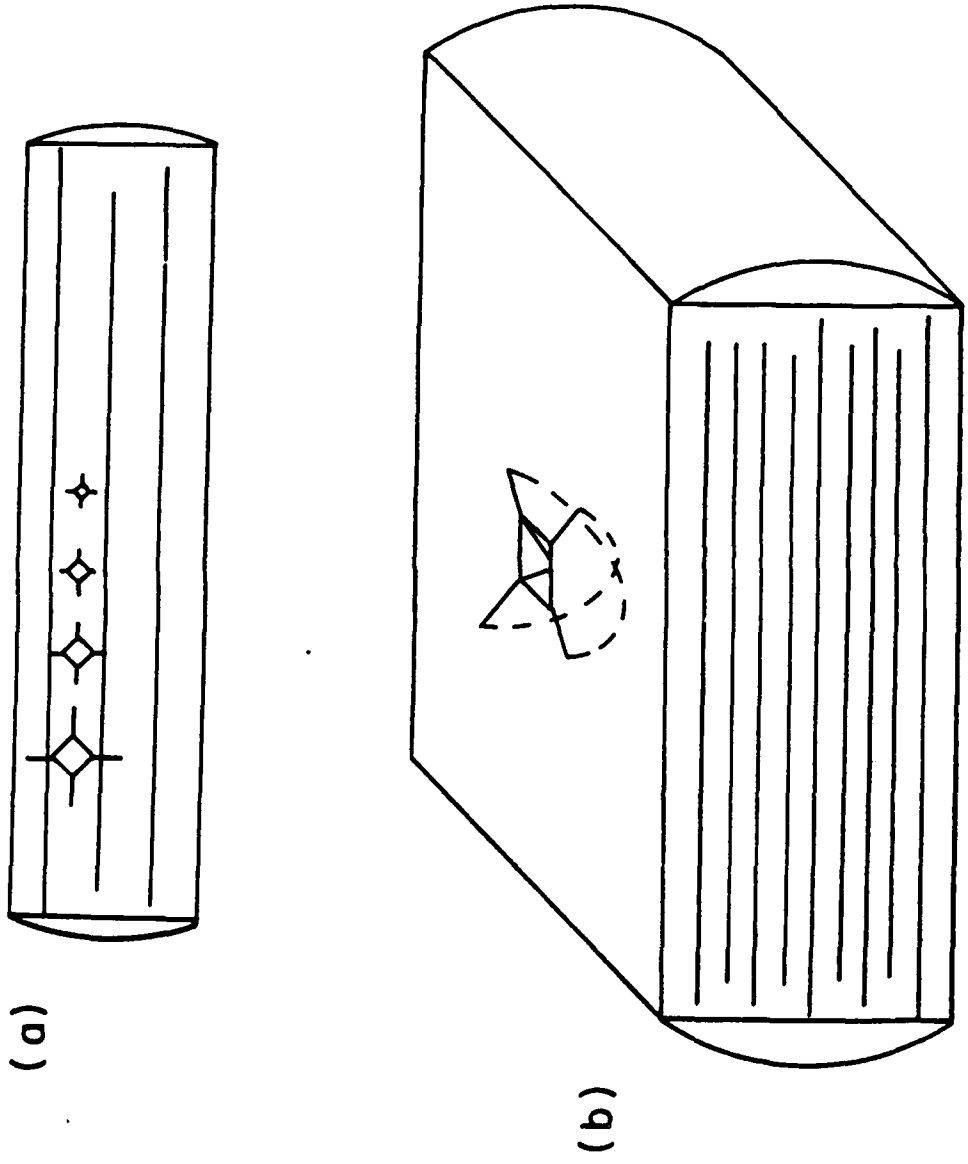
(a)
(b)

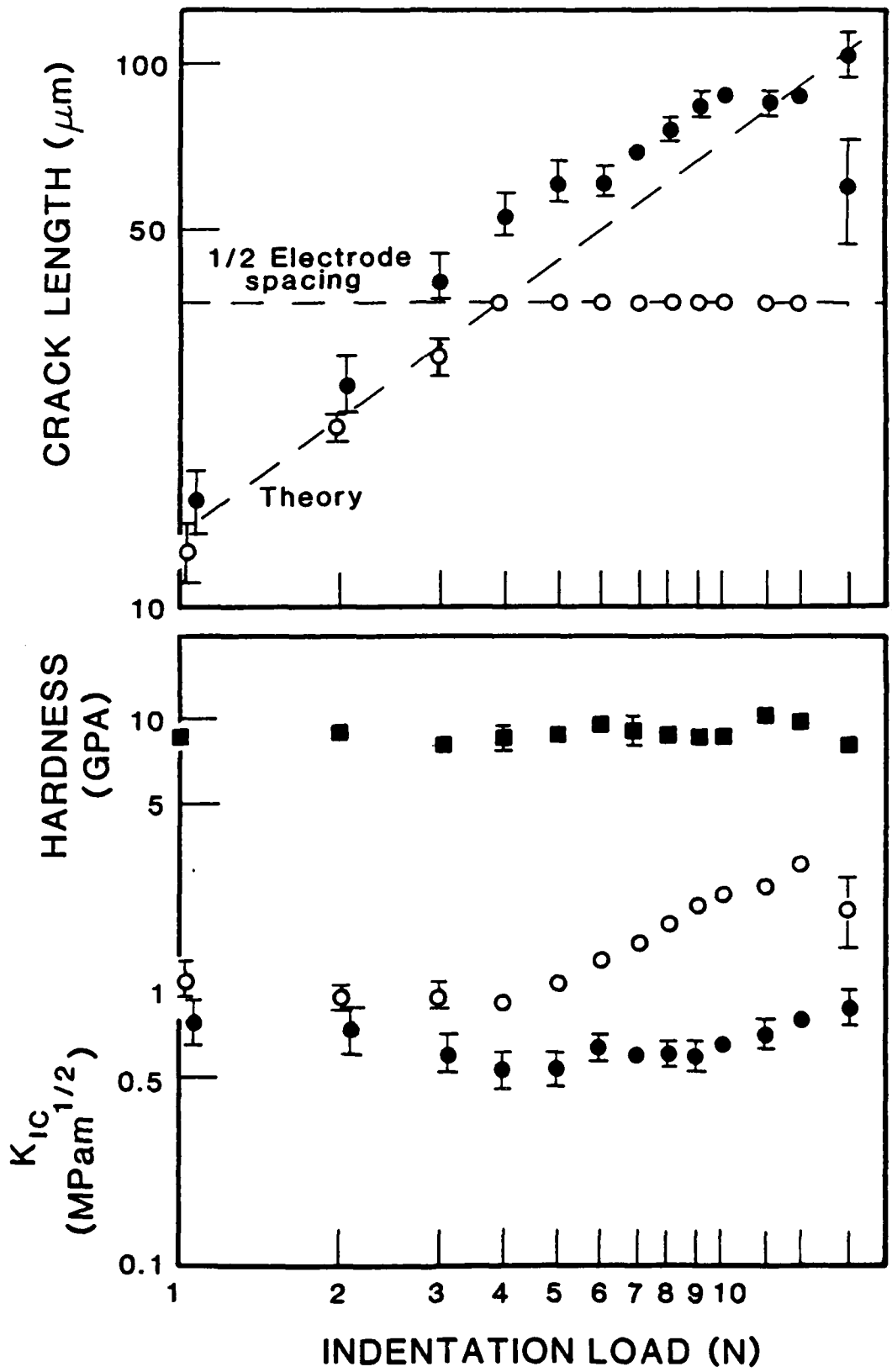
CRACK LENGTH (μm)
100
50
10
1/2 Electrode spacing
Theory
HARDNESS (GPA)
10
5
1
0.5
0.1
K_{IC} ($MPam^{1/2}$)
1
2
3
4
5
6
7
8
9
10
INDENTATION LOAD (N)

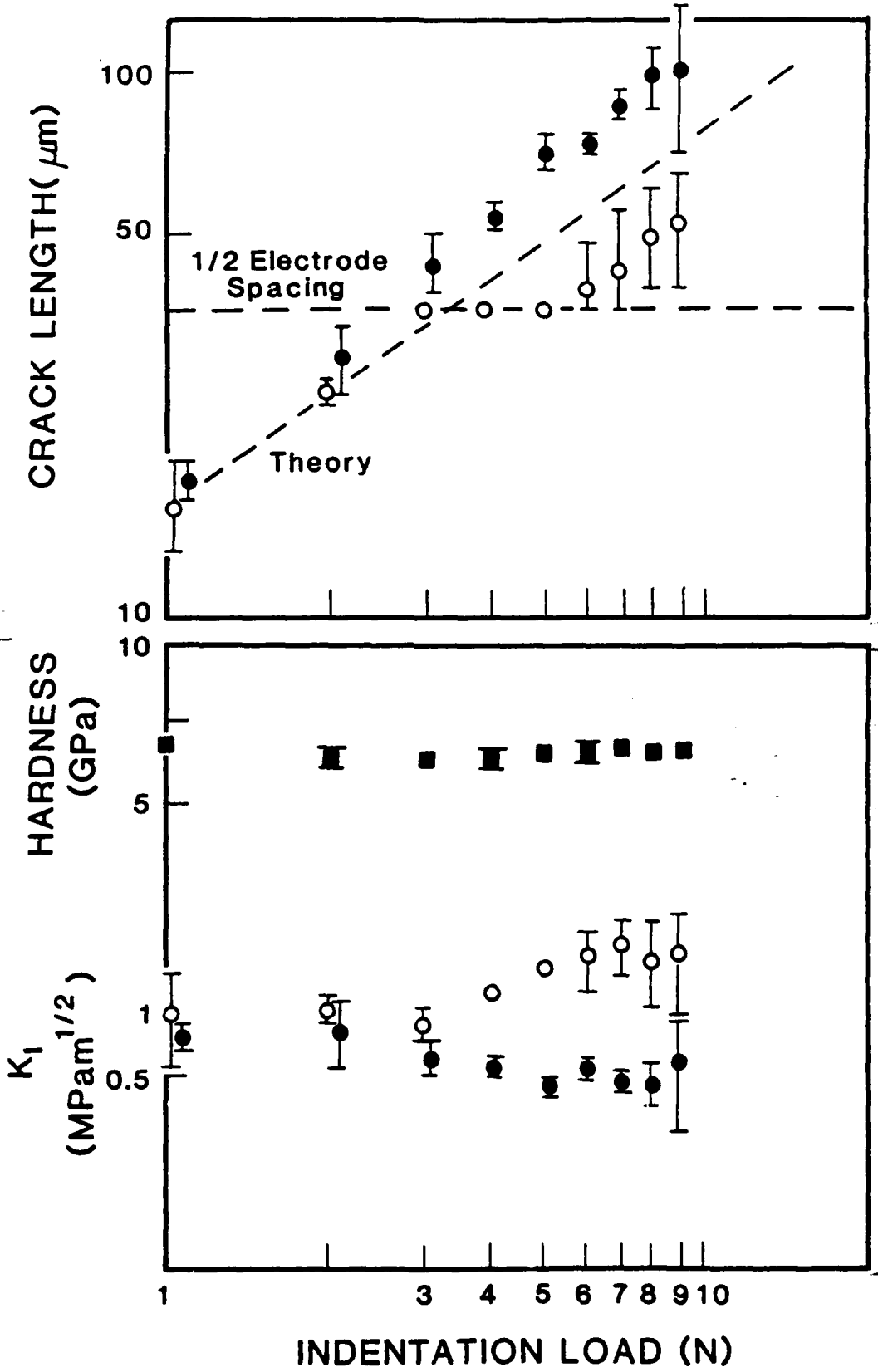
CRACK LENGTH(μm)
100
50
10
1/2 Electrode Spacing
Theory
HARDNESS (GPa)
10
5
K_I ($MPam^{1/2}$)
1
0.5
1
3
4
5
6
7
8
9
10
INDENTATION LOAD (N)

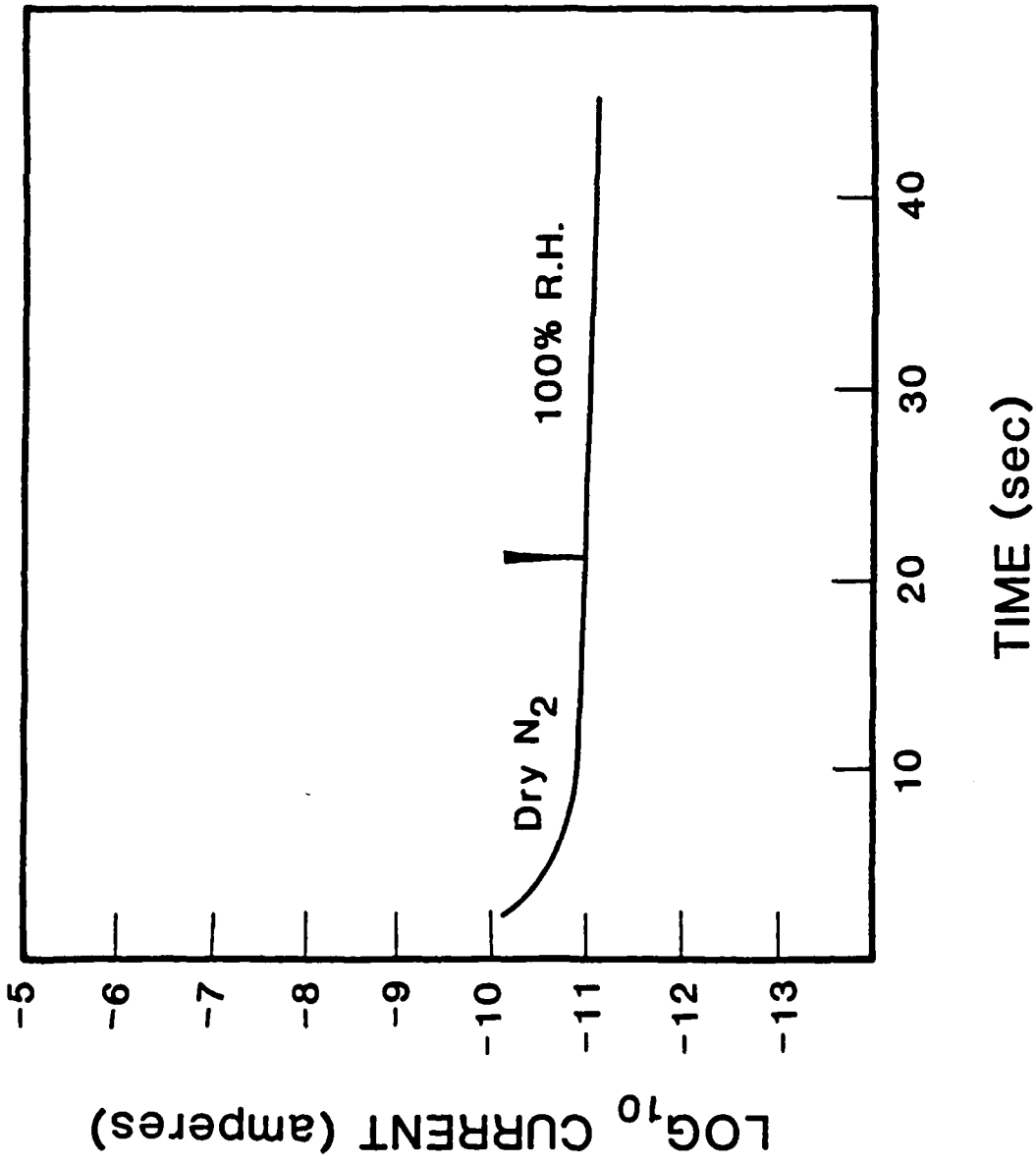
LOG10 CURRENT (amperes)
-5
-6
-7
-8
-9
-10
-11
-12
-13
Dry N2
100% R.H.
10
20
30
40
TIME (sec)

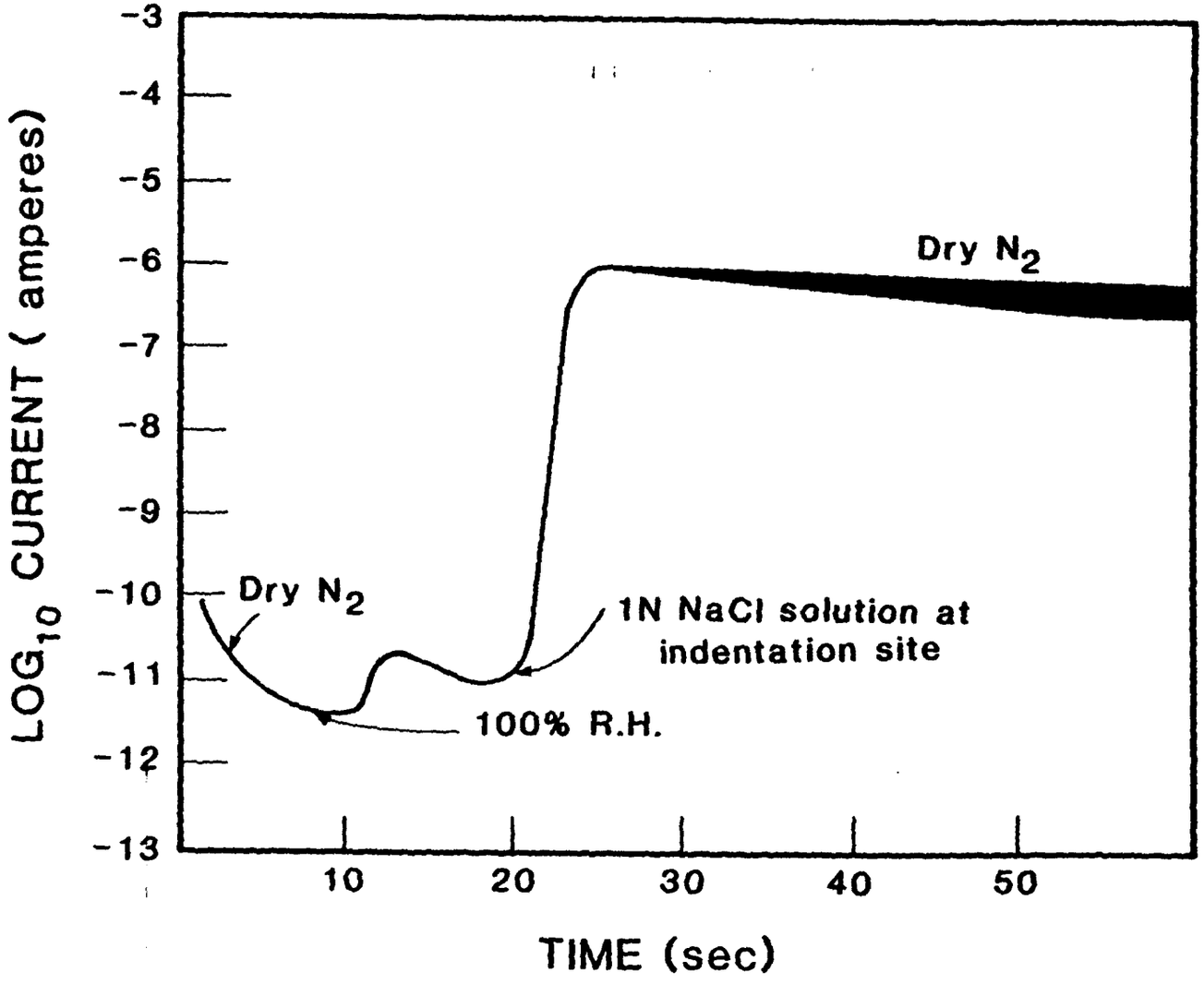
-3
-4
-5
-6
-7
-8
-9
-10
-11
-12
-13
LOG10 CURRENT (amperes)
Dry N2
Dry N2
1N NaCl solution at
indentation site
100% R.H.
10
20
30
40
50
TIME (sec)

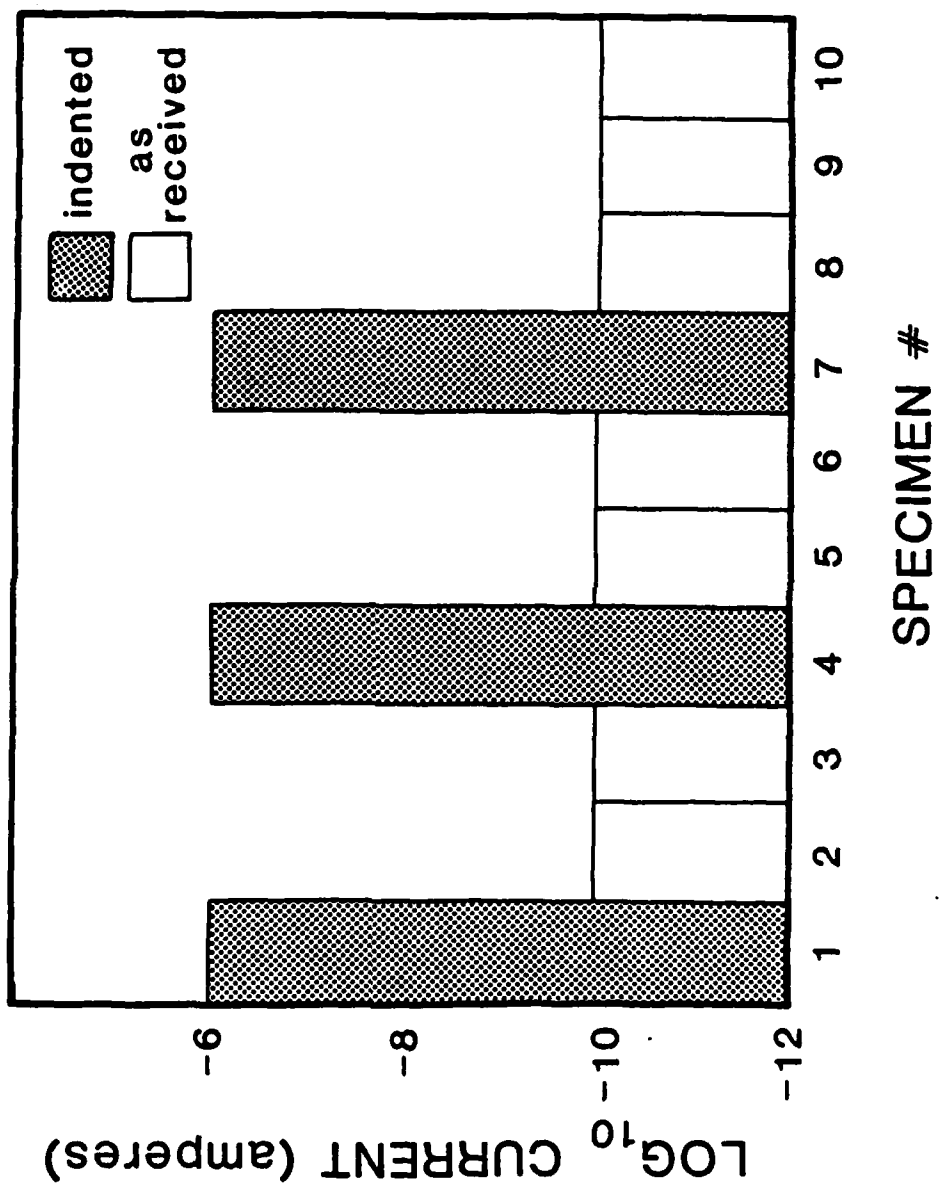
indented
as received
-6
-8
-10
-12
LOG10 CURRENT (amperes)
1
2
3
4
5
6
7
8
9
10
SPECIMEN #

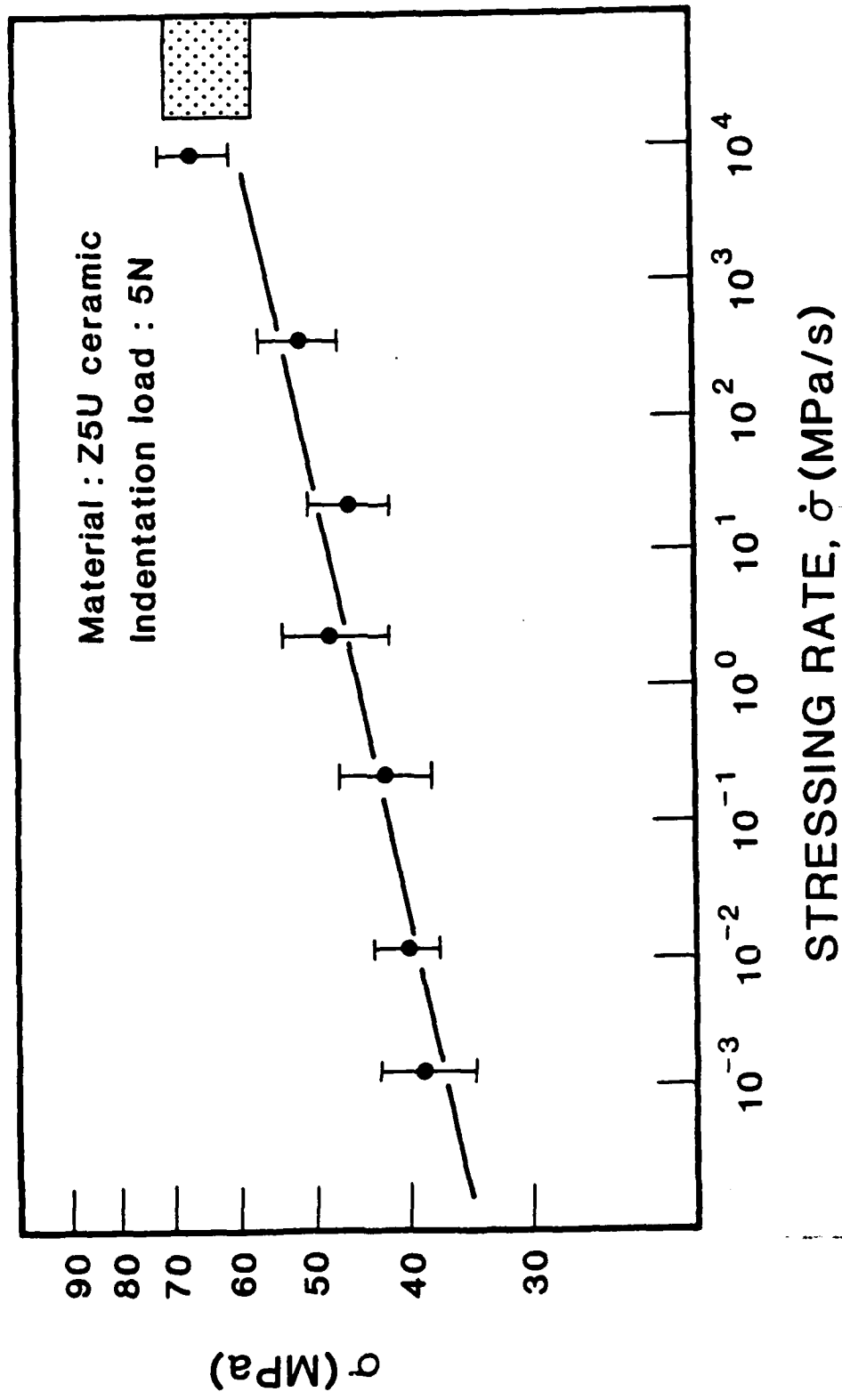
Material : Z5U ceramic
Indentation load : 5N
σ (MPa)
90
80
70
60
50
40
30
STRESSING RATE, σ̇ (MPa/s)
10^-3
10^-2
10^-1
10^0
10^1
10^2
10^3
10^4

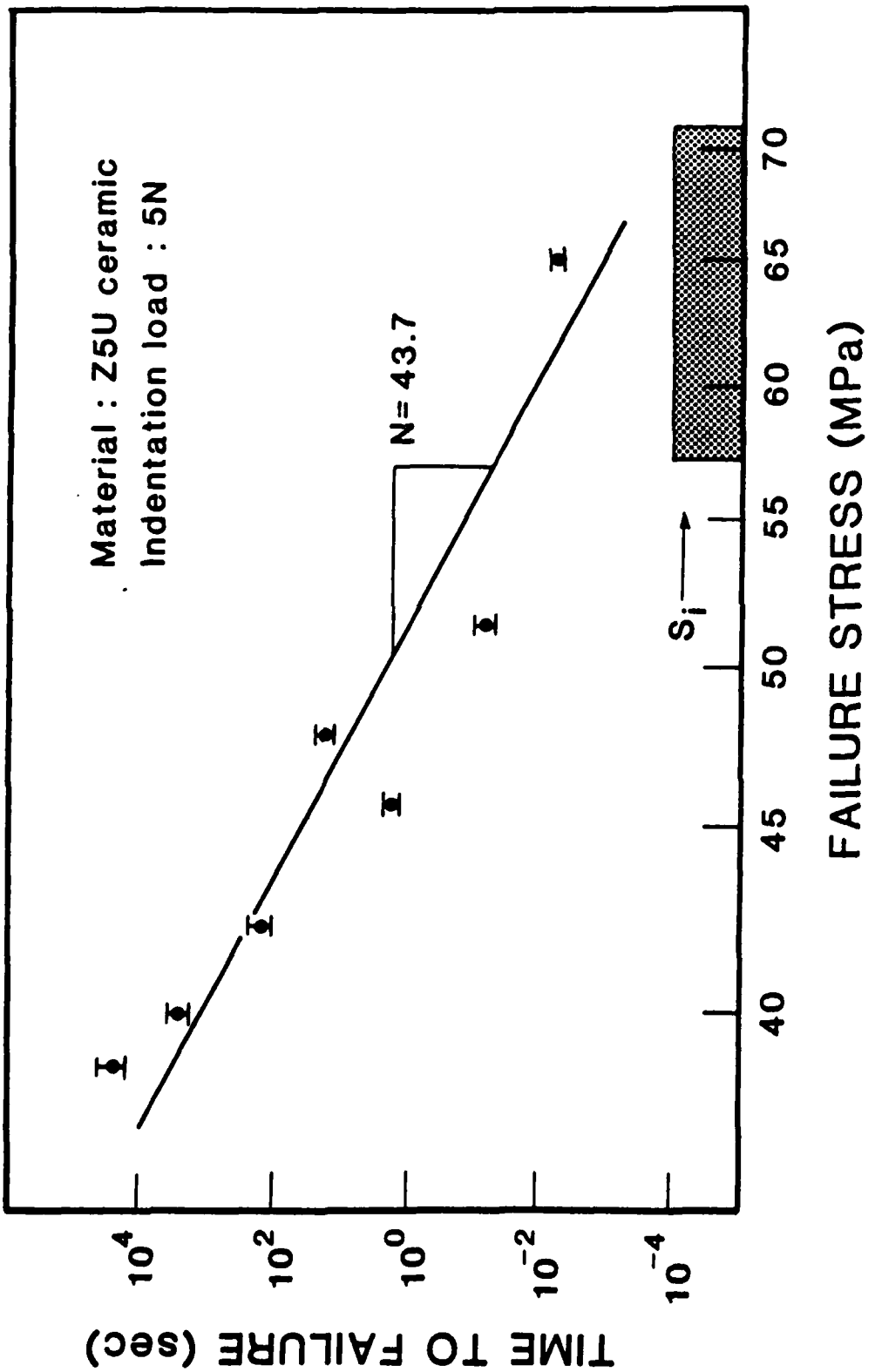
Material : Z5U ceramic
Indentation load : 5N
N= 43.7
S_i
TIME TO FAILURE (sec)
10^4
10^2
10^0
10^{-2}
10^{-4}
40
45
50
55
60
65
70
FAILURE STRESS (MPa)

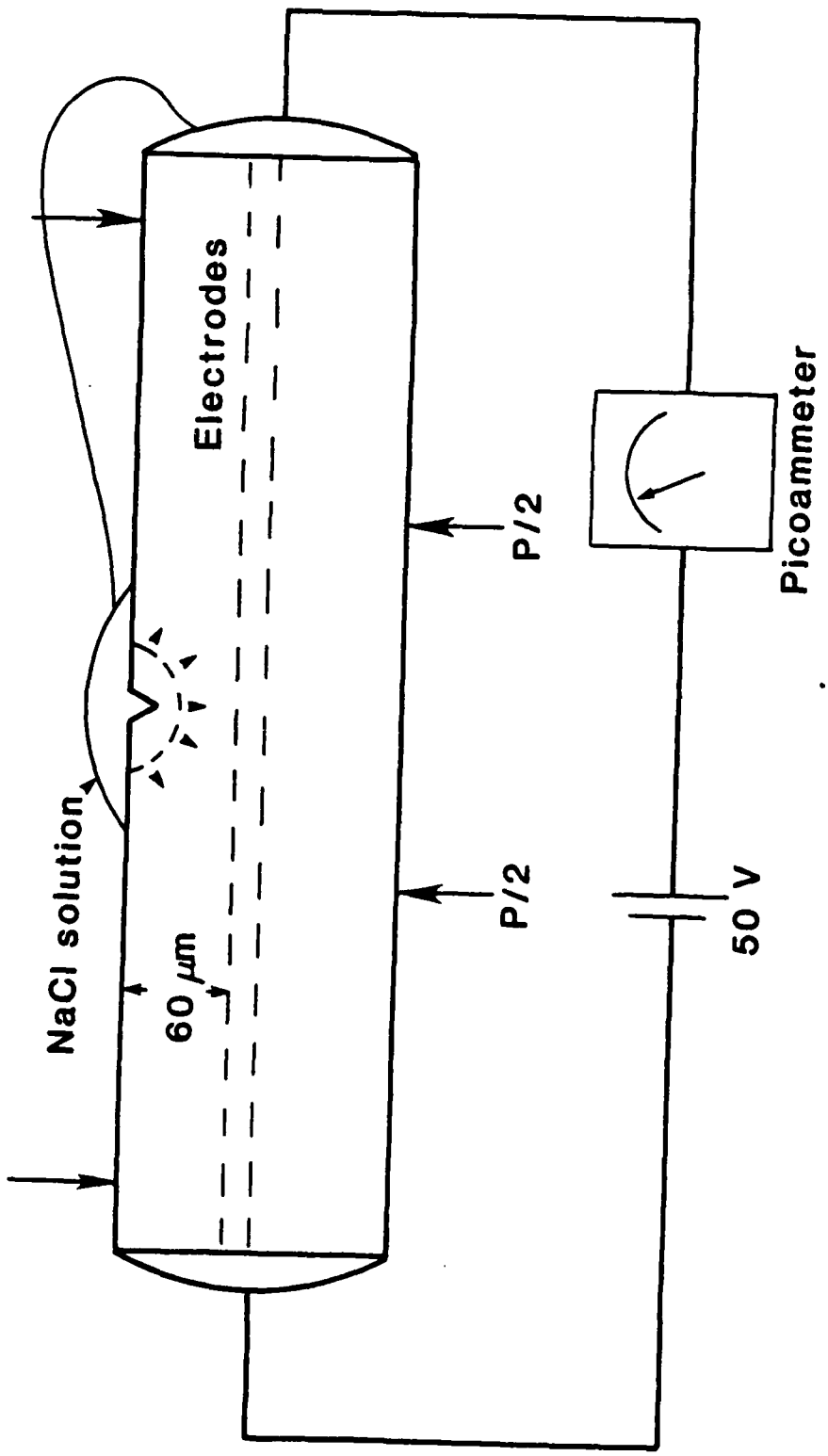
Electrodes
P/2
Picoammeter
NaCl solution
60 μm
P/2
50 V

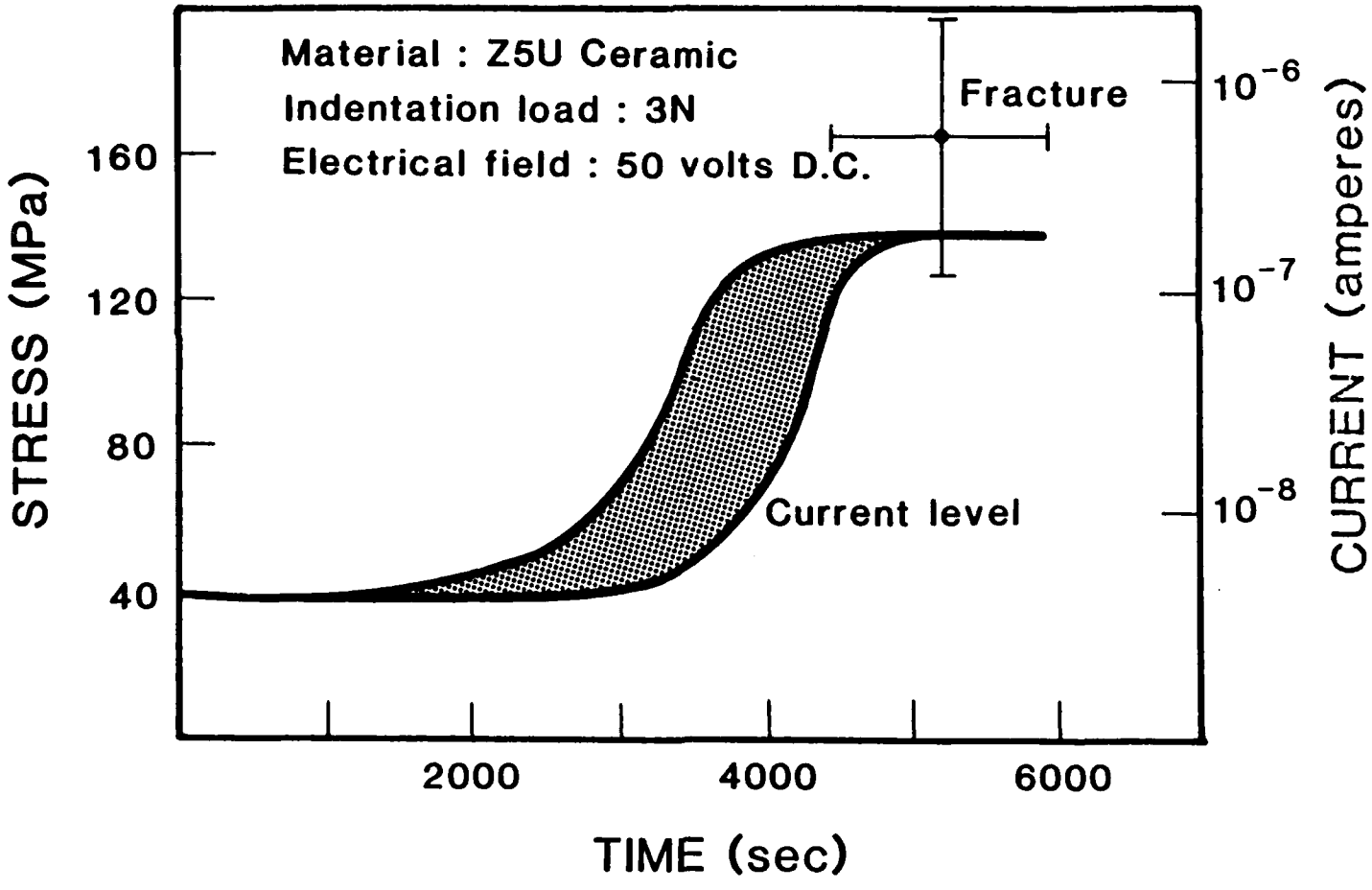
Material : Z5U Ceramic
Indentation load : 3N
Electrical field : 50 volts D.C.
Fracture
Current level
STRESS (MPa)
160
120
80
40
10^{-6}
10^{-7}
10^{-8}
CURRENT (amperes)
2000
4000
6000
TIME (sec)

SECURITY CLASSIFICATION OF THIS PAGE (When Data Entered)

REPORT DOCUMENTATION PAGE

READ INSTRUCTIONS BEFORE COMPLETING FORM

1. REPORT NUMBER	2. GOVT ACCESSION NO. / 3. RECIPIENT'S CATALOG NUMBER
4. TITLE (and Subtitle): Stress Corrosion of Ceramic Materials	5. TYPE OF REPORT & PERIOD COVERED: Annual, 1 Oct. 1983-Sept. 30, 1984
	6. PERFORMING ORG. REPORT NUMBER
7. AUTHOR(s): S.W. Freiman, G.S. White, A.C. Gonzalez, E.R. Fuller, Jr., and D.C. Greenspan	8. CONTRACT OR GRANT NUMBER(s): N00014-84-F-0019
9. PERFORMING ORGANIZATION NAME AND ADDRESS: National Bureau of Standards, Inorganic Materials Division, Gaithersburg, MD 20899	10. PROGRAM ELEMENT, PROJECT, TASK AREA & WORK UNIT NUMBERS
11. CONTROLLING OFFICE NAME AND ADDRESS: Office of Naval Research, 800 North Quincy Street, Arlington, VA 22217	12. REPORT DATE: 1 May 1985
	13. NUMBER OF PAGES: 116
14. MONITORING AGENCY NAME & ADDRESS (if different from Controlling Office)	15. SECURITY CLASS. (of this report): UNCLASSIFIED
	15a. DECLASSIFICATION/DOWNGRADING SCHEDULE

16. DISTRIBUTION STATEMENT (of this Report)

DISTRIBUTION STATEMENT A
Approved for public release
Distribution Unlimited

17. DISTRIBUTION STATEMENT (of the abstract entered in Block 20, if different from Report)

18. SUPPLEMENTARY NOTES

19. KEY WORDS (Continue on reverse side if necessary and identify by block number)
Crack growth; capacitors; fracture; ceramics; glasses

20. ABSTRACT (Continue on reverse side if necessary and identify by block number)

The presence of modifying ions has been shown to affect the rate of, but not the basic mechanism of, bond rupture in silicates. Direct correlations of crack growth and ion exchange/dissolution were obtained in binary alkali silicate glasses. Electrical breakdown times in ceramic capacitors were correlated with rates of crack growth.

DD FORM 1 JAN 73 1473 EDITION OF 1 NOV 65 IS OBSOLETE
S/N 0102-LF-014-6601

SECURITY CLASSIFICATION OF THIS PAGE (When Data Entered)

END

FILMED

7-85

DTIC